



University College London
Department of Biochemical Engineering

A Cell Engineering Approach to Enzyme-Based Fed-Batch Fermentation

*Submitted to University College London for the Degree of
Doctor of Philosophy*

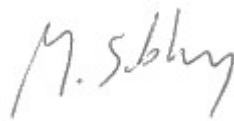
Michael Sibley

Supervised by Prof. John Ward

2018

I, Michael Sibley confirm that the work presented in this thesis is my own. Where information has been derived from other sources, I confirm that this has been indicated in the thesis.

Signed:

A handwritten signature in black ink, appearing to read "M. Sibley". The signature is written in a cursive, slightly slanted style.

Michael Sibley

2018

Abstract

One of the major disadvantages of batch fermentation is the difficulty in achieving high cell densities; in *E.coli* K12, much of this is attributed to the production of acetate via a phenomenon known as overflow metabolism. Although a fed-batch configuration is the standard method for reducing such issues, traditional fed-batch mechanisms require components which become problematic when applying them to smaller scale systems such as shake flasks. As a result, a number of slow release carbon techniques have been developed; one of which uses the enzymatic degradation of starch to slowly release glucose into the culture medium following the addition of an amylolytic enzyme. This reduces acetate production due to the low initial glucose concentration, leading to an increased cell density, and an increased product yield. To date, these amylolytic enzymes have been added to the culture exogenously, whereas this project aims to employ a cell engineering approach to design and build a self-secreting amylolytic chassis capable of enzyme-based fed-batch fermentation. The study explores the use of starch as an alternative carbon source, and describes the ability of a highly active amylolytic *E. coli* strain secreting *S. thermoviolaceus* α -amylase to degrade and utilise starch as a sole carbon source. Bacterial exo-acting amylolytic enzymes have been identified and cloned into *E. coli* for characterisation studies, with enhanced secretion of the novel *C. violaceum* glucoamylase using the DsbA signal peptide resulting in direct conversion of starch to glucose within the media. Further investigations reveal expression can be negatively regulated using a glucose sensitive promoter, providing a basis for self-regulation. Lastly, vectors have been constructed to simultaneously express the *C. violaceum* glucoamylase and a target recombinant protein (eGFP), resulting in higher biomass and increased recombinant protein expression when grown on starch compared to an equivalent amount of glucose, the first demonstration of a cell engineered approach to enzyme-based fed-batch fermentation.

Impact Statement

This thesis describes a novel solution to one of the most fundamental problems associated with microbial fermentation, achieving high cell densities and increased recombinant protein yields in batch culture. By combining the principles of enzyme-based fed-batch fermentation with engineered amylolytic *E. coli* strains, a proof of concept has been demonstrated which has the potential to provide an alternative to current traditional fed-batch methods. The technology is particularly applicable to lab-scale batch culture, giving scientists an ability to increase recombinant protein yield without requiring them to invest in small scale fed-batch control systems. This opens up possible commercial opportunities, not only competing with currently available enzyme-based fed-batch media products, but offering a significant advantage over them whereby the exogenous addition of amylolytic enzymes is not required. More broadly, this work highlights the capability of cell engineering to enhance bioprocessing, and provides a platform for further projects looking to combine this with other innovative cell engineering approaches to improve overall bioprocessing efficiencies.

Acknowledgements

I would like to thank my primary supervisor Prof. John Ward for his help and support, as well as all other members of the Ward lab who have spared me their time over the past four years. I am particularly grateful to both Maria Bawn and Dragana Dobrijevic for their advice and guidance.

The doctoral experience would not have been complete without such a great group of people around me. Special thanks go to Victoria Wood, Rachael Wood, Roberto Chiochio, Ivano Colao, Tom Johnson, Sushobhan Bandyopadhyay and Ryan Walker-Gray, for all the amazing holidays and the pint or two we've shared over the years.

I would like to thank my family, in particular my Mum, Sister, and Brother-in-law for their continued support during my academic studies, and I would also like to acknowledge my Dad, who despite no longer being with us, has always inspired me to succeed.

Finally, I am extremely grateful to the EPSRC and the Department of Biochemical Engineering at UCL for extending me the opportunity to complete my doctorate.

Table of Contents

Title Page	1
Declaration	2
Abstract	3
Impact Statement	4
Acknowledgements	5
1 Introduction	18
1.1 Chassis engineering to enhance bioprocessing	18
1.2 <i>Escherichia coli</i> as a host organism	19
1.2.1 Carbohydrate metabolism within <i>E. coli</i>	20
1.2.2 Acetate production and overflow metabolism	22
1.3 Methods to alleviate the effects of acetate production	23
1.3.1 Fed-batch fermentation	23
1.3.2 Cell and Metabolic engineering	24
1.3.3 Media composition strategies	26
1.3.4 Strain selection	26
1.4 Enzyme-based fed-batch fermentation	27
1.4.1 Current strategies	27
1.4.2 Cell engineering approach to enzyme-based fed-batch fermentation	28
1.5 Amylolytic enzymes and their substrates	29

1.5.1	Starch	29
1.5.2	α -amylases	30
1.5.2.1	<i>S. thermoviolaceus</i> α -amylase	30
1.5.2.2	The derivation of pQR187	31
1.5.3	Glucoamylases	32
1.6	Secretion of amylolytic enzymes within <i>E. coli</i>	33
1.7	Regulatory strategies for enzyme expression.....	34
1.8	Overview of project	35
2	Materials and Methods	37
2.1	Cell culture	37
2.1.1	<i>E. coli</i> strains	37
2.1.2	Constructs	37
2.1.3	Strain maintenance	39
2.1.4	Competent cell preparation.....	39
2.1.5	Transformation	39
2.2	Standard molecular biology techniques	40
2.2.1	Vector design, construction and confirmation	40
2.2.2	Restriction digestion and ligation	43
2.2.3	Polymerase chain reaction (PCR)	43
2.2.4	Circular polymerase extension cloning (CPEC)	43
2.2.5	Agarose gel electrophoresis.....	46
2.2.6	Gel extraction.....	46

2.2.7	Plasmid isolation and purification.....	46
2.2.8	Chromosomal DNA preparation.....	46
2.2.8.1	<i>Saccharomyces diastaticus</i> genomic DNA preparation	46
2.2.8.2	<i>Thermoanaerobacter tengcongensis</i> genomic DNA preparation	47
2.2.8.3	<i>Chromobacterium violaceum</i> genomic DNA preparation	47
2.2.8.4	<i>Deinococcus geothermalis</i> genomic DNA preparation	47
2.3	Growth media preparation	48
2.3.1	Luria broth (LB) media	48
2.3.2	Terrific broth (TB) media.....	48
2.3.3	Glucose free mineral salt medium (MSM)	48
2.3.4	Starch-agar layer preparation	49
2.4	Growth and expression protocols.....	49
2.4.1	Overnight cultures	49
2.4.2	Shake flasks	49
2.4.3	Automated experiments (microwell plates)	50
2.4.4	EnPresso® Growth System.....	50
2.5	Protein expression studies.....	51
2.5.1	Sodium dodecyl sulphate polyacrylamide gel electrophoresis (SDS-PAGE) ..	51
2.5.2	Amylase assay	52
2.5.3	Determination of extracellular amyolytic enzyme activity	52
2.5.4	Periplasmic release procedure.....	53
2.5.5	Whole cell and clarified lysate preparation	53

2.5.6	Starch degradation assay	53
2.5.7	Glucose (GO) assay.....	54
2.5.8	Fluorescence measurements	54
2.5.9	Ortho-nitrophenyl- β -D-galactopyranoside (ONPG) β -galactosidase assay ...	54
2.5.10	High performance anion exchange chromatography with pulsed amperometric detection (HPAEC-PAD) analysis	55
3	Starch as an alternative carbon source in <i>E. coli</i> fermentation... 56	
3.1	Introduction	56
3.2	Investigating catabolite repression in the presence of starch.....	57
3.3	Utilisation of starch by <i>E. coli</i> via heterologous expression and secretion of an α -amylase from <i>Streptomyces thermoviolaceus</i>	58
3.3.1	Expression of <i>S. thermoviolaceus</i> α -amylase	59
3.3.2	Quantification and the subcellular localisation of α -amylase expressed from pQR187	61
3.3.3	Effects of temperature on the relative activity of <i>S. thermoviolaceus</i> α -amylase	63
3.3.4	Starch degradation studies	64
3.3.5	Hydrolysis products of <i>S. thermoviolaceus</i> α -amylase	65
3.3.6	The influence of starch on the growth characteristics of <i>E. coli</i> K12 secreting α -amylase.....	68
3.3.7	Investigating reduced expression through ribosome binding site modification	69
3.3.7.1	Modified vector primer design and construction	69

3.3.7.2	Activity from modified vector and growth characteristics	72
3.4	The ability of <i>E. coli</i> to degrade starch without exogenous amylase expression ..	74
3.4.1	Variations in starch degradation by non-amylolytic strains	74
3.4.2	Starch as a supplement to enhance heterologous expression in complex media	76
3.4.3	Amylolytic activity associated with <i>E. coli</i> BL21(DE3) is not localised to the extracellular media	77
3.4.4	Starch degradation by whole cell <i>E. coli</i> BL21(DE3) in glucose free mineral salt medium	79
3.5	<i>E. coli</i> secreting <i>S. thermoviolaceus</i> α -amylase utilising starch as a sole carbon source	80
3.6	Discussion and Conclusions	81
4	Novel bacterial glucoamylase discovery and characterisation...	84
4.1	Introduction	84
4.2	Cloning of fungal glucoamylases and expression attempts in <i>E. coli</i>	85
4.2.1	Expression of a glucoamylase derived from <i>Aspergillus niger</i>	85
4.2.2	Cloning and expression of a glucoamylase derived from <i>Saccharomyces diastaticus</i>	88
4.3	Bioinformatics; identification and cloning of putative glucoamylases	90
4.3.1	Identification of putative bacterial glucoamylase	90
4.3.2	Classical restriction digestion and ligation cloning strategy	91
4.3.3	PCR of target enzymes in selected organisms	92
4.3.4	Construction of vectors incorporating histidine tags.....	93

4.4	Characterisation of <i>D. geothermalis</i> , <i>T. tengcongensis</i> and <i>C. violaceum</i> glucoamylases.....	94
4.4.1	Initial expression and cell lysate activity for selected glucoamylases	94
4.4.2	Further analysis of <i>D. geothermalis</i> , <i>T. tengcongensis</i> and <i>C. violaceum</i> glucoamylases.....	95
4.4.2.1	Expression of <i>D. geothermalis</i> , <i>T. tengcongensis</i> and <i>C. violaceum</i> glucoamylases and their conversion of starch to glucose	96
4.4.2.2	Hydrolysis products of <i>D. geothermalis</i> , <i>T. tengcongensis</i> and <i>C. violaceum</i> glucoamylases.....	98
4.4.2.3	Clarified lysate activities for <i>D. geothermalis</i> , <i>T. tengcongensis</i> and <i>C. violaceum</i> glucoamylases.....	100
	101
4.5	Investigating glucoamylase secretion.....	102
4.5.1	Secretion of glucoamylases from native signal sequences.....	102
4.5.2	Improvement of secretion through addition of signal sequences.....	103
4.6	Growth characteristic of <i>E. coli</i> expressing and secreting <i>C. violaceum</i> glucoamylase	107
4.6.1	Effects of temperature on the relative activity of <i>C. violaceum</i> glucoamylase	107
4.6.2	<i>E. coli</i> secreting <i>C. violaceum</i> glucoamylase and its utilisation of starch as a sole carbon source.....	108
4.7	Discussion and conclusion	109

5	Towards a self-secreting enzyme-based fed-batch fermentation system	112
5.1	Introduction	112
5.1.1	Overview of Chapter 5	113
5.2	Expression and secretion of α -amylase within commercially available high density media	115
5.3	Starch-agar layer development for sufficient provision of carbon.....	118
5.3.1	Growth studies using starch-agar layers and <i>E. coli</i> secreting <i>S. thermoviolaceus</i> α -amylase	121
5.3.2	Growth studies using starch-agar layers with <i>E. coli</i> secreting <i>C. violaceum</i> glucoamylase.....	123
5.4	Regulation of <i>C. violaceum</i> glucoamylase expression	124
5.4.1	Cyclic AMP dependant promoter.....	124
5.4.2	Vector design and characterisation of <i>PcstA</i>	125
5.4.3	<i>PcstA</i> regulation of <i>C. violaceum</i> glucoamylase.....	128
5.4.3.1	Vector design	128
5.4.3.2	Characterisation of <i>PcstA</i> regulated <i>C. violaceum</i> glucoamylase secretion	130
5.4.4	The influence of <i>PcstA</i> regulated <i>C. violaceum</i> glucoamylase expression on starch degradation within LB media	131
5.4.5	Growth characteristics of <i>E. coli</i> W3110 expressing <i>PcstA</i> regulated <i>C. violaceum</i> glucoamylase cultured in glucose free MSM with starch-agar layers.....	132

5.5	Co-expression studies as a method for developing a heterologous protein expression system utilising starch as a carbon source	134
5.5.1	Co-expression of <i>S. thermoviolaceus</i> α -amylase and an <i>E. coli</i> derived transketolase.....	134
5.5.2	Co-expression of <i>C. violaceum</i> glucoamylase and an <i>E. coli</i> derived transketolase.....	136
5.6	Dual-expression studies as a method for developing a heterologous protein expression system utilising starch as a carbon source	138
5.6.1	Construction of pQR1716 (pUC19-Amy) and pQR1717 (pUC19-GFP)	138
5.6.2	Construction of dual-expression vectors pQR1718 (pUC19-AmyGFP) and pQR1719 (pUC19-GFPAmy)	140
5.6.3	Expression and activity from dual-expression plasmids	142
5.6.4	Dual-expression using starch as a sole carbon source.....	143
5.6.5	Dual-expression of <i>C. violaceum</i> glucoamylase and eGFP	144
5.7	Discussion and Conclusion	147
6	Conclusions and Future work.....	149
7	References.....	154

List of Figures

Figure 1.1 Schematic diagram of acetate production in <i>E. coli</i> central metabolism	23
Figure 2.1 Schematic diagram of circular polymerase extension cloning for single insertion	45
Figure 3.1 Catabolite repression of soluble potato starch in comparison to glucose.	58
Figure 3.2 pQR187 expression and the quantification of α -amylase activity.....	60
Figure 3.3 <i>S. thermoviolaceus</i> α -amylase activity in periplasmic and extracellular fractions over time.....	62
Figure 3.4 Relative enzyme activity of <i>S. thermoviolaceus</i> α -amylase over a range of temperatures	63
Figure 3.5 Starch degradation by the <i>S. thermoviolaceus</i> α -amylase secreting <i>E.coli</i> strain	64
Figure 3.6 Analysis of hydrolysis products from secreted <i>S.thermoviolaceus</i> α -amylase	67
Figure 3.7 Growth of <i>E. coli</i> W3110 harbouring pQR187 in LB media supplemented with starch	68
Figure 3.8 Diagram of primer design for modified vector construction.....	71
Figure 3.9 The reduction of secreted α -amylase from a modified construct and the effects on growth in LB media containing starch	72
Figure 3.10 Degradation of starch within LB media for both W3110 and BL21(DE3) <i>E.coli</i> cultures	74
Figure 3.11 Heterologous protein expression following supplementation of LB media with either starch or glucose	76
Figure 3.12 Differentiating amyolytic activity associated with <i>E. coli</i> BL21(DE3) between the cellular and extracellular space	78
Figure 3.13 Degradation and utilisation of starch by <i>E. coli</i> BL21(DE3).....	79

Figure 3.14 End point analysis of growth in mineral salt media (MSM) supplemented with starch or glucose	80
Figure 4.1 Diagram of synthesised <i>A. niger</i> glucoamylase gene in initial sub-cloning vector and in expression vector	87
Figure 4.2 <i>S. diastaticus</i> glucoamylase genomic PCR and expression vector design.....	88
Figure 4.3 Functional activity of whole cell lysates for <i>E. coli</i> expressing fungal enzymes ...	89
Figure 4.4 Phylogenetic tree of putative bacterial glucoamylases	90
Figure 4.5 Overview of cloning strategy for putative bacterial glucoamylases.....	91
Figure 4.6 Agarose gel electrophoresis of <i>D. geothermalis</i> , <i>T. tengcongensis</i> , and <i>C. violaceium</i> genomic PCR	92
Figure 4.7 Diagram of pET28a expression cassette	93
Figure 4.8 Glucoamylase expression and lysate activity.....	95
Figure 4.9 Further expression studies and clarified lysate effects on starch degradation and glucose accumulation for <i>D. geothermalis</i> , <i>T. tengcongensis</i> and <i>C. violaceum</i> glucoamylases.....	97
Figure 4.10 Chromatograms of <i>D. geothermalis</i> , <i>T. tengcongensis</i> and <i>C. violaceum</i> glucoamylase hydrolysis products	99
Figure 4.11 Clarified lysate activities for <i>D. geothermalis</i> , <i>T. tengcongensis</i> and <i>C. violaceum</i> glucoamylases expressed in terms of starch degradation and glucose production.....	101
Figure 4.12 Extracellular media activity of <i>D. geothermalis</i> and <i>C. violaceum</i> glucoamylases	102
Figure 4.13 Diagram of signal sequence insertion using complementary oligonucleotides	105
Figure 4.14 Activity of <i>D. geothermalis</i> and <i>C. violaceum</i> glucoamylases following addition of exogenous signal sequences.....	106
Figure 4.15 Relative enzyme activity of <i>C. violaceum</i> glucoamylase over a range of temperatures	107

Figure 4.16 <i>E. coli</i> 's utilisation of starch as a sole carbon source through the expression and secretion of <i>C. violaceum</i> glucoamylase	108
Figure 5.1 Growth curves of α -amylase secreting <i>E. coli</i> cultured in commercially available high cell density media	115
Figure 5.2 α -amylase expression over time in commercially available high density media	117
Figure 5.3 Design of starch-agar layer system for sufficient provision of carbon for high cell density applications	120
Figure 5.4 Increased cell densities for <i>E. coli</i> W3110 expressing <i>S. thermoviolaceus</i> α -amylase using the starch-agar layer system	121
Figure 5.5 Comparison of amylolytic strain growth on high concentrations of starch or glucose in MSM.....	122
Figure 5.6 Growth curves for <i>E.coli</i> expressing <i>C. violaceum</i> glucoamylase.....	123
Figure 5.7 A schematic diagram of the Biobrick standard assembly method for suffix insertion	126
Figure 5.8 Characterisation of <i>PcstA</i> over a range of glucose concentrations using eGFP fluorescence.....	127
Figure 5.9 Schematic diagram for the insertion of <i>C. violaceum</i> glucoamylase gene into the BBa_K118011 backbone	129
Figure 5.10 Characterisation of <i>PcstA</i> regulated <i>C. violaceum</i> glucoamylase secretion in LB media supplemented with 0-20 mM glucose	130
Figure 5.11 <i>PcstA</i> regulated expression of <i>C. violaceum</i> glucoamylase by <i>E. coli</i> and its influence on growth and the degradation of starch within LB media	131
Figure 5.12 <i>PcstA</i> regulated <i>C. violaceum</i> glucoamylase expression and its influence on growth in MSM containing starch-agar layers.....	133
Figure 5.13 SDS-page analysis for the co-expression of <i>S. thermoviolaceus</i> α -amylase and an <i>E. coli</i> derived transketolase	135

Figure 5.14 Co-expression of <i>PcstA</i> regulated <i>C. violaceum</i> glucoamylase and an <i>E. coli</i> derived transketolase	137
Figure 5.15 Construction of pQR1716 (pUC19-Amy) and pQR1717 (pUC19-GFP) using Circular Polymerase Extension Cloning.....	139
Figure 5.16 Vectors designed for dual-expression of eGFP and α -amylase	141
Figure 5.17 eGFP fluorescence and α -amylase activity from dual-expression vectors	142
Figure 5.18 Growth and eGFP expression of <i>E. coli</i> W3110 harbouring the pQR1719 dual-expression vector cultured in glucose free MSM supplemented with 2.5 mg/mL starch...	143
Figure 5.19 Vector designed for dual-expression of eGFP and <i>C. violaceum</i> glucoamylase	144
Figure 5.20 Dual-expression of <i>C. violaceum</i> glucoamylase and eGFP in <i>E. coli</i> W3110 harbouring pQR1720.....	146

List of Tables

Table 1 Constructs used within current study	37
Table 2 Nucleotide sequences for primers and oligonucleotides used in vector construction	41

1 Introduction

1.1 Chassis engineering to enhance bioprocessing

Cell or chassis engineering has been applied widely across the biotechnology industry, using a broad range of different host organisms, in an attempt to enhance the efficiency of bioprocessing [1]. Much of this has been associated with improving upstream processes, encompassing any modifications capable of increasing product yield or reducing cost during fermentation [2], although considerable effort has also been directed towards downstream capture and purification steps [3], with the general aim of increasing bioprocess productivity as a whole.

One particularly recent example, which has actually proved beneficial to both upstream and downstream processes, has been the development of a triosephosphate isomerase knockout *E. coli* strain, in which auxotrophic complementation provides a mechanism for antibiotic-free selection of recombinant plasmids [4]. Plasmid segregational stability is an important issue during fermentation, with poor stability leading to a reduced recombinant protein yield. Although many research settings use antibiotics as a selective marker, this is not the preferable option in industry as scale up not only leads to issues associated with the widespread use of antibiotics, but also an increase in both the cost and complexity of downstream processing. Chassis engineering has, in this case, provided an alternative to antibiotic selection which can address these problems and reduce both overall cost and any additional downstream complications.

Another example, this time where chassis engineering has been applied directly to downstream processing, has been the creation of an *E. coli* strain capable of expressing a staphylococcal nuclease which is targeted to the periplasm [5]. Upon homogenisation this

nuclease is able to hydrolyse the host cells nucleic acid, significantly reducing the viscosity of the homogenate and the subsequent supernatant, tackling a major hindrance to downstream processing and purification. With nuclease co-expression compromising neither growth nor yield of the production strain, this cell engineering method appears to be a very viable option in reducing downstream costs and maximising product manufacturability [6].

To that end, this thesis identifies a particular aspect of bioprocessing which has the potential to be enhanced or improved by the application of host cell engineering. More specifically it focusses on the difficulty in achieving high cell densities in batch fermentations, and describes a cell engineering approach to resolve these challenges.

1.2 *Escherichia coli* as a host organism

Escherichia coli are Gram-negative bacteria used extensively in both research and industrial settings. Owing to a rapid growth rate and relative ease to culture, *E. coli* has been the organism of choice for a huge quantity of molecular and cellular research to date. The wealth of knowledge gained has helped *E. coli* become one of the predominant organisms in the bioprocess industry, and as such a key target for host cell engineering. A major drawback in using this particular organism however, is the difficulty in secreting recombinant proteins into the extracellular media; a particularly advantageous feature from the perspective of downstream processing and purification. Instead, proteins of interest are often constructed to include a targeting sequence which directs them to the periplasmic space between the outer membrane and the cytoplasmic membrane. The periplasm offers certain advantages over the cytoplasm such as containing fewer proteases and providing an oxidative environment conducive to disulphide bond formation [7].

Furthermore, regarding downstream processing, the periplasm contains a much smaller number of native cell proteins compared to the cytoplasm, aiding the purification process.

Although thousands of *E. coli* strains have been found and developed, there are only four (K12, B, C and W) which have been characterised as safe, and which are used widely across laboratories and industry [8]. There is a fifth strain (Crooks) which is also commonly used, and although it has not yet been designated laboratory safe, it is not known to be pathogenic. In addition to this, *E. coli* Nissle, which was originally isolated in 1917 by Alfred Nissle, can actually provide certain health benefits, and as such has been used as a probiotic in the treatment of numerous gastrointestinal disorders [9]. For the purposes of the current study, work has been carried out in both K12 and B strains, predominantly because these strains are some of the most extensively used for recombinant protein production in both academia and industry.

1.2.1 Carbohydrate metabolism within *E. coli*

Early experiments by Monod investigating the phenomenon of diauxic growth [10], showed *E. coli* preferentially use glucose over lactose and other sugars, when present in a mixture. This has led to a vast amount of work into carbon catabolite repression and carbon metabolism pathways predominantly using *E. coli* as a model. It is now known that glucose is transported into *E. coli* via five different permeases [11]; three of which are of the phosphotransferase system (PTS) type, including the regular glucose-PTS, the mannose-PTS and the N-acetyl-glucosamine-PTS, and the final two are galactose induced uptake systems, the galactose permease and the methyl-galactoside permease [12]. Glucose entering via the PTS system is directly converted to glucose-6-phosphate, whereas glucose entering via the latter two permeases requires phosphorylation by glucokinase. In either case glucose-

6-phosphate is the starting molecule for the three major carbon metabolism pathways, glycolysis, the tricarboxylic acid cycle, and the pentose phosphate pathway.

E. coli are also capable of catabolising polymers of glucose. Growth is possible on oligosaccharides up to 7 or 8 glucose units in length, any larger and there is an increasingly reduced growth rate correlated with the size of the oligosaccharide [13]. Short chained glucose polymers, or maltodextrins, are transported via facilitated diffusion into the periplasm through the outer membrane transporter protein, maltoporin (LamB) [14]. Maltose binding protein (MBP), the *malE* gene product residing in the periplasm, is responsible for recognising maltodextrins and sequestering them to the MalF, MalG, and MalK membrane bound complex for transport into the cytoplasm [15]. MBP is capable of binding molecules as large as amylose and starch [16], with some evidence suggesting a proportional relationship between binding affinity and maltosaccharide chain length [17]. Only maltodextrins with a chain length of 6 glucose units or fewer are transported into the cytoplasm [18], explaining the difficulty *E. coli* have in catabolising larger maltodextrins. The combined action of three cytoplasmic enzymes, amylomaltase, maltodextrin phosphorylase, and maltodextrin glucosidase, degrade these maltodextrins to form glucose and α -glucose-1-phosphate. These two molecules require the presence of glucokinase and phosphoglucomutase for their respective conversions to glucose-6-phosphate and subsequent entry into central carbon metabolism pathways [19].

In the context of fermentation, the carbon source on which *E. coli* can achieve their highest growth rate is in most conditions glucose [20], however the provision of glucose at high concentrations, when *E. coli* are cultured aerobically, can lead to a phenomenon known as overflow metabolism, ultimately reducing growth rate and product yield [21, 22].

1.2.2 Acetate production and overflow metabolism

During rapid glucose uptake in aerobic conditions, the flux of acetyl-coA is directed away from the tricarboxylic acid (TCA) cycle and towards the production of acetate in a process known as overflow metabolism [23]. This phenomenon leads to a diversion of carbon away from potential biomass and recombinant protein product, as well as resulting in acetate accumulation in the media lowering pH, leading to both a reduction in growth [22] and recombinant protein yield [21]. Overflow metabolism occurs when cells grow above a threshold specific growth rate, with the threshold being strain dependant and linked to the cells maximum oxygen uptake rate. Under glucose limited growth, the growth rate can be controlled by reducing the availability of glucose, which provides the basis of fed-batch fermentation (see section 1.3.1). The molecular mechanisms behind overflow metabolism are yet to be fully resolved, particularly regarding its regulation, however, there is evidence to suggest it arises due to a limitation in the respiratory system whereby NADH is unable to be re-oxidised at a sufficient rate [24]. Given that the flux from acetyl-CoA through the TCA cycle produces NADH, whereas the flux from acetyl-CoA to acetate does not, this could be a mechanism to prevent further accumulation of reduced co-factors within the cell.

Acetate production itself is fairly well understood, with the predominant pathway involving the phosphate acetyl-transferase (Pta) and acetate kinase (AckA) enzymes, which convert acetyl-coA to acetyl-phosphate, and acetyl-phosphate to acetate respectively [25], and a secondary pathway involving the oxidative decarboxylation of pyruvate by pyruvate oxidase (PoxB) (Fig 1.1) [26, 27].

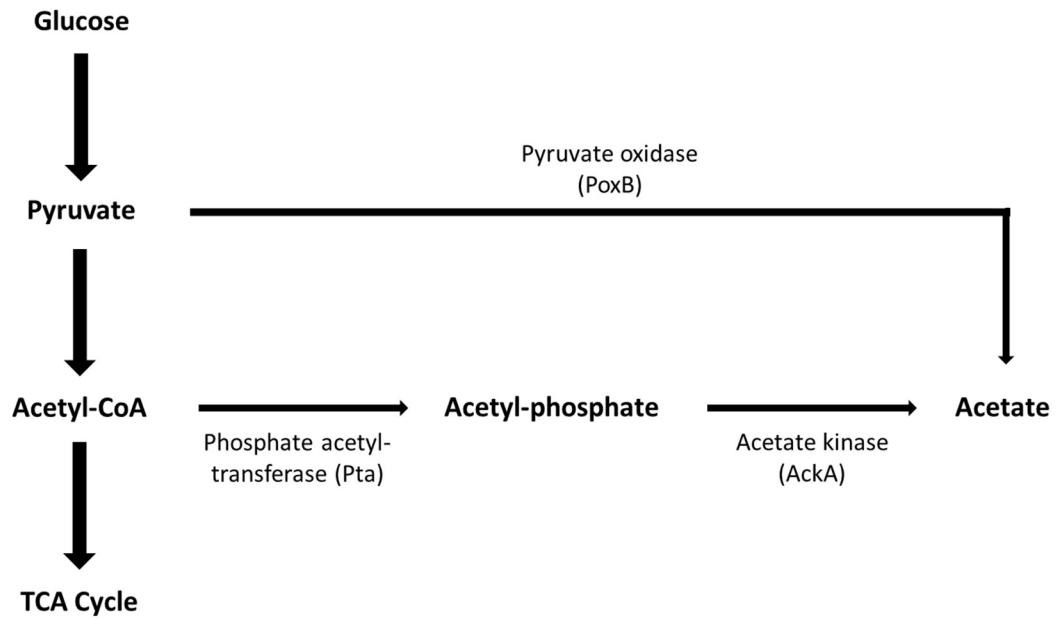


Figure 1.1 Schematic diagram of acetate production in *E. coli* central metabolism
 Acetate production in *E. coli* central carbon metabolism via the Pta/AckA or the PoxB pathways.

1.3 Methods to alleviate the effects of acetate production

Numerous methods have been developed in an effort to overcome the detrimental effects of acetate on *E. coli* recombinant protein fermentations [28]. This section outlines these attempts with the aim of providing a context to the current project.

1.3.1 Fed-batch fermentation

As discussed, the development of traditional glucose-limited fed-batch fermentation has gone some way to alleviate acetate accumulation, and is the method most commonly used in industry for achieving high cell densities and increased recombinant protein yield. These traditional systems vary extensively in the manner of substrate delivery; some are programmed with pre-determined feed rates e.g. constant or exponential, while others rely

on automatic feedback control [29]. Regardless of the mechanism, traditional fed-batch fermentation is often an impractical solution for smaller scale fermentations owing to the sophistication of the control systems required, as well as other technical difficulties including unsatisfactory flow and mixing of small, concentrated feed volumes. Many of these issues are being challenged through the development and increased availability of miniature bioreactors, for example the ambr® 250 from Sartorius or the DASbox® from Eppendorf, however shake flasks still provide an inexpensive and effective way of reproducibly performing many types of industrially-relevant cell cultivations for process development, and are therefore still widely used across industry and academia [30].

An alternative approach to the traditional fed-batch fermentation concept, which is relevant to shake flasks, has been the development of substrate delivery via an internal supply mechanism [31, 32]. An example specific to glucose supply uses silicone elastomer discs containing glucose crystals which, when immersed in media, release glucose by diffusion [33]. This has had the result of significantly increasing biomass yield, as well as potential recombinant protein expression. Another, more recent slow-release innovation, has been the idea of releasing glucose from its polymeric form via enzymatic degradation [34]. This system provides a basis for the current project and is discussed in more detail below (section 1.4).

1.3.2 Cell and Metabolic engineering

Other attempts at limiting acetate accumulation have been focussed on cell and metabolic engineering strategies. Broadly these have aimed at either reducing glucose consumption or reducing acetate production. As already discussed, glucose uptake is controlled predominantly by the PTS system; when knocked out and replaced with galactose permease the effect on glucose metabolism is a reduction in acetate accumulation and a

subsequent improvement of fermentation product yield [35, 36]. Another successful method of limiting glucose uptake has been to overexpress the PTS repressor protein Mlc, through modification of the *mhc* promoter, resulting in a 50% reduction in acetate and an associated increase in protein yield [37]. A number of methods have also been used to reduce acetate production directly, by diverting the flux of carbon away from acetate formation, either by targeting the enzymes responsible for its formation or by diverting the carbon to other compounds which are not as detrimental to growth and protein expression. An example of the former is seen following the mutation of the *Pta* gene, eliminating phosphotransacetylase [21], an enzyme involved in the primary pathway for acetate formation. A downside to this particular target is a subsequent increase in either lactate or pyruvate. The latter approach includes the introduction of enzymes which convert molecules residing at the end of glycolysis into compounds other than acetate. An example being the introduction of acetolactate synthase from *Bacillus subtilis* which converts pyruvate to acetoin, the effect of which doubled recombinant protein yield [38]. The major problem with some of these methods is that they do not necessarily prevent the diversion of carbon away from more useful forms such as biomass or product yield. An alternative genetic approach has been to divert acetate precursors towards the carboxylic acid cycle whereby the carbon can remain available to the cell. Overexpression of phosphoenolpyruvate (PEP) carboxylase, which converts PEP (an acetate precursor) to oxaloacetate, is able to significantly reduce acetate formation [39], however this in turn lowers the amount of PEP available for PTS-mediated glucose uptake which decreases overall growth rate [40]. Attempts have also been focussed on the potential molecular causes of overflow metabolism, as seen when excess NADH is removed by the recombinant expression of a *Streptococcus pneumoniae* NADH oxidase, allowing for a 10% increase in model protein expression [41].

1.3.3 Media composition strategies

Given that glucose in particular leads to acetate accumulation, previous studies have shown that replacing glucose with other utilisable carbon sources such as mannose [42] or fructose [43] can reduce acetate and subsequently increase biomass and recombinant protein expression. Despite the reduced maximum growth rate, there is evidence to suggest glycerol, when used as a carbon source post induction, is superior to glucose in terms of reducing acetate accumulation [44]. It has also been demonstrated that supplementing defined media with certain amino acids such as glycine and methionine can alleviate the inhibition of the specific growth rate caused by acetate [45]. Carbon sources are not the only area of interest, a recent study has presented the idea of implementing an alkaline shift, where by *E. coli* are cultured at pH8 in order to minimise the effects of acetate stress, improving both cell growth and recombinant protein expression [46].

1.3.4 Strain selection

It is known that central carbon metabolism varies between differing *E. coli* strains. B strains such as BL21(DE3) are able to employ a glyoxylate shunt resulting in reduced acetate levels, a mechanism beyond the capability of K12 strains [47-51]. As such K12 strains are more susceptible to the detrimental effects of overflow metabolism, an aspect explored further in this study with respect to selecting a suitable host to apply a cell engineering approach to control carbon utilisation.

1.4 Enzyme-based fed-batch fermentation

An alternative approach to traditional fed-batch fermentation is to provide the culture with necessary glucose in batch, but in a form which is not metabolically active i.e. using a polymerised version of glucose such as starch, and accessing the glucose via the use of amylolytic enzymes.

1.4.1 Current strategies

A current strategy developed by BioSilta, which has already been commercialised, uses the concept of glucose limited fed-batch fermentation, but rather than from an external feed, glucose is instead provided to the cells via the enzymatic degradation of starch [34] i.e. metabolically inactive polysaccharide is converted into metabolically active monosaccharide following the addition of an amylolytic enzyme (in this case an amyloglucosidase or glucoamylase isolated from *A. niger* (E.C.3.2.1.3.; Amylase AG 300L, Novozymes, Bagsvaed, Denmark)). Initially, starch is added to the culture flask in the form of a storage gel from which it continuously dissolves into the medium. The rationale for using a storage gel was based on the assumption that one gram of glucose yields approximately 0.5 g (dry weight) of cells and as such the developers needed to design a system which could supply enough glucose to reach desired cell densities. The developers embedded the gels with 10 % (100 g/L) starch, which they calculated would be enough to give a theoretical cell density of 30 g/L dry cell weight. This is equivalent to an OD₆₀₀ of approximately 100. Their experimental work to determine the most appropriate concentration of glucoamylase found that glucose limited growth controlled by enzymatic degradation could reach an optimum cell density with an OD₆₀₀ of 20 to 30, or approximately 6 to 9 g/L dry cell weight. Importantly, during experiments in which cell density achieved these high levels, acetate accumulation remained low, and pH and pO₂

remained stable. In contrast, when higher concentrations of the enzyme were tested, cell density fell away to an OD₆₀₀ of 10, highlighting the importance of glucose concentration in the media and its correlation with cell density.

Later modifications and subsequent commercialisation led to the development of Biosilta's EnPresso® growth system which incorporates the necessary nutrients and supply of starch within two tablets. These are added to sterile water at both the beginning and again part way through the culture period (see section 2.4.4 for protocol details). The EnPresso® growth system was used during this study as a proof of concept for a cell engineering approach to enzyme-based fed-batch fermentation.

1.4.2 Cell engineering approach to enzyme-based fed-batch fermentation

An important aspect of the EnPresso® growth system described above is the required addition of glucoamylase throughout the culture. Although undeniably easier than providing a constant feed of glucose, it still to some extent defeats the original objective. A cell engineering approach, however, in which a cell expresses and secretes its own amylolytic enzyme, would provide a number of advantages. Firstly it would alleviate the need for an experimenter to intervene at multiple points during the culture, and secondly the expression of the amylolytic enzyme could be regulated in such a way to provide glucose at a rate correlated to cell density, or indeed controlled via a feedback mechanism linked to culture conditions i.e. glucose concentration. This study is concerned with applying an innovative solution to overflow metabolism by designing and constructing an *E. coli* chassis which is capable of self-secreted enzyme-based fed-batch fermentation.

1.5 Amylolytic enzymes and their substrates

Amylolytic enzymes or amylases constitute one of the most significant classes of enzymes within biotechnology, and are applied across industries as diverse as food, textile, paper and detergent manufacturing [52]. Given the abundance of their substrate, starch, and the importance of starch as a biological energy store, a wealth of different amylases are produced by organisms across every domain of life. Recent attempts to classify amylolytic enzymes have been based on their structure and primary sequence [53], and have been compiled in the Carbohydrate Active Enzyme (CAZY) database [54], a resource used in this study to identify putative enzymes for characterisation. One aspect of considerable importance is the product profile following starch hydrolysis, which varies greatly depending on class of amylolytic enzyme used. The two classes used extensively throughout this project are the endo-acting α -amylase (EC 3.2.1.1) (primarily Glycoside hydrolase family 13) (section 1.5.2) and the exo-acting glucoamylase (EC 3.2.1.3) (Glycoside hydrolase family 15) (section 1.5.3).

1.5.1 Starch

Starch, an amylolytic enzyme substrate, is a heterogeneous polysaccharide consisting of amylose, a water insoluble linear polymer of glucose linked by α -1,4 glycosidic bonds, and amylopectin, a water soluble branched polymer of glucose containing both α -1,4 and α -1,6 glycosidic bonds [55]. Traditionally the relationship between biotechnology and amylolytic enzymes has been one of microbial production for use in the starch industry. However, it is also possible to utilise starch directly for conversion into useful and/or valuable products. As mentioned previously, starch is a ubiquitous source of biomass and as such has the potential to provide an excellent source of carbon for fermentative processes. Given that starch is a natural precursor to glucose, and often forms part of agricultural waste streams,

its production has the potential to be more economically viable than that of glucose. Currently however, compared to soluble potato starch, the type of starch used throughout this study, glucose remains the least expensive option, presumably due to the disparity in manufacturing scales.

Until recently there have been very few attempts at engineering *E. coli* to utilise starch directly [56]. This study explores the use of soluble potato starch as an alternative carbon source in *E. coli* fermentation, and investigates a potential increase in achievable biomass through a controlled release of glucose via its direct enzymatic degradation.

1.5.2 α -amylases

The most common and well characterised class of amylolytic enzymes are α -amylases (EC 3.2.1.1), which hydrolyse the α -1,4 glycosidic links within the constituent polysaccharides of starch (amylose and amylopectin), to form shorter chain maltodextrins. Both activity and substrate specificity of α -amylases vary, but a common feature is endo-activity, meaning they predominantly generate oligosaccharides rather than glucose.

1.5.2.1 *S. thermoviolaceus* α -amylase

The α -amylase used in this study was originally cloned from *Streptomyces thermoviolaceus* (CUB74 strain) [57], and has since been sequenced [58]. The gene encodes a 460 amino acid protein which, following cleavage of a 28 amino acid signal peptide, has a molecular weight of 47 kDa [58]. Paper chromatographic analysis has indicated that the major hydrolysis products of *S. thermoviolaceus* α -amylase are maltotetraose, maltotriose and maltose [57]. Although the initial rationale for cloning the *S. thermoviolaceus* α -amylase was to express a recombinant thermophilic α -amylase in *E. coli*, for potential use in the starch industry, the enzyme became a useful tool for investigating the properties of protein retention within the periplasm. The native signal sequence targets *S. thermoviolaceus* α -

amylase to the periplasm where a certain proportion of the enzyme is able to leak out into the extracellular media. The ease with which the activity of amylase can be determined by measuring the degradation of starch using potassium iodide/iodine solution, along with the thermophilic nature of this particular amylase (providing an opportunity to reduce the possibility of any activity from endogenous amylases by using an increased temperature) allowed for the development of an assay to determine activity within extracellular, periplasmic, or cytoplasmic fractions (see section 2.5.5). As a result the method was used to investigate the variation in outer membrane permeability across multiple *E. coli* strains (C. French and J. Ward, unpublished).

1.5.2.2 The derivation of pQR187

In this study *S. thermoviolaceus* α -amylase has been expressed using the vector pQR187. pQR187 was constructed and supplied by J. Ward (unpublished). The original cloning of the *S. thermoviolaceus* α -amylase gene [57] was carried out using *E. coli* JM107 transformed with pUC8 containing the *Bam*HI genomic library of *S. thermoviolaceus*. The one colony displaying extensive amylase activity, detected via starch hydrolysis, contained a recombinant plasmid, designated pQR300, (pUC8 containing a 5.7 kb insert). Cloning the 5.7 kb *Bam*HI fragment in the opposite orientation to the *lacZ* promoter (pQR303) resulted in amylase negative *E. coli* colonies, meaning expression of the α -amylase gene was regulated by the *lacZ* promoter rather than a native promoter. From mapping and sub-cloning experiments it was found that the coding sequence of the gene was localised to a 1.7 kb *Bam*HI-*Sph*I DNA fragment (pUC18 containing the 1.7 kb *Bam*HI-*Sph*I insert was designated pQR307) [57]. A 3.4 kbp *Hind*III/*Pst*I fragment containing the *S. thermoviolaceus* α -amylase gene was excised from pQR300 and cloned into pBGS19 to form pQR126. This particular sub-cloning step removed a 150 bp region of upstream DNA which contained the endogenous promoter. The reduced distance between the translational start site and the *lacZ* promoter allowed for a fivefold increase in production of α -amylase [59]. pBGS19 itself

is a 4.4 kbp kanamycin resistant pUC analogue which contains the multiple cloning region from pUC19 (multiple cloning site originally derived from M13mp19) [60]. pQR126 was later modified to contain a *Pst*/*Eco*RI 200 bp *cer* fragment from pKS450 (a pUC-based vector containing the *cer* region from ColE1 [61]), to increase the segregational stability of the plasmid [62], forming pQR187.

1.5.3 Glucoamylases

Glucoamylases, or amyloglucosidases (EC 3.2.1.3), hydrolyse terminal α -1,4 glycosidic links successively from the non-reducing ends of polysaccharides. This exo-acting ability predominantly generates glucose as opposed to other maltodextrins. The majority of previously characterised glucoamylases are of fungal origin, primarily from *Aspergillus niger* and *Rhizopus oryzae* [63], and are the leading type used in industry. For the most part, fungal glucoamylases are highly glycosylated, which is thought to be important for their stability [64], meaning they are often difficult to successfully express in *E. coli*. However, a notable exception includes the heavily glycosylated glucoamylase STA1 from *Saccharomyces cerevisiae* (var. *diastaticus*), which has been successfully expressed in *E. coli* previously [65]. Owing to the lack of examples in the literature, an aspect of this project involves the identification and characterisation of putative bacterial glucoamylases, to facilitate expression and secretion within a starch utilising *E. coli* chassis. One of the few examples of a bacterially derived glucoamylase which has been heterologously expressed in *E. coli* is the thermostable glucoamylase (TtcGA) from *Thermoanaerobacter tengcongensis* MB4 [66]. This was initially carried out to investigate an alternative and a possible improvement to traditional thermostable enzymes of fungal origin for industrial applications. Despite not necessarily requiring thermostability in this particular application, TtcGA has provided a basis for the identification and characterisation of other novel putative bacterial glucoamylases.

1.6 Secretion of amylolytic enzymes within *E. coli*

As previously stated, one of the draw backs of using *E. coli* as an expression system is the difficulty associated with recombinant protein secretion. Much of the rationale behind this particular project is based on previous work by C. French and J. Ward (unpublished) investigating periplasmic release as a method of protein extraction for downstream processing. The work compared periplasmic retention in a number of different K12 strains including W3110, and highlighted the ability of *E. coli* to secrete a periplasmically targeted amylolytic enzyme into the surrounding culture medium. This idea has been extended in this study to further characterise secretion via periplasmic leakage, and investigate whether this is a viable method to engineer *E. coli* to utilise starch as a carbon source and ultimately provide a basis for a self-secreting enzyme-based fed-batch fermentation system. The initial work carried out by C. French and J. Ward indicated potential differences between different *E. coli* strains in the periplasmic retention of protein (unpublished), a factor which could influence strain selection when designing a system based on periplasmic leakage. There is also the possibility that different proteins may have differing levels of retention within the periplasm, another factor which has the potential to influence the type of amylolytic enzyme used, and the subsequent ability to degrade starch extracellularly.

Regarding the targeting of amylolytic enzymes to the periplasm in the first place, *S. thermophilus* α -amylase contains a native signal sequence, but exogenous sequences have also been explored following fusion to novel bacterial glucoamylases in an attempt to improve secretion. The translocation of polypeptides across the cytoplasmic membrane into the periplasm of Gram-negative bacteria can occur by three main pathways; the sec pathway [67], the signal recognition particle (SRP) pathway [68] and the Tat pathway [69]. Both the Sec and SRP pathways use the SecYEG channel protein for translocation; however the signal peptide directing the former is recognised by the SecB protein whilst signal

peptides directing the latter are recognised by the SRP protein. The two binding proteins recruit different translocation machinery leading to unfolded post-translational translocation and co-translational translocation respectively. In contrast, the third pathway, the Tat pathway, primarily translocates fully folded proteins and uses its own distinct channel protein, TatA [70]. Two previously characterised and widely used signal peptides are investigated in this study, the DsbA signal sequence (originally derived from thiol disulfide oxidoreductase found in many bacterial species including *E. coli*) [71] [72] (SRP pathway) and the PelB signal sequence (originally derived from the pectate lyase B from *Pectobacterium carotovorum*) [73] (Sec pathway), as well as native signal peptides if present.

As a clarification, this study will refer to secretion as the targeting of amylolytic enzymes to the periplasm and their subsequent release into the extracellular media via the leakage of periplasmic contents.

1.7 Regulatory strategies for enzyme expression

The expression of an amylolytic enzyme within a self-secreting fed-batch system can be regulated in a number of different ways depending on the desired outcome. Much of the initial work carried out in this study uses the *S. thermoviolaceus* α -amylase regulated by the *lac* promoter, using Isopropyl β -D-1-thiogalactopyranoside (IPTG) as the inducer. However, within a fed-batch system it would be preferable to avoid the necessity of induction, as this requires external input and to some extent defeats the original purpose. If a constitutive promoter is used, a great deal of fine tuning would be required to determine the appropriate level of expression, and even then expression levels may not be optimal throughout the whole culture. Alternatively, if the amylolytic enzyme is negatively regulated by its own hydrolysis product, theoretically a constant concentration of glucose

within the media could be maintained throughout the culture. In this study a novel glucoamylase from *Chromobacterium violaceum* has been cloned and expressed in *E. coli* under a Cyclic Adenosine Monophosphate (cAMP) sensitive promoter. This glucose repressible promoter (*PcstA*) was derived from *E. coli* JM109 and is ordinarily involved in the regulation of carbon starvation response genes (*cstA*) which are up regulated during glucose starvation [74]. The mechanism behind this is based on the ability of cAMP to induce conformational change in the catabolite gene activator protein (CAP), enhancing its binding to CAP-dependent promoters [75], and promoting expression. In the absence of glucose, levels of intracellular cAMP are increased [76], leading to the binding of CAP to the promoter and subsequent transcription of target genes. In high glucose concentrations, intracellular cAMP is reduced, leading to a reduction in bound CAP, and a subsequent reduction in gene transcription. Based on previous work by the 2008 Edinburgh iGEM team, *PcstA* has been shown to be sensitive to glucose within the range of 0-10 mM, corresponding to 0-2 mg/mL, well within the range typically used in traditional fed-batch fermentation [77].

1.8 Overview of project

In summary, this project aims to investigate the potential use of starch as an alternative carbon source in *E. coli* fermentation, and in doing so applies a cell engineering approach to enzyme-based fed-batch fermentation. Chapter 3 highlights the ability of *E. coli* to heterologously express and secrete *S. thermoviolaceus* α -amylase, to not only degrade starch at rates not previously reported, but also to utilise as a sole carbon source. Chapter 4 includes the identification and characterisation of novel bacterial glucoamylases, the optimisation of their secretion, and the subsequent creation of an *E. coli* strain which can convert starch directly to glucose. The final Chapter focusses on developing these

amylolytic strains and applying them in a self-secreting enzyme-based fed-batch fermentation system, to enhance both biomass and recombinant protein yield in shake flasks.

2 Materials and Methods

2.1 Cell culture

2.1.1 *E. coli* strains

The *E. coli* strains used for growth and expression experiments within this study were the K12 strain W3110 (F- λ -rph-1 *Inv(rrnD-rrnE)*) [78], and the B strain BL21(DE3) [79] (F- *ompT gal dcm lon hsdS_B(r_B-m_B-)* *gal dcm (DE3)* (Novagen). HST08 (Stellar™ chemically competent, Clontech) and TOP10 (chemically competent, Thermo Fisher Scientific) were used for sub-cloning experiments.

2.1.2 Constructs

Plasmid constructs used in this study, and their descriptions are shown in table 1.

Table 1 Constructs used within current study

Plasmid	Description	Reference
pQR187	pBGS19 derivative, <i>lac</i> promoter, Kan ^r	J. Ward (unpublished)
pQR1700	Modified pQR187, <i>lac</i> promoter, Kan ^r	This study
pEX-K4-niger_Gluc	Sub-cloning vector containing <i>A. niger</i> glucoamylase, Kan ^r	Eurofins Genomics
pET29a(+)	T7 promoter, Kan ^r	Novagen
pQR1701	pET29a containing <i>A. niger</i> glucoamylase, T7 promoter, Kan ^r	This study
pQR1702	pET29a containing <i>S. diastaticus</i> glucoamylase, T7 promoter, Kan ^r	This study
pQR1703	pET29a containing <i>D. geothermalis</i> glucoamylase, T7 promoter, Kan ^r	This study
pQR1704	pET29a containing <i>T. tengcongensis</i> glucoamylase, T7 promoter, Kan ^r	This study
pQR1705	pET29a containing <i>C. violaceum</i> glucoamylase, T7 promoter, Kan ^r	This study
pET28a(+)	T7 promoter, Kan ^r	Novagen

Plasmid	Description	Reference
pQR1706	pET28a containing <i>D. geothermalis</i> glucoamylase, T7 promoter, Kan ^r	This study
pQR1707	pET28a containing <i>T. tengcongensis</i> glucoamylase, T7 promoter, Kan ^r	This study
pQR1708	pET28a containing <i>C. violaceum</i> glucoamylase, T7 promoter, Kan ^r	This study
pQR1709	pQR1703 with DsbA signal sequence, T7 promoter, Kan ^r	This study
pQR1710	pQR1703 with PelB signal sequence, T7 promoter, Kan ^r	This study
pQR1711	pQR1705 lacking native signal sequence, T7 promoter, Kan ^r	This study
pQR1712	pQR1711 with DsbA signal sequence, T7 promoter, Kan ^r	This study
BBa_K118011	pSB1C3 containing <i>PcstA</i> , Cam ^r	iGEM 2016 Distribution Kit
pQR1344	pET29a containing eGFP, T7 promoter, Kan ^r	D. Dobrijevic (unpublished)
pQR1714	BBa_K118011 containing eGFP, <i>PcstA</i> , Cam ^r	This study
pQR1715	BBa_K118011 containing <i>C. violaceum</i> glucoamylase with attached DsbA signal sequence, <i>PcstA</i> , Cam ^r	This study
pQR411	pMMB67HE containing <i>E. coli</i> TK, native TK constitutive promoter, Amp ^r	Ingram et al 2007 [80]
pUC19	<i>lac</i> promoter, Amp ^r	Yanisch-Perron et al 1985 [81]
pQR1716	pUC19 containing <i>S. thermoviolaceus</i> α -amylase, <i>lac</i> promoter, Amp ^r	This study
pQR1717	pUC19 containing eGFP, <i>lac</i> promoter, Amp ^r	This study
pQR1718	pUC19 containing <i>S. thermoviolaceus</i> α -amylase followed by eGFP, <i>lac</i> promoter, Amp ^r	This study
pQR1719	pUC19 containing eGFP followed by <i>S. thermoviolaceus</i> α -amylase, <i>lac</i> promoter, Amp ^r	This study
pQR1720	pUC19 containing eGFP followed by <i>C. violaceum</i> glucoamylase with DsbA signal sequence, <i>lac</i> promoter, Amp ^r	This study

Kan^r – Kanamycin resistance, Amp^r – Ampicillin resistance, Cam^r – Chloramphenicol resistance

2.1.3 Strain maintenance

E. coli strains and constructs were maintained and propagated using selective LB agar plates. Glycerol stocks were prepared by re-suspending a colony off a selective plate in 5 mL LB (with appropriate antibiotic) and incubating overnight at 37°C. 500 µL of culture was then added to a cryovial containing 500 µL of 50% (w/v) glycerol and stored at -80°C. Antibiotics and other supplements were used where necessary at the following concentrations: kanamycin (20 µg/mL); ampicillin (50 µg/mL); chloramphenicol (30 µg/mL); IPTG (0.4 mM); and starch (soluble potato starch, Sigma) at 7.5 mg/mL for LB agar plates.

2.1.4 Competent cell preparation

To prepare chemically competent cells, 500 µL of overnight culture of *E. coli* W3110 or BL21(DE3) was used to inoculate 50 mL LB for incubation at 37°C, 250 rpm. When the culture reached an OD₆₀₀ of 0.3-0.4, cells were harvested by centrifugation for 10 minutes at 2000 g, at 4°C. The pellet was re-suspended in 10 mL of ice-cold 100 mM MgCl₂ and then centrifuged again for 10 minutes at 2000 g, at 4°C. The pellet was re-suspended in 1.25 mL ice-cold 100 mM CaCl₂ and incubated on ice for 90 minutes. Following the 90 minute incubation, 200 µL of 50% glycerol was added to the cell suspension, which was subsequently aliquoted into vials for storage at -80°C. For transformation of newly constructed vectors high efficiency competent cells were used (Stellar™ Competent Cells, Clontech, or TOP10 Competent cells, Thermo Fisher Scientific).

2.1.5 Transformation

For pre-prepared chemically competent cells, aliquots were removed from -80°C storage and thawed on ice. Once equilibrated on ice either 4 µL of ligation or 1 µL (of 20 ng/µL) plasmid DNA was added to 50 µL of thawed cells, mixed and incubated on ice for a further

45 minutes. Cells were heat shocked at 42°C for 90 seconds, left on ice for a further two minutes, and then added to 1 mL of LB medium. This was incubated at 37°C for one hour before plating (50 – 100 µL of cell suspension evenly spread per agar plate, and incubated at 37°C for 18 hours). The transformation protocol for high efficiency competent cells varied slightly in that the DNA/thawed cells mixture was incubated on ice for 30 minutes and the heat shock was 42°C for 45 seconds, followed by addition of 450 µL of pre warmed S.O.C medium (2% tryptone, 0.5% yeast extract, 10 mM NaCl, 2.5 mM KCl, 10 mM MgCl₂, 10 mM MgSO₄, and 20 mM glucose) (Thermo Fisher Scientific).

2.2 Standard molecular biology techniques

2.2.1 Vector design, construction and confirmation

All vectors, primers and oligonucleotides were designed using SnapGene (version 1.1.3) software. Oligonucleotides were synthesised and supplied by Eurofins Genomics. For use in PCR (see section 2.2.3), lyophilised oligonucleotides were re-suspended in miliQ water and diluted to a concentration of 10 µM. For use in ligation (see section 2.2.2), equimolar concentrations of complementary oligonucleotides were mixed, heated to 98°C and allowed to cool to room temperature. Vectors were constructed using traditional restriction digestion and ligation (section 2.2.2) or by circular polymerase extension cloning (section 2.2.4). Confirmation of correct construction was carried out by restriction analysis and sequencing (Source Bioscience or Eurofins Genomics).

Table 2 Nucleotide sequences for primers and oligonucleotides used in vector construction

Primer/Oligo	Nucleotide Sequence	Vector(s) constructed
Forwardamy2.1	ACTGAAGCTTTAATGATAAGGAGGACAGCTATG GCCAGCAGAACGCTCTCGGGCGCG	pQR1700
Reverseamy2	AGCTCTGCAGTCAGCAGCTCGTCCTGCCGTTGTG CAG	
diast_Gluc forward	TGGTGCTCGAGTTAGTTCCCCGTCT	pQR1702
diast_Gluc reverse	GAAGGAGATATACATATGGTAGGCCTCAAAAAT CC	
ABF45027.fw	ATTCGACATATGAGTGACGCTTCCGC	pQR1703, pQR1706
ABF45027.rv	ATCAAGCTCGAGTCACCCGTTCTGCGCG	
Q8R917_3.Fw	ATTCGACATATGTTGAAGAGGATTGGAAT	pQR1704, pQR1707
Q8R917_3.Rv	ATCAAGCTCGAGTTATCTCTCCCCTAATACATAC	
AAQ61151.fw	ATTCGACATATGAAACACCCGTCCTG	pQR1705, pQR1708
AAQ61151.rv	ATCAAGCTCGAGTCACCAGTTCACCTGATCAT	pQR1705, pQR1708
AAQ61151.rv	ATCAAGCTCGAGTCACCAGTTCACCTGATCAT	pQR1711
AAQ61151_2.fw	ATTCGACATATGGGGGAGGCATTCCGCG	
PcstA_eGFP.Rv	TACTAGTAGCGGCCGCTGCAGTTACTTGTACAGC TCGTC	pQR1714
PcstA_rbsGFP.fw	GCCGCTTCTAGAAGGAGTAAATAATGGTGAGCA AGGGC	
K118011-CVprimer2-Dsb	TTCCCCTCTAGAAGGAGTAAATAA	pQR1715
K118011_CV1.rv	ATCAAGGATCCTCACCAGTTCACCTGAT	
K118011Bamh1.fw	CATGATGGATCCTCCGGCAAAAAGGGC	
K118011Bamh1.rv	GGCCGCTACTAGTATGTC	
AmyCPEC1.fw	GGCCAGTGAATTCTCAGCAGCTCGTCCT	pQR1716
AmyCPEC1.rv	CACACAGGAAACAGCTATGGCCAGCAGAACG	
pUC19CPEC1.fw	CGTTCTGCTGGCCATAGCTGTTTCCTGTGTG	
pUC19CPEC1.rv	AGGACGAGCTGCTGAGAATTCACCTGGCC	
CPEC2_GFP.fw	ACGGCCAGTGAATTCTTACTTGTACAGCTCG	pQR1717
CPEC2_GFP.rv	ACACAGGAAACAGCTATGGTGAGCAAGGG	
CPEC2_pUC19.fw	CCCTTGCTCACCATAGCTGTTTCCTGTGT	
CPEC2_pUC19.rv	CGAGCTGTACAAGTAAGAATTCACCTGGCCGT	
AmyCPEC1.rv	CACACAGGAAACAGCTATGGCCAGCAGAACG	pQR1718
CPEC2_GFP.fw	ACGGCCAGTGAATTCTTACTTGTACAGCTCG	
CPEC2_pUC19.rv	CGAGCTGTACAAGTAAGAATTCACCTGGCCGT	

Primer/Oligo	Nucleotide Sequence	Vector(s) constructed
CPEC7_Amy.fw	CTTGCTCACCATTATTTACTCCTTCAGCAGCTCG	pQR1718
CPEC7_GFP.rv	CGAGCTGCTGAAGGAGTAAATAATGGTGAGCAA G	
pUC19CPEC1.fw	CGTTCTGCTGGCCATAGCTGTTTCCTGTGTG	
CPEC8_Amy.fw	ACGGCCAGTGAATTCTCAGCAGCTC	pQR1719
CPEC8_Amy.rv	GCTGTACAAGTAAAGGAGTAAATAATGGCCAGC AGA	
CPEC8_GFP.fw	TCTGCTGGCCATTATTTACTCCTTTACTTGTACAG C	
CPEC8_GFP.rv	CACACAGGAAACAGCTATGGTGAGCAAGG	
CPEC8_pUC19.fw	CCTTGCTCACCATAGCTGTTTCCTGTGTG	
CPEC8_pUC19.rv	GAGCTGCTGAGAATTCAGTGGCCGT	
CPEC8_GFP.rv	CACACAGGAAACAGCTATGGTGAGCAAGG	pQR1720
CPEC8_pUC19.fw	CCTTGCTCACCATAGCTGTTTCCTGTGTG	
CPEC9_CVprimer2Dsb.fw	ACGGCCAGTGAATTCTCACCAGTTCAC	
CPEC9_CVprimer2Dsb.rv	GCTGTACAAGTAAAGGAGTAAATAATGAAAAA ATTTGGCTG	
CPEC9_GFP.fw	CAGCCAAATTTTTTTCATTATTTACTCCTTTACTTG TACAGC	
CPEC9_pUC19.rv	GTGAACTGGTGAGAATTCAGTGGCCGT	
DsbAss forward	CTAGAAGGAGTAAATAATGAAAAAATTTGGCT GGCGCTGGCGGGCCTGGTGCTGGCGTTTAGCGC GAGCGCGCA	pQR1709, pQR1712
DsbAss reverse	TATGCGCGCTCGCGCTAAACGCCAGCACCAGGC CCGCCAGCGCCAGCCAAATTTTTTTCATTATTTAC TCCTT	
PelBss forward	CTAGAAGGAGTAAATAATGAAATATCTGCTGCC GACCGCGGCGGGCCTGCTGCTGCTGGCGG CGCAGCCGGCGATGGCGCA	pQR1710
PelBss reverse	TATGCGCCATCGCCGGCTGCGCCGCCAGCAGCA GCAGGCCCCGCCCGCGGTCGGCAGCAGATATT TCATTATTTACTCCTT	

2.2.2 Restriction digestion and ligation

Restriction enzymes were obtained from New England Biolabs. For a typical digest with a total volume of 25 μL , 5 units of restriction enzyme was used to digest up to 0.5 μg of DNA, along with 2.5 μL of associated 10X NEBuffer. Reactions were carried out at 37°C for 1-3 hours. For further use of DNA in ligation reactions restriction enzymes were heat inactivated by incubation at 70°C for 10 minutes. Ligation reactions were carried out overnight at room temperature using T4 DNA ligase (New England Biolabs). A typical ligation reaction with a total volume of 20 μL contained 1 μL T4 DNA ligase, 2 μL 10X T4 DNA ligase buffer and 50 ng of vector DNA, with insert amount calculated using a 1:3 vector to insert molar ratio (NEBcalculator).

2.2.3 Polymerase chain reaction (PCR)

PCR reactions used Phusion® High-Fidelity PCR master mix with HF Buffer (New England Biolabs). Typical PCR reactions with a total volume of 20 μL contained 10 μL of 2X Phusion Master Mix, 1 μL of each primer (10 μM) and less than 10 ng of template (plasmid) DNA (or up to 250 ng of genomic DNA). Thermo-cycling conditions included an initial denaturation period of 30 seconds at 98°C, followed by 25 cycles of denaturation (98°C for 15 seconds), annealing (45-72°C, or approximately 2°C below the lowest primer T_m , for 30 seconds), and extension (72°C for 30 seconds per 1000 base pairs), with a final extension of 72°C for 8 minutes. PCR products were confirmed using agarose gel electrophoresis and purified using gel extraction (see sections 2.2.5 and 2.2.6).

2.2.4 Circular polymerase extension cloning (CPEC)

For plasmids constructed using CPEC (Fig 2.1), vectors and inserts were amplified by Phusion® High-Fidelity PCR master mix with HF Buffer (New England Biolabs) (using the

same conditions as described in section 2.2.3). CPEC reactions were carried out in total volumes of 50 μL containing 25 μL Phusion[®] High-Fidelity PCR master mix with HF Buffer, purified vector (200 ng) combined with purified insert at a 1:1 molar ratio. The thermocycling conditions for CPEC reactions used an initial denaturation period of 30 seconds at 98°C, followed by cycles of denaturation (98°C for 15 seconds), annealing (55°C for 30 seconds), and extension (72°C for 25 seconds per 1000 base pairs) and a final extension of 72°C for 5 minutes. One cycle was performed for single insert CPEC, but for multiple inserts this was increased to 20 cycles. CPEC reaction product was used directly for transformation (4 μL CPEC product in 50 μL competent cells). Figure 2.1 is a schematic diagram showing the cloning of a single insert using CPEC. Primers used for insert and vector amplification are designed to overlap both the insert and vector, allowing the resultant PCR products to act as a template for each other in the final CPEC reaction.

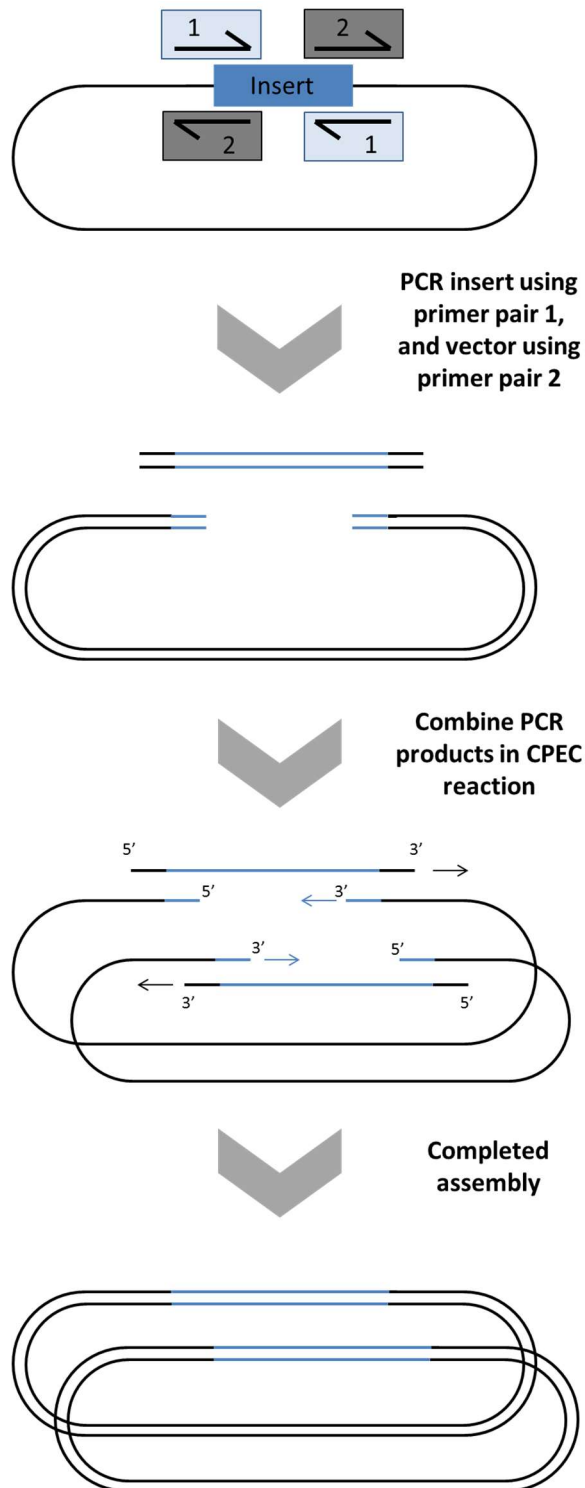


Figure 2.1 Schematic diagram of circular polymerase extension cloning for single insertion
 Construct designed *in silico* with a primer pair at each intersection between vector and insert. Primer pair 1 and primer pair 2 used to amplify insert and vector respectively in separate PCR reactions using appropriate templates. Gel extracted and purified PCR products combined for CPEC reaction in which they act as templates for each other. Final constructs can be transformed into chemically competent cells for propagation.

2.2.5 Agarose gel electrophoresis

DNA fragments were separated using agarose gel electrophoresis, carried out with 1% (w/v) agarose (Sigma) dissolved in Tris-Borate-EDTA (TBE) (89 mM Tris-Borate, 2 mM EDTA) plus a 1 in 10,000 dilution of SYBR safe (Invitrogen). Gels were submerged in TBE running buffer within a horizontal electrophoresis tank (Thermo Fisher Scientific) and subjected to 100-120 volts for 45-90 minutes. DNA samples were prepared with 6X loading dye (Thermo Fisher Scientific), and HyperLadder 1kb (Bioline) was used as the DNA marker.

2.2.6 Gel extraction

DNA fragments were extracted from agarose gels and purified using a QIAquick Gel Extraction Kit (Qiagen), following the protocol provided.

2.2.7 Plasmid isolation and purification

Plasmids were isolated from single colonies and propagated in LB media (containing appropriate antibiotic). Plasmid DNA was then purified using a QIAprep Miniprep Kit (Qiagen) following the standard protocol.

2.2.8 Chromosomal DNA preparation

The genomic DNA from a number of microbial species was used for cloning within this study, some of which required preparation before being used as a PCR template.

2.2.8.1 *Saccharomyces diastaticus* genomic DNA preparation

Saccharomyces diastaticus was supplied as a slant by the University of Reading, and was subsequently re-streaked onto YPD agar plates and incubated at 30°C for 48 hours. A colony was then suspended in 20 µL of 0.25% (v/v) SDS, vortexed and centrifuged at 17000 g for 5 minutes. The supernatant was diluted 1 in 50 for use in PCR.

2.2.8.2 *Thermoanaerobacter tengcongensis* genomic DNA preparation

Thermoanaerobacter tengcongensis was supplied lyophilised by The Leibniz Institute DSMZ (DSM number 15242 *Caldanaerobacter subterraneus* subsp. *tengcongensis*), and was re-suspended in 1 mL of 20% (w/v) glycerol. This stock was diluted 1 in 10 with sterile water. Lysozyme was added to this dilution to give a final concentration of 50 µg/mL and the mixture was incubated at 37°C for 15 minutes. SDS was then added to give a final concentration of 1% (v/v), turning the mixture clear and viscous. 250 µL of this solution was combined with a vortexed mixture of P2 (250 µL) and N3 (350 µL) reagents (QIAprep Miniprep Kit, Qiagen) and centrifuged for 10 minutes at 17000 g. The supernatant was loaded onto a spin column (QIAprep Miniprep Kit, Qiagen) with the standard miniprep protocol followed from this point onwards. The genomic DNA was eluted with 100 µL EB buffer, and used directly for PCR.

2.2.8.3 *Chromobacterium violaceum* genomic DNA preparation

Chromobacterium violaceum was supplied by J. Ward as a glycerol stock, from which 250 µL was processed as above (section 2.2.8.2).

2.2.8.4 *Deinococcus geothermalis* genomic DNA preparation

Deinococcus geothermalis was supplied by J. Ward as a glycerol stock and prepared into genomic DNA suitable for PCR by M. Bawn.

2.3 Growth media preparation

2.3.1 Luria broth (LB) media

Miller's LB Broth (Sigma Aldrich), containing 10 g/L Tryptone, 10 g/L NaCl and 5 g/L yeast extract, was prepared by dissolving 25 g in 1 L of water. The media was autoclaved at 121°C for 15 minutes.

2.3.2 Terrific broth (TB) media

Terrific broth (Sigma Aldrich), containing 12 g/L Tryptone, 24 g/L yeast extract, 9.4 g/L K_2HPO_4 , and 2.2 g/L KH_2PO_4 , was prepared by dissolving 47.6 g plus an additional 8 mL of glycerol into 1 L of water, and was autoclaved at 121°C for 15 minutes.

2.3.3 Glucose free mineral salt medium (MSM)

Glucose free mineral salt medium (MSM) was adapted from Krause *et al* 2010 [82] and was prepared by dissolving (per L of water) 2.0 g Na_2SO_4 , 6.12 g $(NH_4)_2SO_4$, 0.50 g NH_4Cl , 14.60 g K_2HPO_4 , 3.60 g $NaH_2PO_4 \cdot H_2O$, 1.00 g $(NH_4)_2$ -H-citrate, 3 mM $MgSO_4$, 0.1 g thiamine hydrochloride, and 2 mL of SM6 trace element solution (composed of 104 g/L Citric acid, 5.22 g/L $CaCl_2 \cdot 2H_2O$, 2.06 g/L $ZnSO_4 \cdot 7H_2O$, 2.72 g/L $MnSO_4 \cdot 4H_2O$, 0.81 g/L $CuSO_4 \cdot 5H_2O$, 0.42 g/L $CoSO_4 \cdot 7H_2O$, 10.06 g/L $FeCl_3 \cdot 6H_2O$, 0.03 g/L H_3BO_3 , 0.02 g/L $Na_2MoO_4 \cdot 2H_2O$). The solution was filter sterilised using 0.22 μm Millipore Express™ PLUS stericup® with a vacuum pump. MSM was prepared in three formats, either glucose free MSM (see section 2.3.4), MSM supplemented with 2.5 mg/mL glucose (Sigma), or MSM supplemented with 2.5 mg/mL starch (soluble potato starch, Sigma). To assist with dissolving starch the latter required pre-autoclaved water containing enough starch for a final concentration of 2.5 mg/mL prior to addition of the other constituents and filter sterilisation.

2.3.4 Starch-agar layer preparation

Starch-agar layers were prepared within 500 mL baffled shake flasks, and were used in conjunction with glucose free MSM media. Firstly, a 50 mL solution of 50 mg/mL starch and 2 mg/mL agar was added to the flask and autoclaved at 121°C for 15 minutes. Once cooled, 50 mL of pre-autoclaved 50 mg/mL agar was poured on top of the original layer and allowed to cool. Finally, 50 mL of glucose free MSM was added to the flask as the liquid media, which is displaced by the solid starch-agar layers and remains predominantly above the layers within the flask.

2.4 Growth and expression protocols

2.4.1 Overnight cultures

All growth and expression studies were inoculated with either a 1 in 20 dilution from an overnight culture, or inoculated to an initial OD₆₀₀ of 0.1 or 0.25. Overnight cultures were generally 5 mL LB in a 50 mL falcon tube (containing appropriate antibiotic) seeded from a glycerol stock, and grown at 37°C at 250 rpm.

2.4.2 Shake flasks

Shake flask cultures generally followed a standard protocol with the exception of the EnPresso® growth system (see section 2.4.4). For growth and expression experiments, unless otherwise stated, 500 mL baffled conical shake flasks were used, containing 50 mL of selected media. In addition to media an antibiotic, if needed, was supplied at the following concentrations: kanamycin (20 µg/mL); ampicillin (50 µg/mL); chloramphenicol (30 µg/mL). For induction of all inducible promoters used in this study, 0.4 mM IPTG was added when the culture had reached an OD₆₀₀ of 0.6-0.8, or at inoculation, for growth experiments

involving amylolytic strains. Shake flask cultures were carried out at varying temperatures and durations depending on the nature of the experiment (see individual experiment for detail), but all were performed in a standard orbital incubated shaker (innova™ 4330, New Brunswick Scientific) at either 250 or 180 rpm.

2.4.3 Automated experiments (microwell plates)

Automation experiments used a Tecan Evo150 platform with integrated Eppendorf Thermomixer, Tecan Infinite M200 Pro plate reader and Hettich centrifuge. Set up required polypropylene 96-deep square well (96-DSW) culture plates, 96-standard round well (96-SRW) plates, reagent troughs and disposable microconductive tips. A sterile environment was maintained by a Walker class 2 biosafety cabinet equipped with laminar flow and HEPA filtration system. Liquid handling steps were devised by F. Truscott, and implemented using Freedom EVOware® software. All experiments used a total culture volume of 800 µL per well (96-DSW), agitation at 800 rpm, and a temperature of 37°C over a period of 8 or 24 hours depending on the experiment. Cell density was measured in 96-SRW plates using OD₆₀₀, and, when required, GFP fluorescence intensity was measured using an excitation wavelength of 483 nm and an emission wavelength of 535 nm (Tecan Infinite M200 Pro).

2.4.4 EnPresso® Growth System

For shake flask growth using the EnPresso® growth system, the standard protocol developed by BioSilta was followed, with some alterations applied specifically to amylolytic strains. A pre-culture was grown from a glycerol stock (or a single colony from an agar plate) in 2 mL LB containing an appropriate antibiotic (see section 2.4.2 for concentrations) for 6-8 hours at 37°C, 250 rpm. This culture was then used as inoculum (a 1 in 25 dilution) and added to 50 mL sterile water in a 500 mL shake flask containing one white bag (of two

tablets composed of minerals, vitamins, trace elements, inorganic and organic nitrogen for pH control, and a polysaccharide substrate), the required antibiotic, and 25 μ L of reagent A (containing amyloglucosidase) (for amyolytic strains reagent A was replaced with 0.4 mM IPTG). Cultures were incubated overnight for 15-18 hours at 30°C, 250 rpm. Further nutrients were added to the culture in the form of a booster tablet (composed of nutrients and polysaccharide substrate), along with IPTG for induction and a further 25 μ L of reagent A (neither of which were added to flasks containing amyolytic strains). Cultures were incubated for an additional 24 hours at 30°C, 250 rpm before harvest. For the amyolytic strains the first culture period was at 37°C rather than 30°C and the second culture period following the addition of the booster tablet was 25°C rather than 30°C, in order to optimise the cell densities achieved.

2.5 Protein expression studies

2.5.1 Sodium dodecyl sulphate polyacrylamide gel electrophoresis (SDS-PAGE)

The expression of heterologously expressed protein was analysed using SDS-PAGE. Either whole cell lysate or clarified lysate samples (see section 2.5.5) were mixed with NuPAGE® LDS sample buffer (4X) and incubated at 70°C for 10 minutes. They were subsequently centrifuged at 17000 g for 5 minutes and loaded onto NuPAGE® Bis-Tris Mini Gels (Novex) and run using 20X MOPS buffer (ThermoFisher Scientific) (50 mM MOPS, 50 mM Tris Base, 0.1% SDS, 1 mM EDTA, pH 7.7) at 200 volts for 50 minutes. Gels were stained with InstantBlue™ (Sigma Aldrich) for 1 hour and de-stained with water for 12-24 hours on a rocker.

2.5.2 Amylase assay

Amylase activity was determined by measuring the rate of degradation of starch-iodine complex, a method adjusted from Blanchin-Roland and Masson [83]. An appropriate dilution of sample from either the periplasmic or extracellular fraction was made up to 0.5 mL with 15 mM sodium phosphate buffer (pH5.8). Unless otherwise stated this was 50 μ L of sample in 450 μ L sodium phosphate buffer. This dilution was then incubated to an assay temperature of 50°C for *S. thermoviolaceus* α -amylase, or 37°C for the glucoamylase enzymes. The reaction was initiated by the addition of 0.5 mL starch solution (5 mg/mL) made up in 15mM sodium phosphate buffer (pH5.8). Subsequent 50 μ L samples were then taken at numerous time points and added to 1 mL of potassium iodide/iodine solution (freshly prepared by adding 200 μ L 2.2%I₂/4.4%KI (w/v) into 100mL of 2% (w/v) KI solution) with the corresponding decrease in absorbance at 600 nm measured. Unless otherwise stated one unit of enzyme activity for *S. thermoviolaceus* α -amylase is defined as the disappearance of 1 mg/mL of starch/iodine complex per minute at 50°C, and one unit of enzyme activity for the glucoamylase enzymes is defined as the disappearance of 1 mg/mL of starch-iodine complex per minute at 37°C.

2.5.3 Determination of extracellular amylolytic enzyme activity

For the determination of secreted amylolytic enzyme within the extracellular media, 1 mL of culture was centrifuged at 17000 g for 5 minutes with the resultant supernatant collected as the extracellular media fraction. To quantify activity from this fraction, samples were directly added to the amylase assay (section 2.5.2).

2.5.4 Periplasmic release procedure

The following procedure was used for analytical scale periplasmic release. 1 mL of culture was centrifuged at 17000 g for 5 minutes. The resultant pellet was re-suspended in 200 μ L of extraction buffer (20% (w/v) sucrose, 1 mM Na₂EDTA, 200 mM Tris.HCL, 500 μ g/mL lysozyme (Sigma)) and incubated at room temperature for 15 minutes. 200 μ L of distilled water was then added and the mixture was incubated for a further 15 minutes before being centrifuged at 17000 g for 10 minutes. The supernatant was collected as the periplasmic fraction, with activity determined via direct addition to the amylase assay (section 2.5.2).

2.5.5 Whole cell and clarified lysate preparation

In expression studies and some activity assays, whole cell lysates and clarified cell lysates were measured. Samples (1 mL) of culture were centrifuged at 17000 g for 5 minutes. The resultant pellet was re-suspended in 300 μ L phosphate buffered saline (PBS) (pH7.4) and sonicated (3 cycles of 20 seconds on, 20 seconds off with an amplitude of 10 microns, MSE Soniprep 150). The ensuing whole cell fraction was further centrifuged at 17000 g for 5 minutes and the supernatant collected as the clarified lysate.

2.5.6 Starch degradation assay

Starch degradation within culture media was determined using an adaptation of the amylase assay, whereby a 50 μ L sample of clarified culture media was added directly to 1 mL of potassium iodide/iodine solution (freshly prepared by adding 200 μ L 2.2%I₂/4.4%KI (w/v) into 100mL of 2% (w/v) KI solution). The absorbance was measured against a potassium iodide/iodine solution blank at 600 nm, with a standard curve prepared to determine concentration. For concentrations of starch beyond the linear range of the

spectrophotometer the sample of clarified culture media was diluted appropriately and added to the potassium iodide/iodine solution in the same ratio.

2.5.7 Glucose (GO) assay

The Glucose (GO) assay kit (supplied by Sigma) was used as per the technical bulletin provided. Samples were diluted with deionised water to between 20 and 80 µg glucose per mL. Reactions were initiated following the addition of 2 mL of glucose oxidase/oxidase reagent to 1 mL of sample, and incubated at 37°C for 30 minutes. The reaction was quenched by the addition of 2mL of 12 N H₂SO₄, and the subsequent absorbance was measured against a reagent blank at 540 nm. Glucose concentration was determined using a standard curve.

2.5.8 Fluorescence measurements

Fluorescence intensity of eGFP from samples of neat cell culture dispensed in either 24 or 96 microwell plates, were measured using excitation and emission wavelengths of 483 nm and 535 nm respectively (Tecan Infinite M200 Pro). Gain was optimised for each experiment conducted. Fluorescence units were displayed either irrespective of cell density, or were normalised to OD₆₀₀ depending on the specific experiment conducted.

2.5.9 Ortho-nitrophenyl-β-D-galactopyranoside (ONPG) β-galactosidase assay

Ortho-nitrophenyl-β-D-galactopyranoside (ONPG) is a colorimetric substrate for β-galactosidase, allowing for the determination of β-galactosidase activity and subsequent inference of catabolite repression. Assays took place in a 96 microwell plate and involved the addition of 150 µL of substrate solution (3 mM ONPG, 10 mM MgCl₂, and 0.1 mM 2-mercaptoethanol in PBS) to 200 µL of sample clarified lysate. The mixture was incubated at

30°C for 30 minutes and then quenched with 5 µL of 1 M sodium carbonate. Absorbance was measured at 410 nm (Tecan Infinite M200 Pro), indicative of the amount of ONPG hydrolysis product ortho-nitrophenol present in the sample lysate. Units of β-galactosidase activity were defined as change in absorbance at 410 nm per minute, and were normalised to OD₆₀₀.

2.5.10 High performance anion exchange chromatography with pulsed amperometric detection (HPAEC-PAD) analysis

HPAEC-PAD analysis was used to detect and quantitate mono- and small chain oligo-saccharides resulting from the amylolytic hydrolysis of starch. Detection was carried out by injecting 25 µL samples into a Reagent-Free Ion Chromatography System (ICS 5000+, Dionex) equipped with a Dionex CarboPac™ PA100 anion exchange column (2 x 250 mm) fitted with a Dionex CarboPac™ PA100 guard column (2 x 50 mm), and an electrochemical detector system. Elution was carried out using a linear gradient of 100 mM NaOH at 0 minutes, to 60 mM NaOH and 400 mM NaOAc at 18 minutes, followed by a step of 40 mM NaOH and 600 mM NaOAc for a further 2 minutes. The column was re-equilibrated for 5 minutes with 100 mM NaOH. The flow rate remained at 0.25 mL min⁻¹ with a system pressure of approximately 2500 psi. Data collection and analysis was performed with Chromeleon software version 7.

3 Starch as an alternative carbon source in *E. coli* fermentation

3.1 Introduction

Starch has the potential to offer a number of advantages over more traditionally used carbon sources in *E. coli* fermentations. Firstly from a sustainability perspective starch represents a huge source of biomass, much of which constitutes agricultural waste streams, for example potato pulp from the potato industry. Given the increasing importance of developing a renewable and sustainable biomass-based economy, the direct utilisation of starch by *E. coli* presents an opportunity to convert this source of naturally occurring biomass into useful products, possibly reducing the reliance on petroleum derived hydrocarbons. In fact in a recent study by Rosales-Colunga *et al*, an *E. coli* K12 strain was engineered to express and secrete an α -amylase, a first step towards developing a microbial platform capable of using agro-industrial wastes to produce valuable compounds [56].

Starch may also serve a more general purpose by providing a means to tackle one of the root causes of overflow metabolism in batch fermentations. As a polysaccharide starch is understood to be metabolically inert to *E. coli*, and as such could conceivably be present in media without effecting growth or expression. If an *E. coli* strain engineered to degrade starch into utilisable carbon were to grow in such media, the strain would be able to self-feed and depending on the rate of hydrolysis, mimic fed-batch fermentations which commonly use glucose as the feed carbon source. Furthermore, it is widely known that glucose leads to catabolite repression, affecting a number of commonly used promoters for expression e.g. the *lac* promoter. With carbon present in the form of starch rather than

glucose, this has the potential to alleviate catabolite repression and give an experimenter more options when designing expression systems.

This Chapter will explore some of the properties and characteristics of using starch as a source of carbon for *E. coli*, and describes an α -amylase producing strain originally constructed at University College London, highlighting its increased capability of degrading starch compared to current strains in the literature, as well as its ability to grow using starch as a sole carbon source.

3.2 Investigating catabolite repression in the presence of starch

Using the ortho-nitrophenyl- β -D-galactopyranoside (ONPG) assay described in the materials and methods (section 2.5.9), the properties of starch as a potential catabolite repressor were investigated. Results from an initial single experimental run demonstrated that when *E. coli* W3110 was grown in LB containing 10 mg/mL starch combined with 10 mg/mL lactose, β -galactosidase was expressed; whereas when W3110 was grown in LB containing 10 mg/mL glucose combined with 10 mg/mL lactose, β -galactosidase was not expressed (Fig 3.1a). It is widely known from literature that glucose represses the *lac* operon, significantly impacting an experimenter's choice of promoter when designing an expression system in traditional media. This result suggests that catabolite repression is not exerted when starch, unlike glucose, is present in the media, and as such could allow for a more flexible approach in terms of promoter use within expression systems.

The data also show a clear increase in the optical density obtained from the starch containing culture compared with the glucose containing culture (Fig 3.1b). This has been explored further in Fig 3.10.

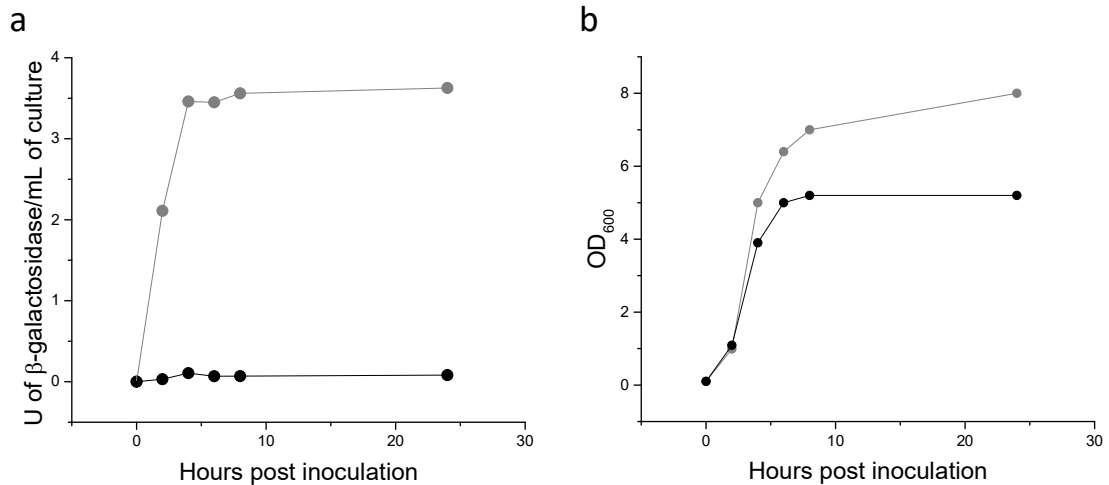


Figure 3.1 Catabolite repression of soluble potato starch in comparison to glucose.

Single experimental run for *E. coli* W3110 cultured in LB containing 10 mg/mL lactose for 24 hours at 37°C, 250 rpm, supplemented with 10 mg/mL starch (grey) or 10 mg/mL glucose (black). a) Accumulation of ONPG hydrolysis product ortho-nitrophenol measured using absorbance at 410 nm (Tecan infinite 200 pro) and expressed as units of β -galactosidase activity (defined as change in absorbance at 410 nm per minute, normalised to OD₆₀₀). b) Growth curves for each condition throughout the culture period.

3.3 Utilisation of starch by *E. coli* via heterologous expression and secretion of an α -amylase from *Streptomyces thermoviolaceus*

In order to utilise starch as a carbon source *E. coli* must first be engineered to hydrolyse it. Unpublished work carried out by C. French and J. Ward used an α -amylase from *Streptomyces thermoviolaceus* CUB74 [57] to investigate periplasmic leakage into the media by different K12 strains of *E. coli*. The enzyme itself is particularly active and trivial to assay, and was therefore a useful tool in determining relative enzyme concentration both inside and outside the periplasm. Periplasmic leakage of *S. thermoviolaceus* α -amylase has as a result been used as a basis for this current study, with amylolytic activity in the media being used to hydrolyse starch into a utilisable carbon source to sustain *E. coli* growth.

3.3.1 Expression of *S. thermoviolaceus* α -amylase

The *S. thermoviolaceus* α -amylase has been expressed using the vector pQR187 (section 1.5.2.2). Fig 3.2a shows a schematic diagram of the multiple cloning site of pQR187 containing the 1383 bp *S. thermoviolaceus* α -amylase gene alongside the *lac* promoter (65 bp upstream of the gene) and the *cer* stability fragment (1955 bp downstream of the gene). The 65 bp and 1955 bp sections flanking the gene are untranslated regions of genomic DNA which fell between the restriction sites (*Hind*III and *Pst*I) used for the original cloning. When induced with 0.4 mM IPTG, colonies of *E. coli* W3110 harbouring pQR187 under the selection of 20 μ g/mL kanamycin expressed and secreted α -amylase into the surrounding agar (Fig 3.2b). The agar contained 7.5 mg/mL soluble potato starch and was stained blue/purple with potassium iodide/iodine solution, with visible halos around each colony indicating starch hydrolysis.

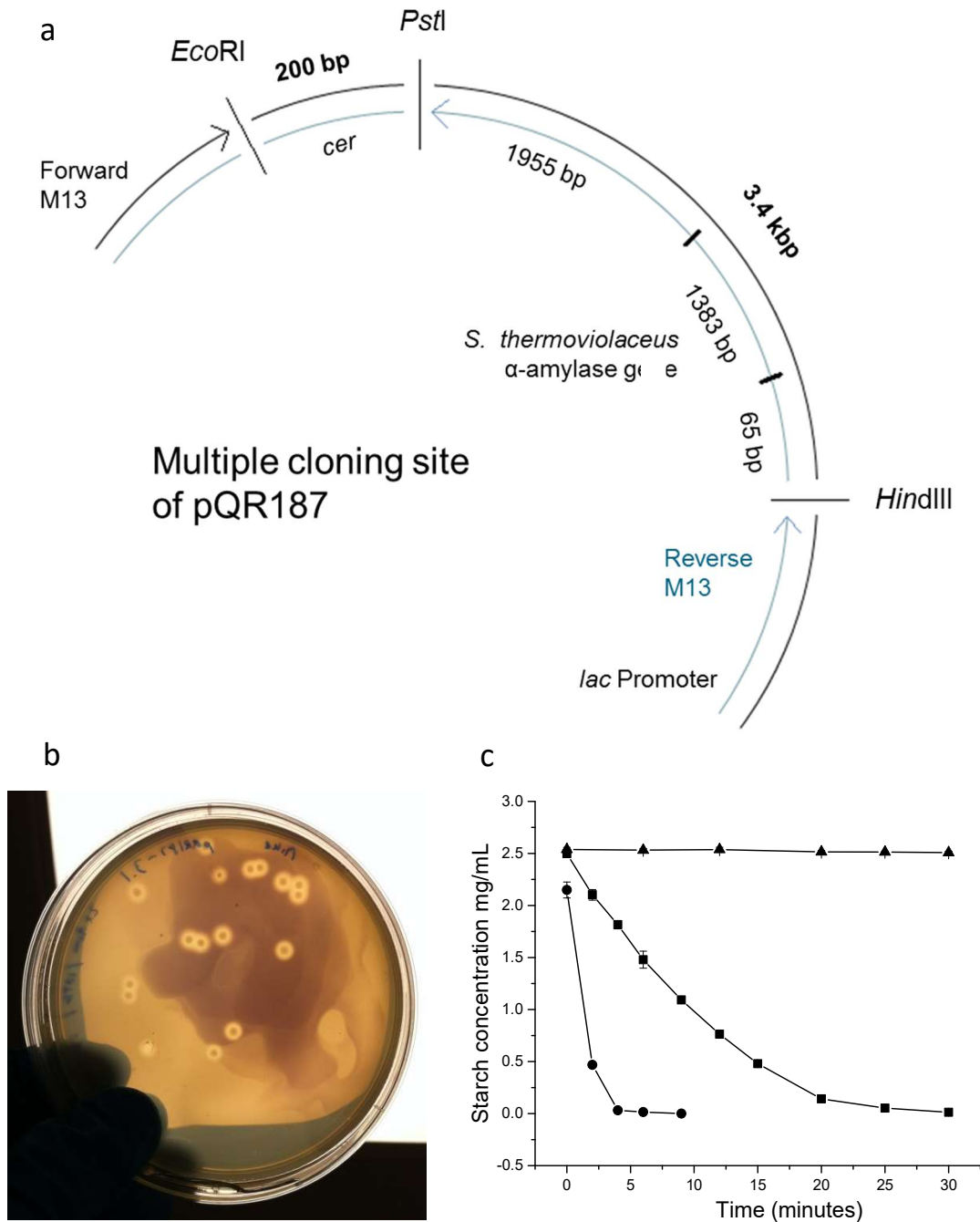


Figure 3.2 pQR187 expression and the quantification of α -amylase activity

a) Schematic diagram of pQR187 containing the *S. thermoviolaceus* derived α -amylase gene fragment (1383 bp) including untranslated regions upstream (65 bp) and downstream (1955 bp) of the gene, as well as the *cer* stability fragment (200 bp). b) *E. coli* W3110 harbouring pQR187 cultured on LB-agar containing 7.5 mg/mL starch, 0.4 mM IPTG and 20 μ g/mL kanamycin following incubation at 37°C for 24 hours and subsequent addition of potassium iodide/iodine solution (see materials and methods). c) Amylase assay of the periplasmic fraction (circle) and extracellular media fraction (square) of W3110 harbouring pQR187 (induced with 0.4 mM IPTG at an OD_{600} of 0.6-0.8) cultured at 37°C, 250 rpm for 24 hours, alongside amylase assay buffer (15 mM sodium phosphate buffer (pH5.8)) containing 2.5 mg/mL starch serving as a negative control (triangle). Error bars represent standard deviation, n=3.

3.3.2 Quantification and the subcellular localisation of α -amylase expressed from pQR187

To quantify α -amylase activity an assay measuring the rate of decrease of a coloured starch/iodine complex originally developed by Blanchin-Roland and Masson (1989) [83], and modified by C. French and J. Ward [59, 84], was refined in this study (section 2.5.2) to measure the subcellular localisation of α -amylase. *E. coli* W3110 harbouring pQR187 cultured over 24 hours (induced with 0.4 mM IPTG at an OD₆₀₀ of 0.6-0.8) was processed in triplicate to obtain periplasmic and extracellular fractions to demonstrate the robustness of the assay (Fig 3.2c). Both periplasmic and extracellular fractions showed a degradation of starch within the assay over time, as opposed to the 2.5 mg/mL starch only control. It is worth noting that due to the assay conditions the periplasmic fraction appeared to have a greater activity than the extracellular fraction; however this is a misrepresentation as the periplasmic fraction was concentrated approximately three fold due to the nature of the periplasmic extraction process (section 2.5.4). Figures 3.3a and 3.3b show the normalised activity of each fraction expressed as units per mL of culture volume (defined as the disappearance of 1 mg/mL of starch/iodine complex per minute at an assay temperature of 50°C).

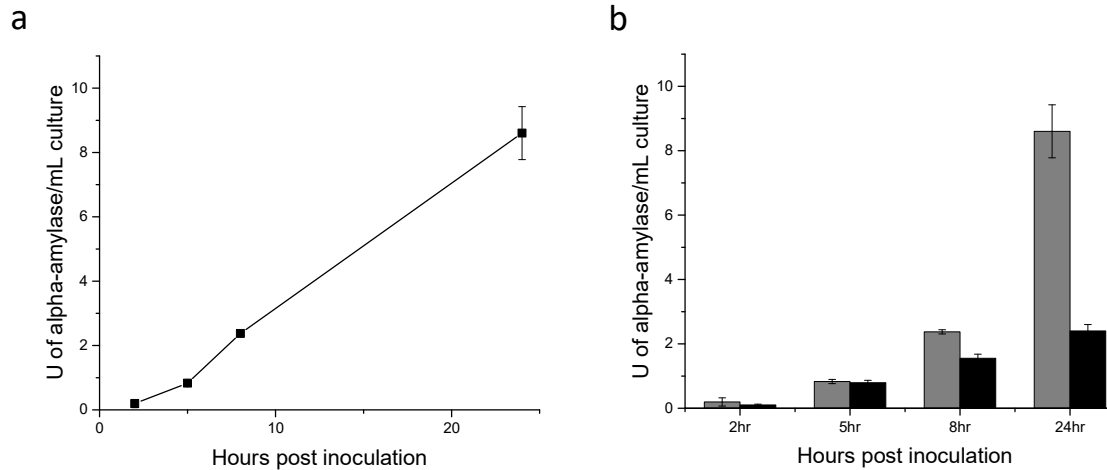


Figure 3.3 *S. thermoviolaceus* α-amylase activity in periplasmic and extracellular fractions over time

E. coli W3110 harbouring pQR187 induced with 0.4 mM IPTG at inoculation and cultured at 37°C, 250 rpm for 24 hours. a) α-amylase activity in the extracellular media throughout the culture period, expressed as units of α-amylase per mL of culture. b) α-amylase activity in the extracellular media (grey) compared with α-amylase activity in the periplasmic fraction (black) throughout the culture period, expressed as units of α-amylase activity per mL of culture. Error bars represent standard deviation, n=3.

As expected the extracellular activity of α-amylase (i.e. secreted α-amylase mediated via the leakage of periplasmic contents) increased throughout the time course of the culture (Fig 3.3a). The same is true, but to a lesser extent, for periplasmic activity (Fig 3.3b). As a result there was an increasing divide between amylase secreted into the media and amylase remaining in the periplasm throughout the culture. One possible explanation for this is that the periplasmic space has a certain capacity and once that capacity has been reached, leakage becomes more apparent. For the purposes of this project though it is the increase in extracellular amylase activity which has the potential to be useful, particularly from the perspective of developing a self-feeding strategy; as cell mass increases, more amyolytic activity in the media is required for an increased release of utilisable carbon, which is itself in turn required to sustain cell growth.

3.3.3 Effects of temperature on the relative activity of *S. thermoviolaceus* α -amylase

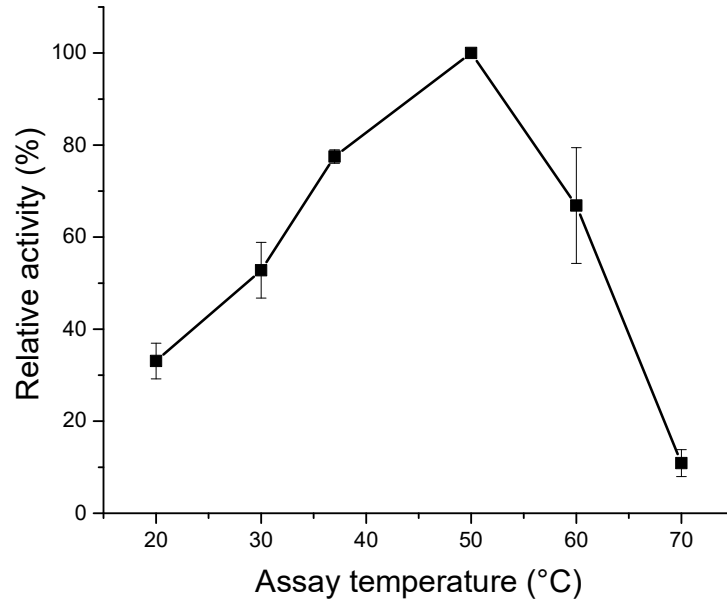


Figure 3.4 Relative enzyme activity of *S. thermoviolaceus* α -amylase over a range of temperatures

S. thermoviolaceus α -amylase activity in the extracellular media for 24 hour cultures of *E. coli* W3110 harbouring pQR187 in LB (induced with 0.4 mM IPTG at an OD₆₀₀ of 0.6-0.8), determined using amylase assays carried out at a range of temperatures (20°C to 70°C). Activity expressed as a percentage of the standard assay carried out at 50°C. Error bars represent standard deviation, n=3.

As an enzyme derived from a thermophilic organism, the *S. thermoviolaceus* α -amylase is known to be active at high temperatures [57, 85]; in fact the idea behind its original cloning was to find amylases which were active at high temperatures for potential use in the starch industry. The assay used to determine activity in previous Figures was carried out at 50°C, largely to reduce the possibility of background activity from endogenous amylases, as these would be denatured at this temperature. However, for a true comparison with previously engineered amylolytic strains of *E. coli*, the activity of the enzyme at traditional culture temperatures was investigated. Fig 3.4 shows extracellular α -amylase activity relative to

50°C for temperatures ranging from 20°C to 70°C. The optimum appeared to be around 50°C, although there was still considerable activity (approximately 50%) at 30°C. Despite *S. thermoviolaceus* α -amylase being a thermostable enzyme, its activity at the typical culture temperatures for *E. coli* growth remains high enough for it to be a useful enzyme for this particular application. Unlike the previous experiment investigating the relative activities of α -amylase in the periplasm and the extracellular media, the assays carried out in Fig 3.4 used samples from cultures which were induced at an OD₆₀₀ of 0.6 to 0.8, rather than at inoculation, as an attempt to optimise the amount of enzyme expressed.

3.3.4 Starch degradation studies

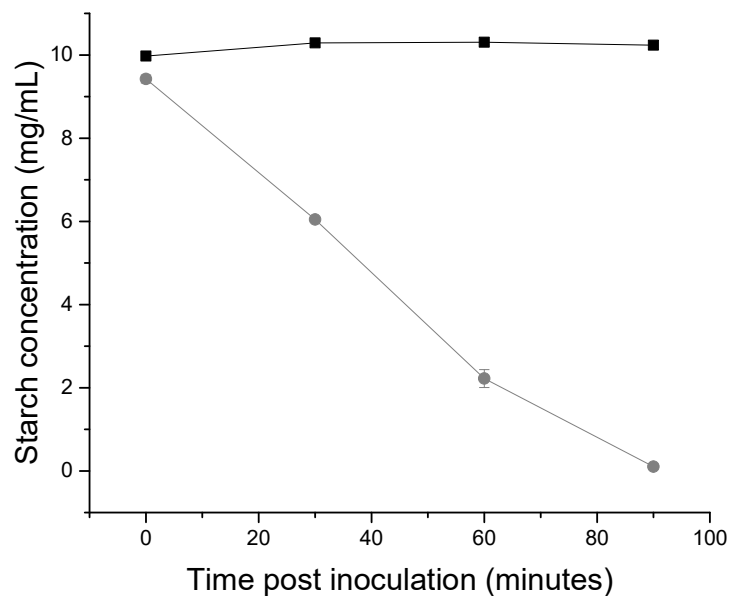


Figure 3.5 Starch degradation by the *S. thermoviolaceus* α -amylase secreting *E. coli* strain *E. coli* W3110 harbouring pQR187 cultured in LB containing 10 mg/mL starch. Inoculated with overnight culture (1 in 20 dilution) and induced from time point zero with 0.4 mM IPTG. Starch concentration measured from absorbance of starch/iodine complex at 600 nm, following addition of media sample to potassium iodide/iodine solution. Flasks were incubated at 37°C and shaken at 250 rpm, with samples extracted from media containing cells (grey) and media alone (black). Error bars represent standard deviation, n=3.

Knowing that *S. thermoviolaceus* α -amylase from pQR187 has considerable enzymatic activity in the media when expressed in *E. coli* W3110, it seemed pertinent to measure the rate of starch degradation within a culture set-up. Starch dissolved to a concentration of 10 mg/mL in LB was degraded to undetectable levels (using the starch degradation assay) within 100 minutes of the cultures initiation (inoculum from an overnight culture from a 1 in 20 dilution, induced with 0.4 mM IPTG at inoculation) (Fig 3.5). It is worth noting that the degradation of starch is likely due in some part to α -amylase being present in the overnight inoculum media. Despite the inoculum being uninduced, α -amylase expression on pQR187 is controlled by the *lac* promoter which is known to be leaky, due to titration of the low levels of the *lac* promoter repressor protein [86]. However, even when taking this into account, compared to the degradation rate seen in previous studies [56], whereby similar levels of starch degradation took tens of hours rather than tens of minutes, the combination of W3110 and pQR187 makes for a much more potent amylolytic strain. Work by Rosales-Colunga *et al* designed their constructs to contain a positive feedback loop, where the secretion of an endogenous α -amylase was promoted by the hydrolysis products of that same enzyme, in an attempt to maximise secretion. What is clear is that pQR187, on an IPTG inducible promoter, expresses and secretes α -amylase with substantially higher activity in the surrounding media than has been seen in those previous attempts. As a basis for a microbial platform with the ability to convert agro-industrial wastes into useful compounds, this has significant advantages.

3.3.5 Hydrolysis products of *S. thermoviolaceus* α -amylase

The hydrolysis products of *S. thermoviolaceus* α -amylase were identified using high performance anion exchange chromatography (section 2.5.10). Fig 3.6 shows the results from amylase assays carried out (at 37°C) using samples from the extracellular media of 24 hour (37°C, 250 rpm) W3110-pQR187 cultures. As the assay proceeded, the concentration

of starch within the assay decreased (Fig 3.6a); indicating α -amylase was present in the media. In the same sample, the concentration of both maltose and maltotriose increased (Fig3.6b). A chromatogram 80 minutes into the amylase assay (Fig 3.6c) clearly displays the presence of oligosaccharides up to approximately 20 glucose units, exemplifying the endo-acting nature of this α -amylase. When chromatograms from each time point throughout the assay are super-imposed it becomes clear that the longer oligosaccharides decreased in concentration over time, whereas the shorter oligosaccharides (maltose to maltotetrose) increased in concentration (Fig 3.6d). This finding supports the initial characterisation of this enzyme [57], confirming that the predominant hydrolysis products are maltose, maltotriose and maltotetrose.

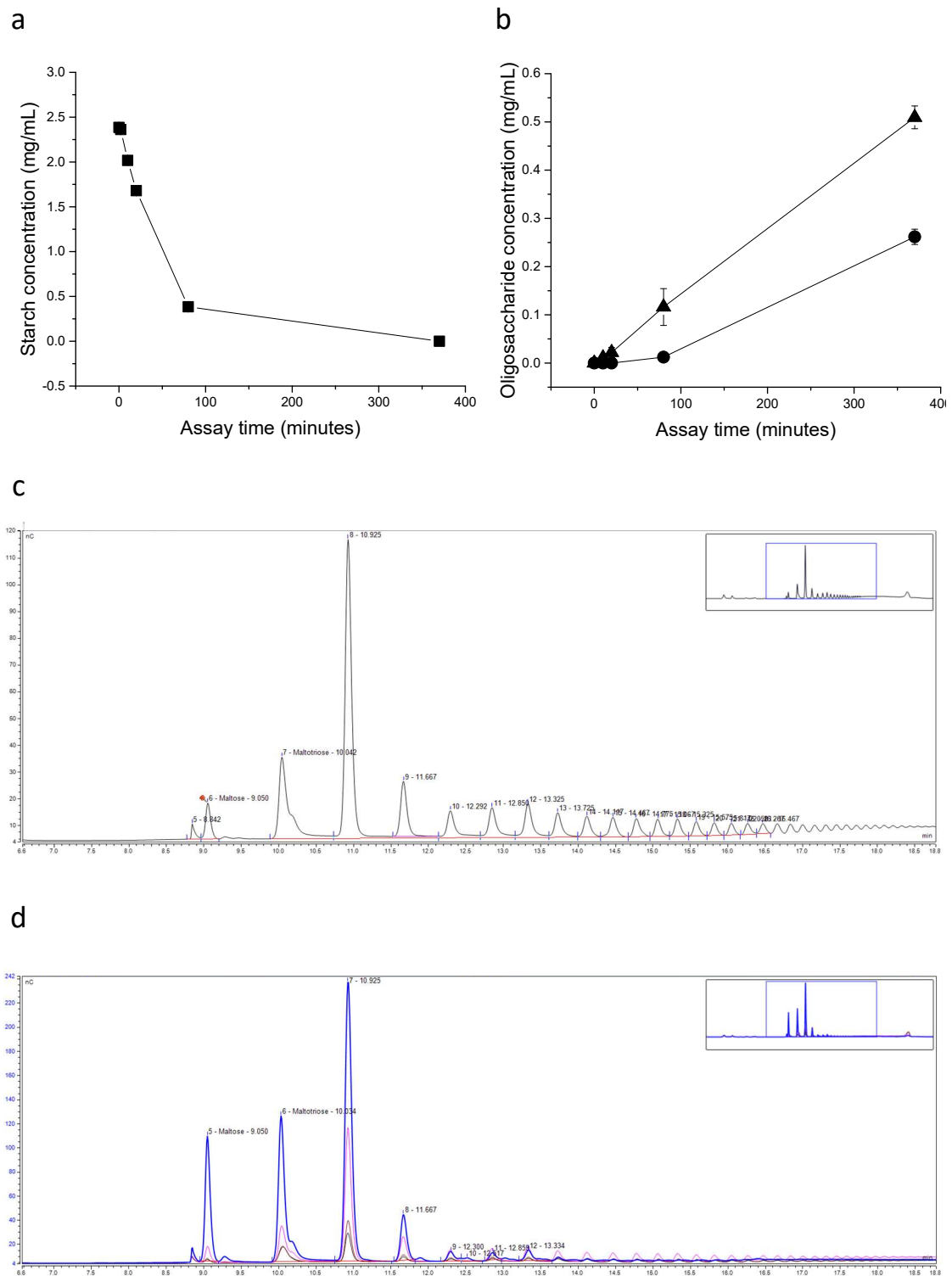


Figure 3.6 Analysis of hydrolysis products from secreted *S.thermoviolaceus* α -amylase

S.thermoviolaceus α -amylase activity within the extracellular media from 24 hour cultures of *E. coli* W3110 harbouring pQR187, inoculated with a 1 in 20 dilution of overnight culture and induced at an OD₆₀₀ of 0.6-0.8 with 0.4 mM IPTG, grown at 37°C, 250 rpm. a) Starch degradation throughout assay. b) Maltose (circle) and Maltotriose (triangle) accumulation throughout assay. c) Chromatogram of assay sample at 80 minutes, highlighting sequential peaks representing oligosaccharides increasing in length by single glucose units. d) Amalgamation of assay time points, 10 minutes (black), 20 minutes (brown), 80 minutes (pink) and 370 minutes (blue), indicating differing concentrations between longer oligosaccharides and shorter oligosaccharides. Error bars represent standard deviation, n=3

In the context of engineering an *E. coli* strain to hydrolyse starch into a utilisable carbon source, this work confirms that *S. thermoviolaceus* α -amylase is a promising enzyme. It is capable of being highly expressed from pQR187 in W3110, and in doing so it is secreted into the medium where it has access to its substrate. The hydrolysis of this substrate produces primarily short oligosaccharides which *E. coli* can naturally metabolise [13]. The next section examines how supplementing culture media with starch affects the growth characteristics of *E. coli* W3110 when expressing and secreting *S. thermoviolaceus* α -amylase.

3.3.6 The influence of starch on the growth characteristics of *E. coli* K12 secreting α -amylase

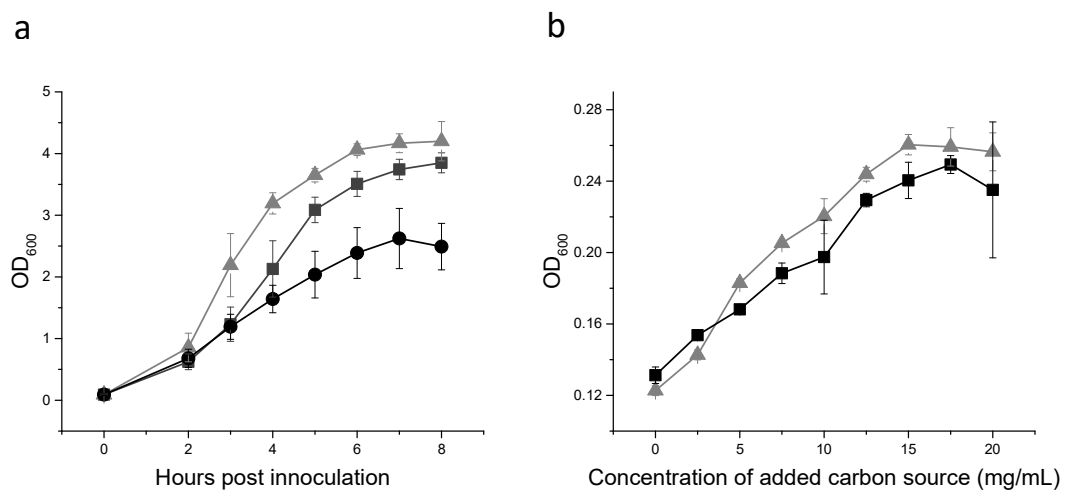


Figure 3.7 Growth of *E. coli* W3110 harbouring pQR187 in LB media supplemented with starch

a) Growth curves for *E. coli* W3110 harbouring pQR187 in shake flasks over 8 hours at 37°C, 250 rpm (induced at inoculation (OD₆₀₀ of 0.1) with 0.4 mM IPTG) in either LB media only (circle), or LB media supplemented with either 10 mg/mL starch (square) or 10 mg/mL glucose (triangle). b) Overnight cell density for W3110 harbouring pQR187 in 96-well plate at 37°C, 800 rpm (induced at inoculation (OD₆₀₀ of 0.1) with 0.4 mM IPTG) in LB media containing increasing concentrations of starch (square) or glucose (triangle). Error bars represent standard deviation, n=3.

E. coli W3110 expressing and secreting *S.thermoviolaceus* α -amylase was able to grow to higher cell densities over eight hours in LB supplemented with 10 mg/mL starch compared with just LB media alone (Fig 3.7a). This was a similar increase to that of cells grown in LB supplemented with an equivalent amount of glucose (10 mg/mL). As the concentration of starch (and glucose for reference) within the media was increased (up to 20 mg/mL), the density following a 24 hour culture in a microwell plate also increased (Fig 3.7b). The presence of starch in the media appeared to provide a benefit over LB alone in terms of achievable final density for cells expressing and secreting α -amylase, and this final density was similar to that seen with an equivalent amount of glucose.

3.3.7 Investigating reduced expression through ribosome binding site modification

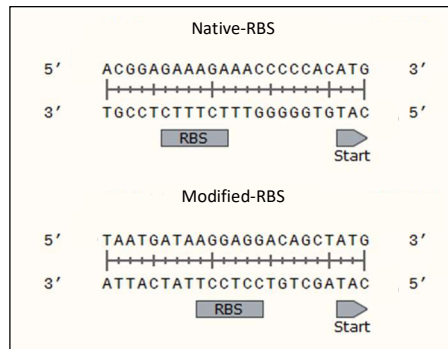
From the perspective of using this enzyme as a method of slowly releasing utilisable carbon from starch, it is fairly clear that pQR187 as a construct leads to excessive secretion of α -amylase into the extracellular space and the subsequent rapid degradation of starch in the medium. Following an attempt to modularise pQR187 through the removal of non-coding regions of DNA both upstream and downstream of the gene, and the replacement of the native ribosome binding site (RBS) with an *E. coli* Shine-Dalgarno consensus sequence (see Fig 3.8), α -amylase secretion was surprisingly reduced. This however provided an interesting opportunity to investigate the effects of decreased α -amylase secretion on growth in media containing starch.

3.3.7.1 Modified vector primer design and construction

The cloning strategy used restriction digestion and ligation, taking advantage of the *Hind*III and *Pst*I sites used in the original construction (section 1.5.2.2). The forward primer (Forwardamy2.1) was designed with an overhang to include the new RBS and a *Hind*III site at the 5' end. The reverse primer (Reverseamy2) was designed with an overhang to include

the *Pst*I site immediately downstream of the stop codon, thus removing non coding regions of DNA both upstream and downstream of the gene present in the original pQR187 vector. The new RBS and spacer region incorporated into the forward primer followed a Shine-Dalgarno consensus sequence and had been used successfully in previous expression studies within the group (D. Jackson, personal communication). Following PCR, which used the original pQR187 vector as a template for the α -amylase, the resultant product was purified and digested with *Hind*III/*Pst*I, and was subsequently ligated to the similarly digested and purified pQR187 backbone. The new vector pQR1700 was confirmed by restriction digestion analysis and sequencing from the M13 primer sites.

a



b

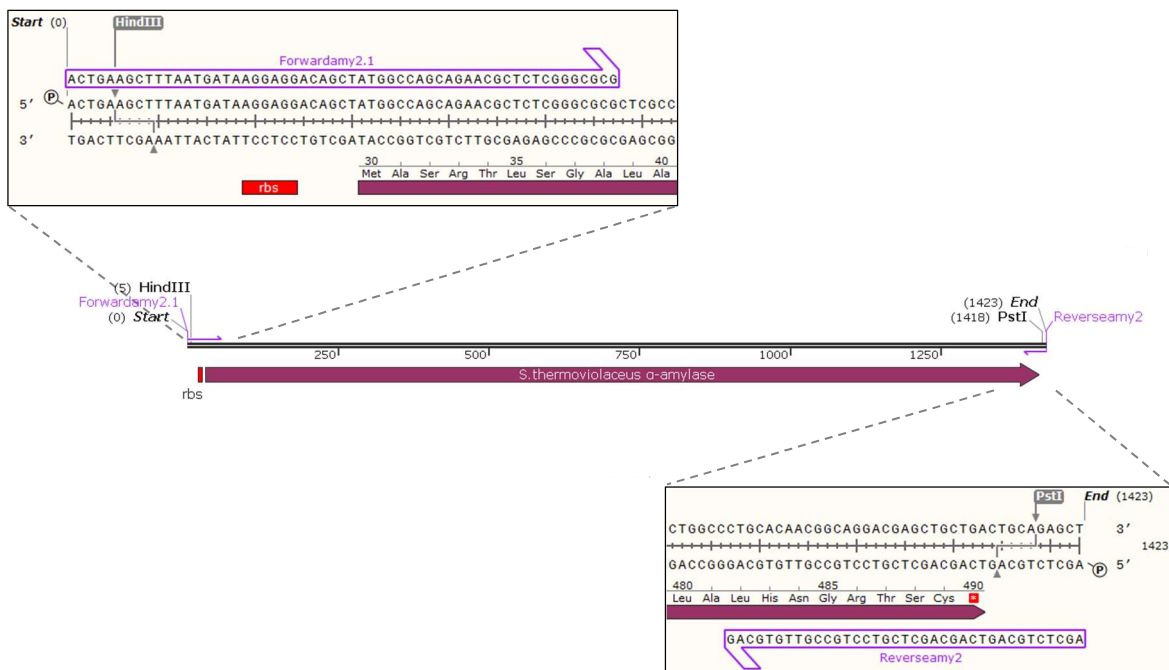


Figure 3.8 Diagram of primer design for modified vector construction

a) Nucleotide sequence displaying twenty base pairs 5' of the start codon, for both the native RBS and the consensus Shine-Dalgarno sequence. b) Forward primer (Forwardamy2.1) designed to include modified ribosome binding site upstream of the start codon, and downstream of the *HindIII* restriction site. Reverse primer (Reverseamy2) designed to include *PstI* restriction site immediately downstream of the stop codon.

3.3.7.2 Activity from modified vector and growth characteristics

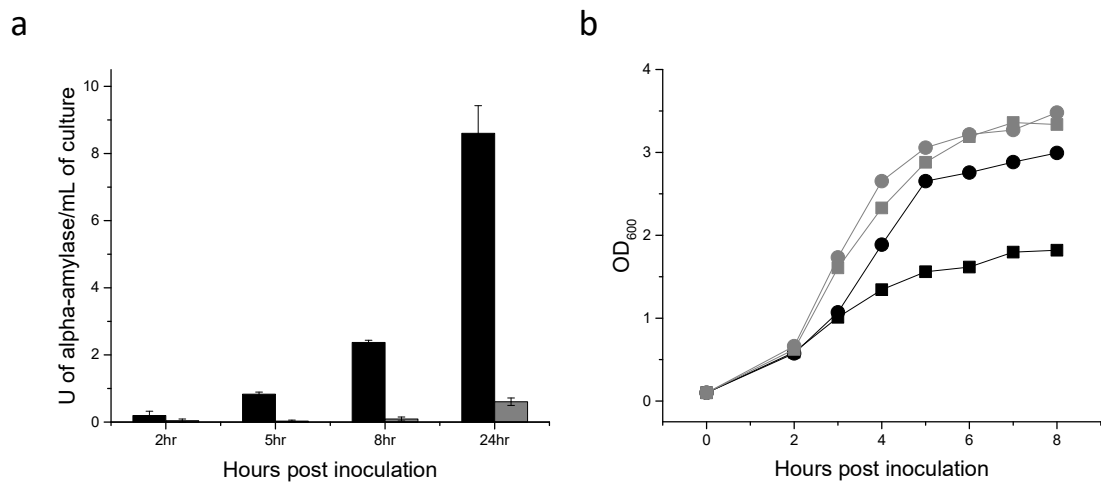


Figure 3.9 The reduction of secreted α -amylase from a modified construct and the effects on growth in LB media containing starch

E. coli W3110 harbouring either pQR187 or pQR1700, cultured at 37°C, 250 rpm and induced with 0.4 mM IPTG at inoculation. a) α -amylase activity in the extracellular media throughout the culture period (24 hours) for pQR1700 (grey) or pQR187 (black), expressed as units of α -amylase per mL of culture. Error bars represent standard deviation, $n=3$. b) Growth curves from single experimental run for W3110 harbouring pQR1700 (grey) or pQR187 (black) cultured in LB (square) or LB supplemented with 10 mg/mL starch (circle).

The vector modifications led to a significant decrease (approximately 10 fold) in secreted α -amylase, at all time points within the culture, compared with the original pQR187 construct (Fig 3.9a). Despite a consensus sequence being used for the ribosome binding site, the combination of replacing the native RBS, decreasing the spacer length, and removing nucleotide bases upstream of the gene, appeared to significantly diminished α -amylase expression.

Growth curves for *E. coli* W3110 harbouring pQR187 were consistent with previous data (Fig 3.7a) which showed an increase in cell density at 8 hours for cultures containing starch compared to cultures grown in LB media alone. Conversely, growth curves for W3110 harbouring pQR1700 did not differ between LB and LB supplemented with starch. Together

this would suggest that the level of α -amylase expression associated with each construct may have influenced growth rate, but in a way not necessarily related to the presence of starch. It is already known that a plasmid, even if no expression is taking place, can increase the metabolic burden on a cell through expression of antibiotic resistance genes and copy number maintenance [87]. It is also known that heterologous expression of a recombinant protein from a plasmid can place a further and more pronounced metabolic burden on the host cell, detrimentally affecting growth rate and final cell density [88]. In addition, the protein in this case is targeted to the periplasm, which can cause crowding of the translocation machinery during overexpression, again leading to a burden on cell growth [89, 90]. Given that cells harbouring the reduced expression construct achieved higher final cell densities, it is not unreasonable to assume that the reduction in final cell density seen by W3110-pQR187 in LB media was related to the over expression of α -amylase. Interestingly, however, very little difference in growth was seen between the two constructs in LB supplemented with starch. One explanation could be that the provision of extra carbon, in either the form of starch or glucose, may in some way salvage the reduced growth seen as a result of overexpression. The modified vector appeared not to be subjected to detrimental growth in the first place, possibly explaining why there was no benefit in terms of growth when supplemented by starch. Importantly the data also suggest the reduced rate of starch degradation within W3110-pQR1700 cultures did not lead to higher cell densities compared to the pQR187 equivalent, indicating that for this particular experimental setup the rate at which utilisable carbon was provided to the culture was not important for cell growth.

3.4 The ability of *E. coli* to degrade starch without exogenous amylase expression

From the literature it is known that *E. coli* express an endogenous amylase encoded by *malS* which is active in the periplasmic space [15, 91]. However, the role of this amylase is currently unclear, with mutants showing only a small disadvantage in terms of growth compared to wildtype when cultured on long maltodextrins [13]. As maltodextrins increase in length beyond approximately eight glucose units, the ability of *E. coli* to utilise them as a sole carbon source begins to diminish. To our knowledge, the ability of *E. coli* to degrade polymers as large as starch, without the addition of an exogenous enzyme, has not previously been reported.

3.4.1 Variations in starch degradation by non-amylolytic strains

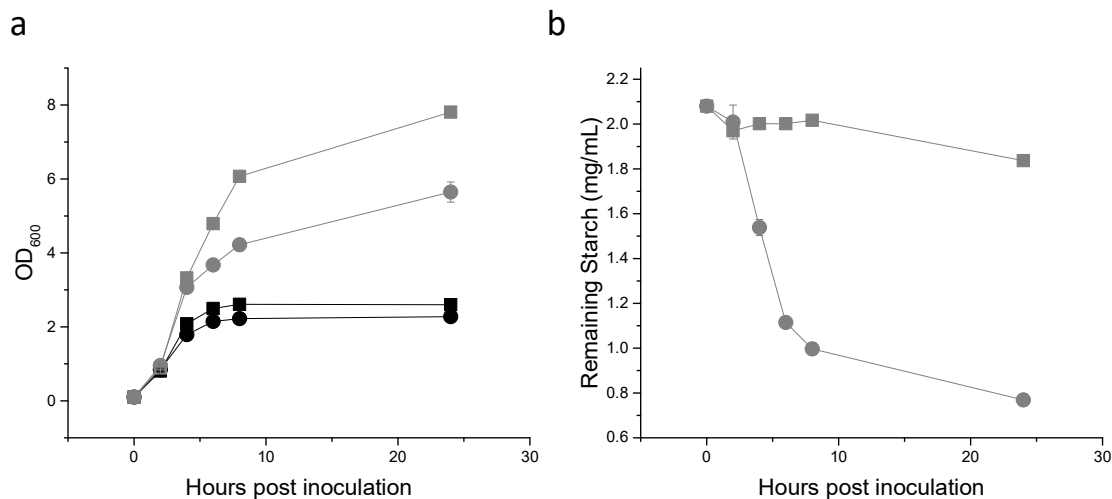


Figure 3.10 Degradation of starch within LB media for both W3110 and BL21(DE3) *E. coli* cultures

a) Growth curves for W3110 (square) and BL21(DE3) (circle) cultured in LB media (black) and LB media supplemented with 2.5 mg/mL starch (grey), at 37°C, 250 rpm over 24 hours (inoculated to an initial OD₆₀₀ of 0.1 from an overnight culture). b) Starch degradation within W3110 (square) and BL21(DE3) (circle) cultures over 24 hours at 37°C, 250 rpm. Remaining starch concentration determined using starch degradation assay with absorbance of starch/iodine complex measured at 600 nm. Error bars represent standard deviation, n=3.

E. coli strains W3110 and BL21(DE3) have not previously been reported to degrade starch; however when grown in LB supplemented with 2.5 mg/mL starch both showed increased densities after 24 hours compared with LB alone (Fig 3.10a). One potential explanation for this is that the starch added was not 100% pure, smaller oligosaccharides may be present in the starch mix as a result of the manufacturing process. Some of these shorter oligosaccharides could conceivably be metabolised by non-amylolytic *E. coli* and lead to an enhancement of growth. W3110 appeared to benefit more in terms of growth by achieving a higher cell density with the addition of starch than BL21(DE3), with very little difference between the two in LB media alone (Fig 3.10a). This suggests an inherent difference between the two strains in their ability to metabolise oligosaccharides.

When measuring starch concentration within the media throughout the culture period, both strains unexpectedly demonstrated starch degradation, however, the extent to which BL21(DE3) degraded starch was significantly greater than W3110, with over 1 mg/mL of degradation in the first 10 hours of the culture period. The ability of BL21(DE3) to degrade starch to such an extent has not been reported previously. Counter intuitively, it was BL21(DE3) that degraded starch to the greatest extent but it was W3110 which was enhanced the most in terms of growth. Presumably the degradation of starch did not necessarily result in the release of utilisable carbon. The limits of the starch degradation assay i.e. the inability of iodine to form a complex with shorter oligosaccharides, mean that oligosaccharides less than approximately 18 glucose units in length are not detected [92]. High performance anion chromatography analysis was also not conclusive, being negative for oligosaccharides up to the detection limit of approximately 20 glucose units in length (data not shown). Together this suggests that either the starch had been hydrolysed into small length oligosaccharides which BL21(DE3) had metabolised for something other than biomass, or that the starch had been hydrolysed into oligosaccharides of lengths which were difficult to detect using these particular techniques. Regardless, BL21(DE3) had the

ability to degrade starch without exogenous amylase expression, and both strains showed some enhancement in growth when starch was added to the media.

3.4.2 Starch as a supplement to enhance heterologous expression in complex media

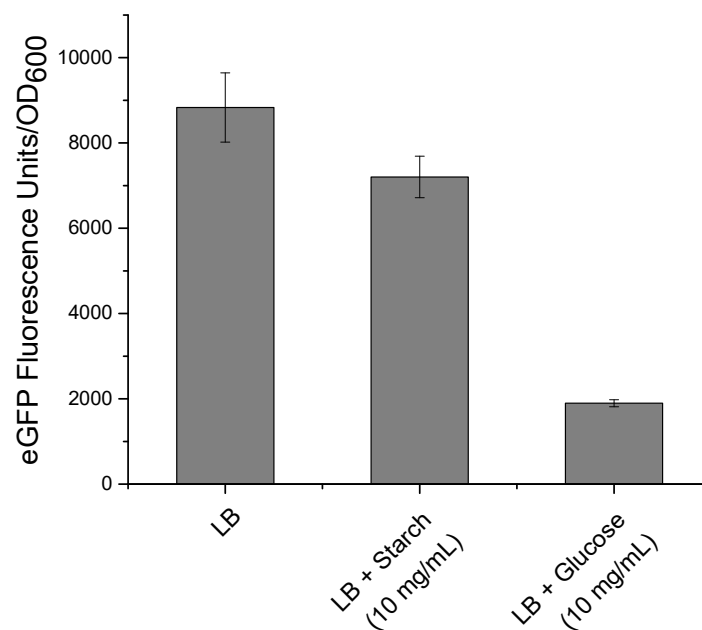


Figure 3.11 Heterologous protein expression following supplementation of LB media with either starch or glucose

E. coli BL21(DE3) harbouring pQR1344 cultured in either LB media, LB supplemented with 10 mg/mL starch, or LB supplemented with 10 mg/mL glucose, induced with 0.4 mM IPTG at an OD₆₀₀ of 0.6-0.8, and incubated at 25°C, 250 rpm for 24 hours. Samples (1mL) from each culture dispensed into a 24 well plate (Thermo Fisher Scientific) and whole cell GFP fluorescence intensity measured (with an excitation wavelength of 483 nm, and an emission wavelength of 535 nm, Tecan infinite 200 pro), normalised to OD₆₀₀ (OD₆₀₀ values for LB alone 4.2 ±0.2; LB supplemented with starch 4.8 ±0.2; and LB supplemented with glucose 5.1 ±0.3). Error bars and values represent standard deviation, n=3.

To assess whether the increase in biomass associated with starch supplements was mirrored by an increase in recombinant protein expression, pET29a with an eGFP [93] insert (pQR1344, supplied by D. Dobrijevic) was transformed into BL21(DE3) and cultures

were grown in either LB alone, LB containing 10 mg/mL starch, or LB containing 10 mg/mL glucose. Expression of eGFP measured by fluorescence intensity (excitation wavelength of 483 nm and of emission wavelength 535 nm, Tecan infinite 200 pro) appeared to be similar in both normal LB and LB supplemented with 10 mg/mL starch, indicating there was no real advantage with using starch for recombinant protein expression, despite the slight increase in cell density (cultures in LB alone had an OD_{600} of 4.2 ± 0.2 whereas those in LB supplemented with starch had an OD_{600} of 4.8 ± 0.2). When an equivalent amount of glucose was added to LB, there was a significant reduction in expression; consistent with previous catabolite repression data (LB supplemented with glucose achieved an OD_{600} of 5.1 ± 0.3). Despite there being no enhancement, the data support the notion that starch itself does not have a detrimental effect on recombinant protein expression, and may offer advantages over the more traditionally used glucose particularly if cells are able to utilise it for growth.

3.4.3 Amylolytic activity associated with *E. coli* BL21(DE3) is not localised to the extracellular media

By routinely using the extracellular fraction of untransformed *E. coli* (either W3110 or BL21(DE3)) as a negative control within the amylase assay, it was already known that there was very little amylolytic activity within this fraction, suggesting that the endogenous enzyme responsible for starch degradation is not secreted but rather associated with the cell itself. To further investigate this, an experiment was devised whereby cultures of W3110 and BL21(DE3) were grown in LB media supplemented with 2.5 mg/mL starch for 4 hours. At this point each culture was split in two, half filtered through a 0.22 μm filter (Millipore) to remove cells and half left unaltered. The concentration of starch in each was subsequently measured. The filtered and unfiltered cultures were incubated separately for another 4 hours at which point the remaining starch concentrations were again measured.

At 4 hours post inoculation when the culture was split, BL21(DE3) had degraded approximately 10% of the starch in the media (Fig 3.12). After 8 hours (4hours following the split) the culture had degraded another 30% whereas the filtered extracellular media had not altered. The disparity between the two conditions confirmed that starch was only degraded in the presence of BL21(DE3) cells i.e. there was no amyolytic activity present in the media alone suggesting the enzyme responsible was not secreted but rather the amyolytic activity was associated with the cell itself. This evidence suggests BL21(DE3) expresses an endogenous amyolytic enzyme, presumably associated with the periplasmic space or outer membrane which is capable of hydrolysing starch, and this is not expressed to the same extent in the W3110 strain.

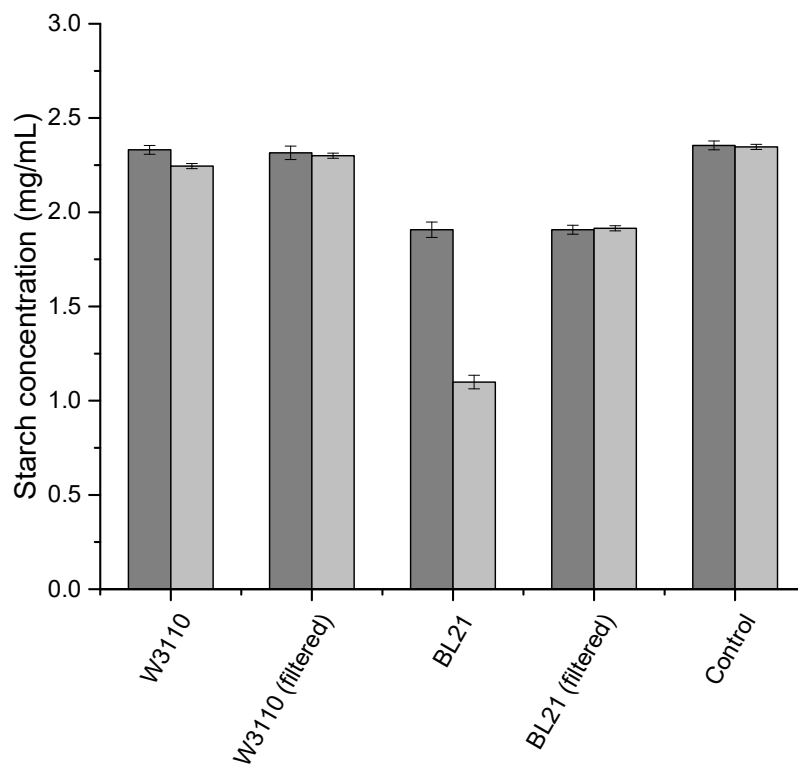


Figure 3.12 Differentiating amyolytic activity associated with *E. coli* BL21(DE3) between the cellular and extracellular space

E. coli W3110 and BL21(DE3) inoculated (1 in 20 dilution from overnight culture) in LB supplemented with 2.5 mg/mL starch. Cultures grown for 4 hours at 37°C, 250 rpm (dark grey), and for a further 4 hours following filtering or non-filtering (light grey). Error bars represent standard deviation, n=3.

3.4.4 Starch degradation by whole cell *E. coli* BL21(DE3) in glucose free mineral salt medium

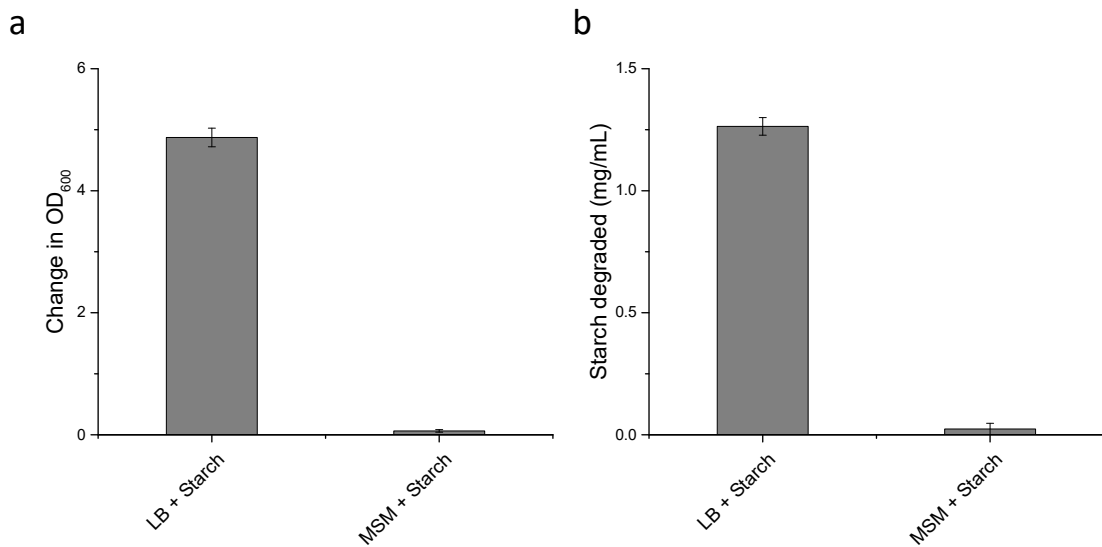


Figure 3.13 Degradation and utilisation of starch by *E. coli* BL21(DE3)

Starter cultures (1 mL) centrifuged and subsequently re-suspended in 5 mL of either LB supplemented with 2.5 mg/mL starch or glucose free MSM supplemented with 2.5 mg/mL starch, incubated at 37°C, 250 rpm for a further 14 hours. a) Change in OD₆₀₀ of re-suspended cells over the 14 hour culture period. b) Amount of starch (mg/mL) degraded in culture media (using starch degradation assay for residual starch measurements with concentration calculated from a standard curve) over the 14 hour culture period. Error bars represent standard deviation, n=3.

To determine the extent to which untransformed *E. coli* may benefit in terms of growth from starch, and to further characterise the native amylolytic activity, a starter culture of BL21(DE3) was centrifuged and subsequently re-suspended in either fresh LB supplemented with 2.5 mg/mL starch, or glucose free mineral salt medium (MSM) (see section 2.3.3 for composition) supplemented with 2.5 mg/mL starch, and incubated for a further 14 hours at 37°C, 250 rpm. With starch as the sole carbon source (i.e. MSM supplemented with starch), re-suspended BL21(DE3) cells were unable to increase in density beyond that of the initial resuspension, whereas BL21(DE3) re-suspended in LB supplemented with starch, showed a significant increase in density (Fig 3.13a). In terms of residual starch remaining in the media after 14 hours, there was no starch degradation in

the MSM cultures, whereas over 1 mg/mL was degraded in LB cultures (Fig 3.13b), consistent with previous results (Fig 3.10). The results indicate BL21(DE3) was unable to degrade or utilise starch when present as a sole carbon source, but could degrade starch in the presence of other utilisable carbon sources.

3.5 *E. coli* secreting *S. thermoviolaceus* α -amylase utilising starch as a sole carbon source

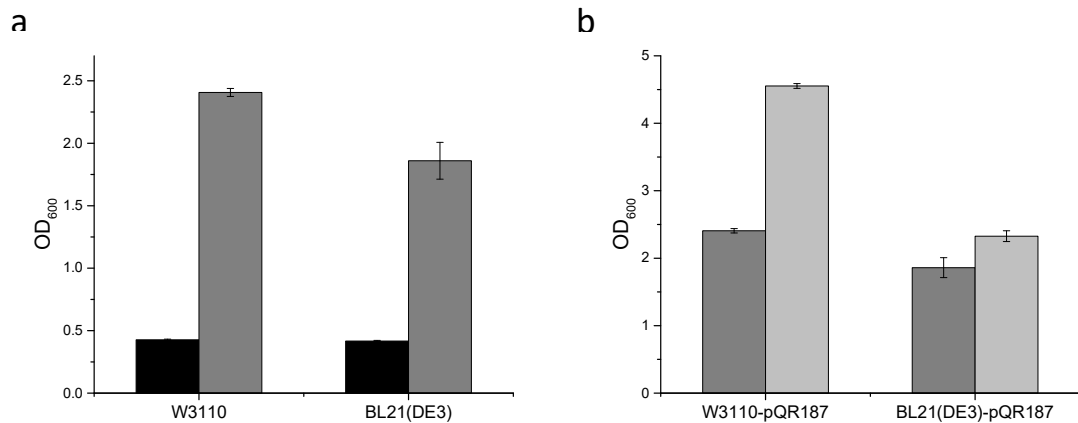


Figure 3.14 End point analysis of growth in mineral salt media (MSM) supplemented with starch or glucose

a) Cell density (OD₆₀₀) of both untransformed (black) and pQR187 harbouring (grey) *E. coli* W3110 and BL21(DE3) cultured over a 24 hour period at 30°C 250 rpm, in glucose free MSM, supplemented with 2.5 mg/mL starch. b) W3110 and BL21(DE3) harbouring pQR187 cultured over a 24 hour period in MSM supplemented with either 2.5 mg/mL starch (dark grey) or 2.5 mg/mL glucose (light grey). Error bars represent standard deviation, n=3.

This study has provided evidence to suggest the addition of starch to LB media offers a benefit in terms of biomass not only for *E. coli* expressing *S. thermoviolaceus* α -amylase, but also provides a benefit for the two untransformed strains investigated. To determine whether the engineered strains have any advantage over the untransformed strains in the context of utilising starch as a carbon source, experiments were carried out in defined media where all carbon sources were accounted for. When grown on glucose free mineral

salt medium (MSM) supplemented with 2.5 mg/mL starch, only *E. coli* expressing and secreting *S. thermoviolaceus* α -amylase was able to grow (Fig 3.14a). The untransformed *E. coli* strains were unable to grow to a density much beyond the initial inoculum after 24 hours of culture. The two *E. coli* strains expressing α -amylase were also grown on MSM supplemented with 2.5 mg/mL glucose, which appeared to be a superior source of carbon particularly for W3110 harbouring pQR187 (Fig 3.14b). The increased cell density seen with glucose over starch indicates that at these concentrations, the negative effects of overflow metabolism on growth brought about by excessive glucose concentrations were not an important factor. At this concentration *E. coli*'s preferred source of carbon, glucose, remained the most beneficial for growth.

3.6 Discussion and Conclusions

Although not widely thought of as a source of carbon in *E. coli* fermentation, starch has been identified in this study as a potential alternative to some of the more traditional carbon sources. When added as a supplement to complex media such as LB, starch appears to offer a significant advantage in terms of growth even for *E. coli* which has not been engineered to degrade it. In fact, this work has identified that *E. coli*, particularly BL21(DE3), is capable of degrading starch without the heterologous expression of an amylolytic enzyme. However, despite achieving higher cell densities in complex media supplemented with starch, BL21(DE3) is unable to grow when starch is used as a sole carbon source in defined media. Incidentally, alongside this inability to grow, degradation of starch seen in LB media is eliminated when cells are re-suspended in defined media containing starch as the sole carbon source. There is also a paradoxical relationship between the two *E. coli* strain's ability to degrade starch, and their ability to benefit in terms of growth from the presence of starch. The reason for this remains unclear; although

W3110 does degrade starch, BL21(DE3) degrades starch more than ten-fold faster, however, it is W3110 that benefits the most in terms of growth from the addition of starch. The mechanism behind starch degradation by untransformed BL21(DE3) cells is associated with the cells themselves, as there is no amylolytic activity in the media once cells have been removed, however further investigation is required to determine the specific products of this degradation, and their eventual route through central metabolism.

The amylolytic activity of *E. coli* strains can be greatly increased through the heterologous expression of *S. thermoviolaceus* α -amylase. *E. coli* W3110, when expressing and secreting *S. thermoviolaceus* α -amylase from pQR187, can degrade starch present in the media at a rate many times faster than that of other engineered strains in the literature [56]. This opens up an opportunity to use this engineered strain as the basis for a microbial platform to convert starch into valuable products. An increase in α -amylase activity in the media over time also shows this has the potential to be applied to a self-feeding system; as the culture proceeds, cell mass increases, expressing and secreting more α -amylase which in turn provides more utilisable carbon for cell mass. However, it has been clearly demonstrated that the rate of α -amylase activity in the media is far beyond that which would be required, even when using the vector with reduced expression. Furthermore, there is a complexity associated with an endo-acting amylase in terms of hydrolysis product profile. The fact that *S. thermoviolaceus* α -amylase does not produce *E. coli*'s preferred carbon source, glucose, in any sufficient quantity, but rather a mixture of oligosaccharides of varying size, complicates the development of a slow release system for utilisable carbon. As such the next Chapter focusses on the possibility of using an exo-acting amylolytic enzyme, or glucoamylase, for the purpose of simplifying the hydrolysis product profile and mimicking enzyme-based fed-batch systems currently in use.

Finally, it has been demonstrated that *E. coli* cells expressing and secreting *S. thermoviolaceus* α -amylase have the capability of using starch as a sole carbon source, and do not require the presence of any other form of carbon within the culture media. Unlike previous strains developed by others [56], the densities achieved by W3110 and BL21(DE3) expressing *S. thermoviolaceus* α -amylase in MSM containing starch are not far off densities achieved in glucose, and can rival those of complex media such as LB. One of the limitations identified in this study thus far has been the difficulty in dissolving high concentrations of starch within the culture media. It has also become clear that LB is only capable of sustaining growth to a certain density, despite the amount of carbon present. To test the hypothesis that starch can offer a growth advantage over glucose by way of avoiding or minimising overflow metabolism, higher concentrations of both starch and glucose are required, as well as a media containing necessary amounts of other nutrients essential for high density growth. This has been investigated in greater detail in Chapter 5.

4 Novel bacterial glucoamylase discovery and characterisation

4.1 Introduction

Glucoamylases offer a particular advantage over α -amylases with respect to developing an enzyme-based feeding strategy. In contrast to α -amylases, their primary hydrolysis product is glucose, rather than a mixture of oligosaccharides of varying length. This simplifies both prediction and measurement from the perspective of glucose release, and also provides *E. coli* with its preferential source of carbon. This Chapter aims to identify and characterise candidate glucoamylases which when expressed and secreted by *E. coli*, can release glucose and enable growth using starch as a sole carbon source.

The characterisation of bacterial glucoamylases is surprisingly uncommon in the literature, with the vast majority of commercially available enzymes of this type derived and produced from fungal sources. One of the difficulties with using fungal enzymes is achieving successful heterologous expression within an *E. coli* host, owed in large part to the post-translational modifications required. To this end, a bioinformatics approach has been applied to identify putative bacterial glucoamylases, with selected candidates cloned and subsequently expressed in *E. coli* for characterisation studies. Further studies have focussed on the suitability of these novel glucoamylases for self-secretion, and eventual application within an enzyme-based fed-batch fermentation system.

4.2 Cloning of fungal glucoamylases and expression attempts in *E. coli*

The most well characterised glucoamylases, primarily because they are used extensively in industrial applications, are derived from fungal sources. In most cases they are produced using their native host; however, there are examples in the literature where fungal glucoamylases have been successfully expressed in *E. coli*. Two examples are investigated here, firstly a glucoamylase from *Aspergillus niger*, which is commonly used within the starch industry, and a glucoamylase from *Saccharomyces diastaticus*, which has previously been heterologously expressed in *E. coli* [65].

4.2.1 Expression of a glucoamylase derived from *Aspergillus niger*

As described in the introduction the enzyme-based fed-batch fermentation system developed by BioSilta uses a glucoamylase derived from *A. niger* (E.C.3.2.1.3) [34]. It therefore seemed appropriate to use this as a starting point within this study. Owing to the fact that the *A. niger* gene encoding glucoamylase (GLAA) contains four introns [94], it was decided to synthesise the coding region of the gene rather than attempting to clone it. Using the Uniprot FASTA sequence (P69328) the amino acid sequence was codon optimised (http://www.bioinformatics.org/sms2/rev_trans.html) for *E. coli*, and reverse translated. The resulting sequence was sent to Eurofins Genomics for synthesis and returned within a sub-cloning vector (pEX-K4-niger_Gluc) (Fig 4.1). During synthesis *Nde*I and *Xho*I restriction sites were inserted to flank the gene 5' and 3' respectively. This allowed for a one step sub-cloning strategy using restriction digestion and ligation. Both parent (pEX-K4-niger_Gluc) and recipient (pET29a) plasmids were digested with *Nde*I/*Xho*I, with subsequent gel extraction and purification of both insert and pET29a backbone. These were ligated together to form pET29a-niger_Gluc, designated pQR1701. Expression vector construction

was confirmed with restriction digestion and sequencing. Expression studies revealed neither a visible band on SDS page at the expected size (approximately 68kDa), nor any functional activity within the whole cell lysate (see Fig 4.3).

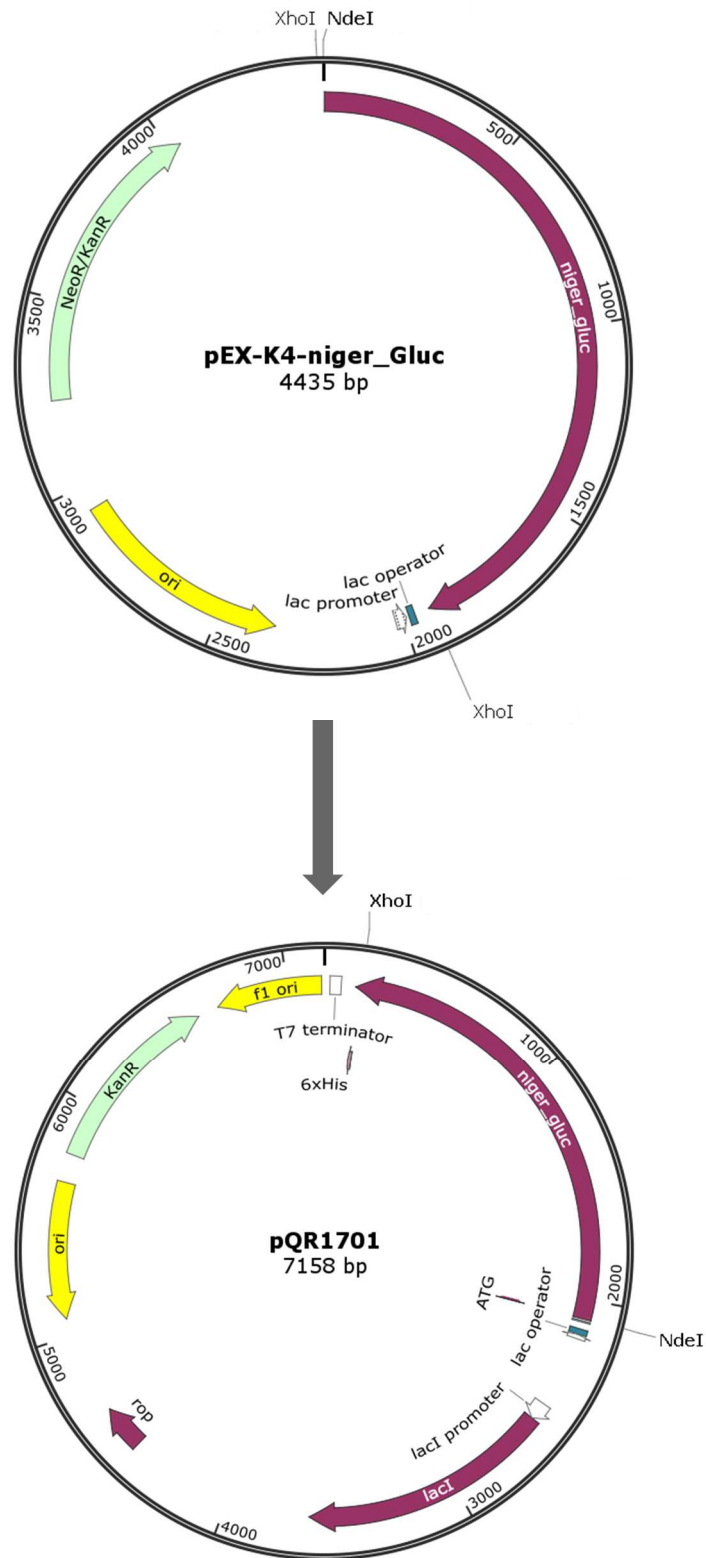


Figure 4.1 Diagram of synthesised *A. niger* glucoamylase gene in initial sub-cloning vector and in expression vector

Synthesised *A. niger* glucoamylase gene from pEX-K4-niger_gluc digested with *NdeI* and *XhoI*, extracted, purified, and ligated to the backbone of *NdeI/XhoI* digested pET29a, forming pQR1701.

4.2.2 Cloning and expression of a glucoamylase derived from *Saccharomyces diastaticus*

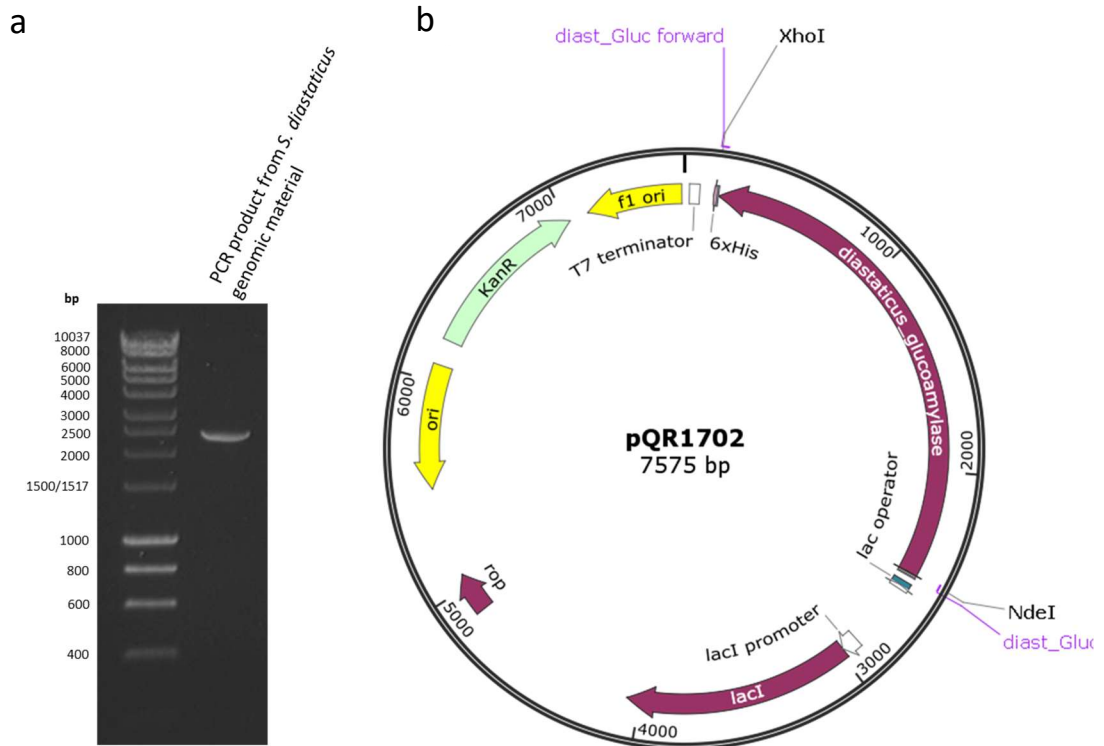


Figure 4.2 *S. diastaticus* glucoamylase genomic PCR and expression vector design

a) Agarose gel electrophoresis of genomic PCR product using diast-Gluc primers, forming a band 2334bps in size. b) Diagram of final expression vector (pQR1702) following *NdeI/XhoI* digestion of purified PCR product and ligation with *NdeI/XhoI* digested and purified pET29a backbone.

Unlike GLAA from *A. niger*, the glucoamylase STA1 derived from *S. diastaticus* has been cloned and expressed in *E. coli* previously [65]. Cloning directly from the *S. diastaticus* genome was therefore attempted (see section 2.2.8.1 for genomic DNA preparation) with the aim of inserting the gene into an expression vector. Primers were designed with overhanging regions to include *NdeI* upstream and *XhoI* downstream of the coding region. PCR (see section 2.2.3 for conditions) resulted in a band at 2334 bp (Fig 4.2a). This was extracted and purified for subsequent digestion with *NdeI* and *XhoI* restriction enzymes, and ligated to similarly digested and purified pET29a backbone, resulting in pET29a-

diast_Gluc designated pQR1702 (Fig 4.2b). Confirmation of final construct was carried out by sequencing.

Again, expression studies revealed no apparent band on SDS page at the expected size (approximately 83 kDa), as well as no functional activity within the whole cell lysate (Fig 4.3). Functional activity data for both fungal enzymes is expressed as starch degradation rather than glucose accumulation, a method validated by using commercially available *A. niger* glucoamylase (E.C.3.2.1.3) (Sigma) as a positive control (data not shown). However glucose accumulation was also measured (Glucose GO assay kit, Sigma-Aldrich) and again neither enzyme showed activity (data not shown). Owing to the rarity of heterologous expression of fungal glucoamylases in *E. coli* hosts, the two attempts here were not pursued any further. Instead attention was turned towards bacterial derived glucoamylases, in particular putative enzymes from organisms which were available in-house.

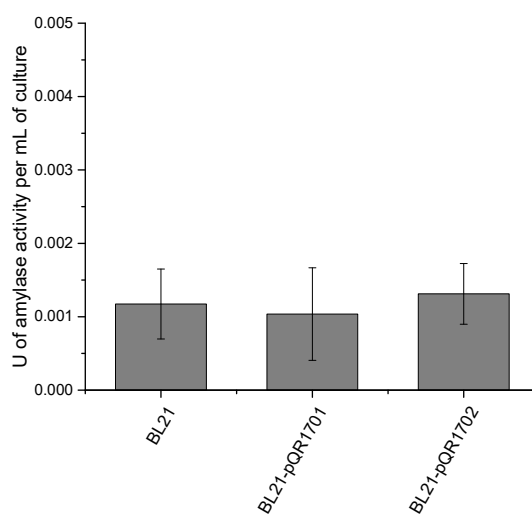


Figure 4.3 Functional activity of whole cell lysates for *E. coli* expressing fungal enzymes
Amylolytic activity of whole cell lysates from BL21(DE3) expressing either pQR1701 or pQR1702. Cultures grown for 24 hrs in LB at 30°C, 250 rpm (induced at OD₆₀₀ of 0.6-0.8). Cells (1mL culture) were centrifuged for 5 minutes at 2000 g and re-suspended in 300 µL PBS for sonication (20 second on, 20 seconds off for 3 cycles). Cell lysates were added directly to the amylase assay with U of amylase activity defined as change in absorbance at 600 nm of starch/iodine complex per minute. Error bars represent standard deviation, n=3.

4.3 Bioinformatics; identification and cloning of putative glucoamylases

4.3.1 Identification of putative bacterial glucoamylase

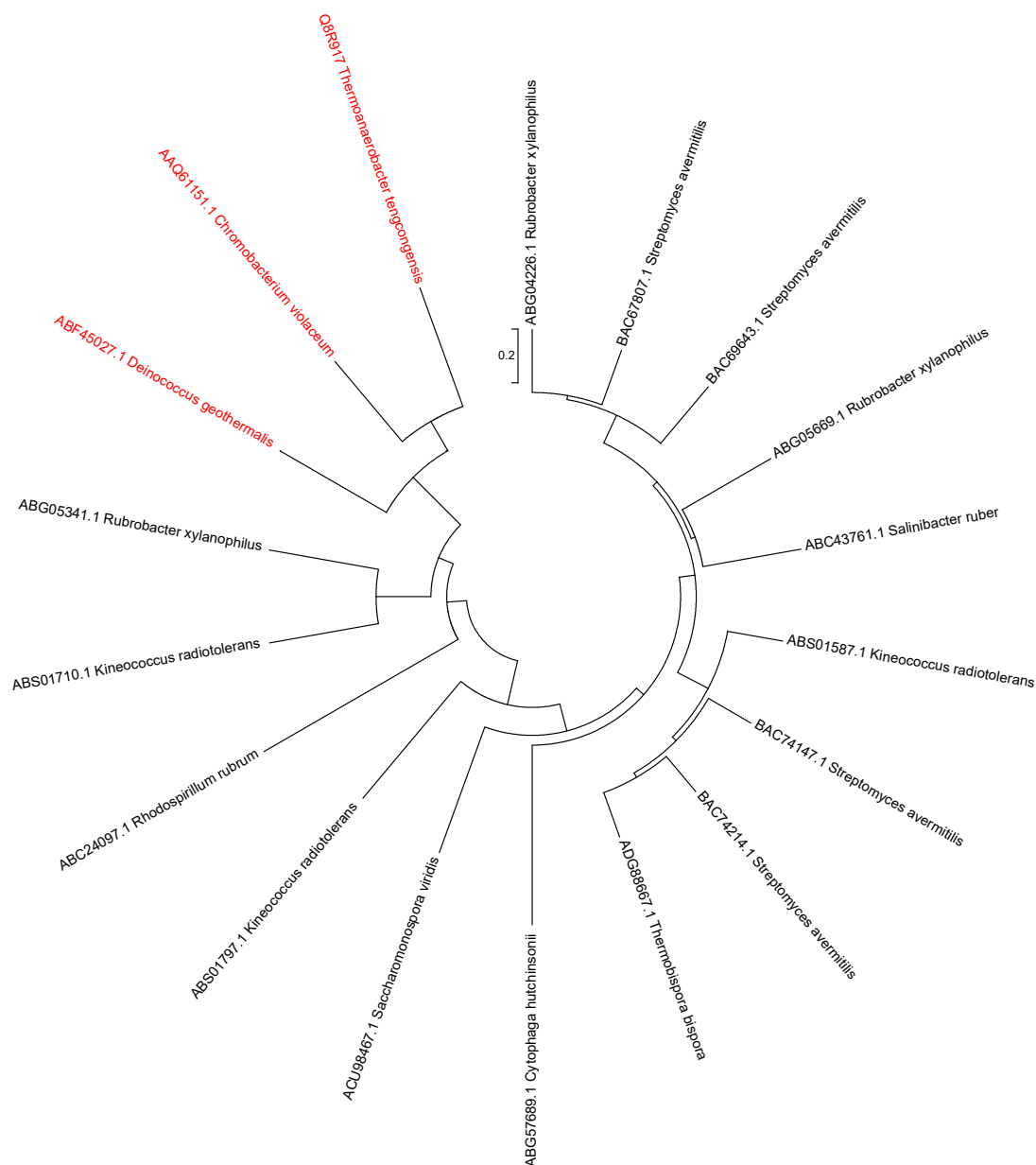


Figure 4.4 Phylogenetic tree of putative bacterial glucoamylases

Putative bacterial glucoamylases cross referenced with organisms available in-house. Enzymes selected for initial screening (red) due to their relatedness to the previously characterised *T. tengcongensis* glucoamylase. Phylogenetic tree created using neighbour-joining method by Molecular Evolutionary Genetics Analysis version 7.0 (MEGA7) software.

To identify putative glucoamylases the carbohydrate-active enzymes (CAZy) database [54] was used to search for bacterial enzymes classified as Glycoside Hydrolase Family 15, which includes glucoamylases (EC 3.2.1.3). Suitable enzymes were cross referenced with available organisms within the laboratory to form 17 potential cloning targets. Following a phylogenetic analysis using Molecular Evolutionary Genetics Analysis version 7.0 (MEGA7) software (Fig 4.4), which included a previously characterised enzyme (from *Thermoanaerobacter tengcongensis*) that had been successfully expressed in *E. coli* by another group [66], two other enzymes from *Deinococcus geothermalis* and *Chromobacterium violaceum* were selected for initial cloning and expression tests based on their relatedness to the *T. tengcongensis* glucoamylase.

4.3.2 Classical restriction digestion and ligation cloning strategy

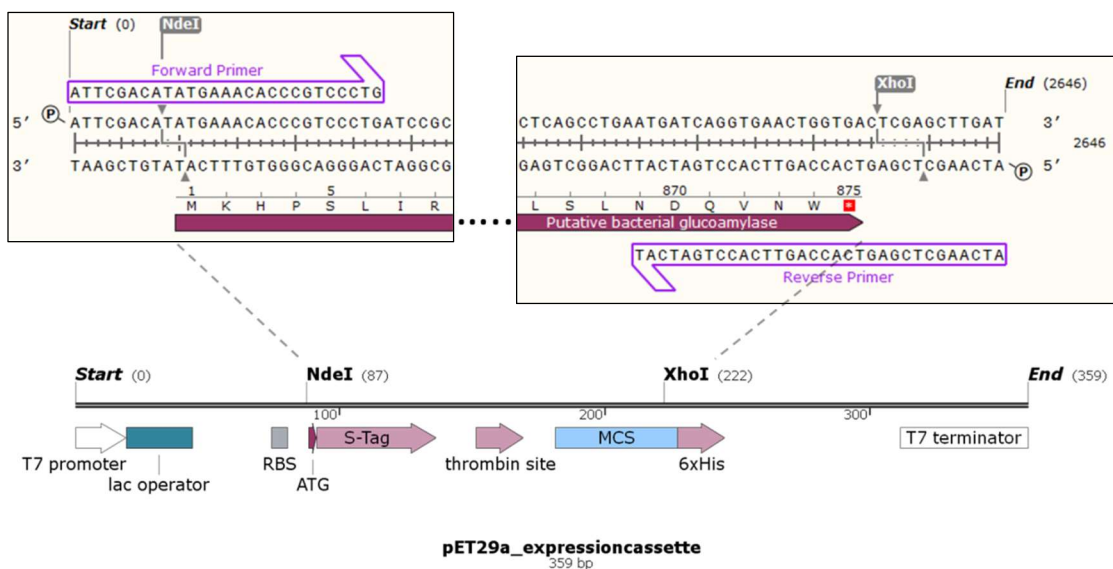


Figure 4.5 Overview of cloning strategy for putative bacterial glucoamylases

Cloning procedure for example putative bacterial glucoamylase (*C. violaceium*). Forward and reverse primers include *NdeI* and *XhoI* in their overhanging regions respectively. Following gel extraction and purification of PCR product, fragments are digested with *NdeI* and *XhoI* and are subsequently ligated to the pET29a backbone which has been similarly digested.

As above (in Fig 4.1 and 4.2), the cloning strategy used for these particular glucoamylases was classical restriction digestion and ligation. Primers for each of the putative glucoamylases were designed to include, within their overhanging regions, an *Nde*I restriction site immediately 5' of the gene and an *Xho*I site immediately following the stop codon 3' of the gene. These restriction sites allowed for insertion into the expression vector pET29a, in which the gene is regulated by the T7 promoter. See Figure 4.5 for an overview.

4.3.3 PCR of target enzymes in selected organisms

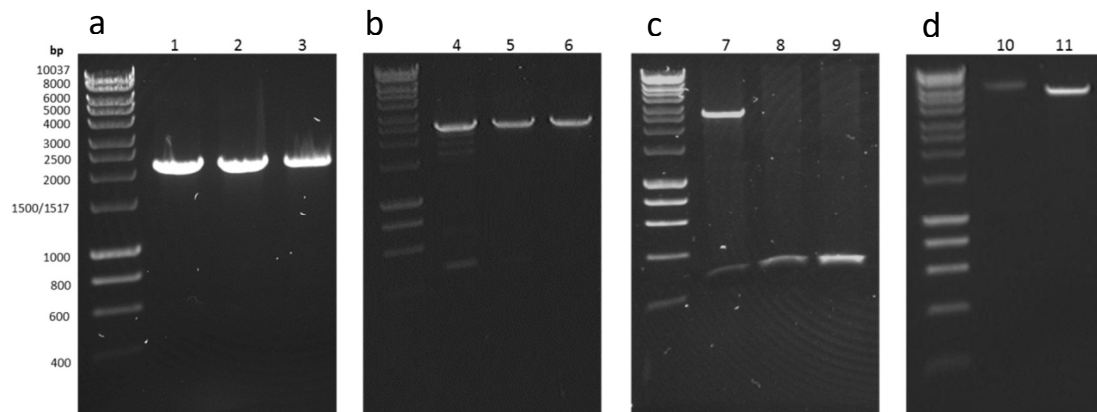


Figure 4.6 Agarose gel electrophoresis of *D. geothermalis*, *T. tengcongensis*, and *C. violaceium* genomic PCR

Agarose gel electrophoresis results for genomic PCR of *D. geothermalis*, *T. tengcongensis*, and *C. violaceium* glucoamylase genes, using an annealing temperature gradient 5°C either side of the lowest primer T_m . a) *D. geothermalis* (lanes 1-3), b) *T. tengcongensis* (lanes 4-6), and c) *C. violaceium* (lanes 7-9). d) Undigested (lane 10) and *Nde*I/*Xho*I digested (lane 11) pET29a.

Genomic material from *D. geothermalis*, *T. tengcongensis*, and *C. violaceium* was extracted (see section 2.2.8 for genomic DNA preparation) and the respective glucoamylase genes were amplified using PCR under standard conditions (section 2.2.3). Using an annealing temperature gradient of 10°C (5°C either side of the lowest primer T_m) each PCR produced bands at the expected size; *D. geothermalis* (2396 bp), *T. tengcongensis* (2111 bp), and *C. violaceium* (2624 bp) (Fig 4.6). Following gel extraction and purification, DNA bands were

digested with *NdeI* and *XhoI* and ligated to purified *NdeI/XhoI* digested pET29a backbone. The resultant constructs, pQR1703, pQR1704 and pQR1705 respectively, were confirmed through restriction digestion analysis and sequencing.

4.3.4 Construction of vectors incorporating histidine tags

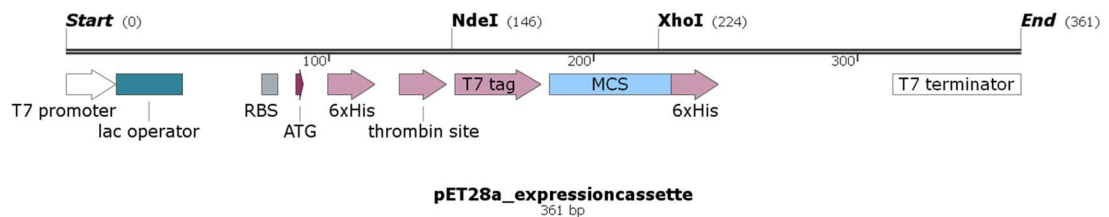


Figure 4.7 Diagram of pET28a expression cassette

pET28a expression cassette highlighting the 6xHis tag upstream of the *NdeI* restriction site and downstream of the ATG start codon, allowing for a His-tag fusion to the N-terminus of genes cloned into *NdeI/XhoI* restriction sites.

To allow for potential purification of these glucoamylases at a later stage it was appropriate to design a set of constructs whereby the new enzymes were fused to a histidine tag. As the previous primers were designed to include a stop codon between the gene and the *XhoI* restriction site, pET29a would not allow for inclusion of a His-tag to the C-terminus of the genes. Rather than redesigning the primers and repeating the PCRs, it was instead decided to attach a His-tag to the N-terminus of the genes by using the N-terminal His-tag of pET28a (Fig 4.7). This was advantageous as the same digested PCR products from the previous pET29a constructions could be used, given that the multiple cloning sites of pET28a and pET29a are identical. Cloning into pET28a therefore followed the same strategy as cloning into pET29a, with correct construction of the three vectors confirmed through sequencing. These were designated pQR1706, pQR1707 and pQR1708 for *D. geothermalis*, *T. tengcongensis*, and *C. violaecium* glucoamylases respectively.

4.4 Characterisation of *D. geothermalis*, *T. tengcongensis* and *C. violaceum* glucoamylases

Following successful construction of the bacterial glucoamylase expression vectors, initial expression studies were carried out to determine whether a functional enzyme could be expressed within *E. coli*.

4.4.1 Initial expression and cell lysate activity for selected glucoamylases

Initially, following growth in LB for 24 hours at 30°C, 250 rpm (induced with 0.4 mM IPTG at an OD₆₀₀ of 0.6-0.8), crude cell lysates of *E. coli* BL21(DE3) harbouring either pQR1703, pQR1704 or pQR1705 were run on SDS page (Fig 4.7a). This revealed a high level of expression for *D. geothermalis* glucoamylase, with a prominent band at 87.5 kDa. However there were no clear expression bands for *T. tengcongensis* or *C. violaceum* glucoamylases, which were expected to be situated at 79.1 kDa and 92.7 kDa respectively. Despite there not being any obvious expression using SDS page analysis, the clarified lysates were tested for amylolytic activity using the amylase assay described previously (section 2.5.2). In both cases, along with the *D. geothermalis* glucoamylase crude lysate, starch degradation was detected. Moreover, the starch degradation products were measured using an enzymatic glucose assay kit (Glucose GO assay kit, Sigma-Aldrich) with all three lysates displaying accumulation of glucose. In fact, when the enzymatically determined mass of starch and glucose were combined at an arbitrary time point within the assay (16 hours in this case), the total mass equalled the initial mass of starch (2.5 mg/mL) present at the beginning of the assay (Fig 4.7b). This indicated that the predominant hydrolysis product for all three enzymes was glucose, confirming their classification as exo-acting glucoamylases.

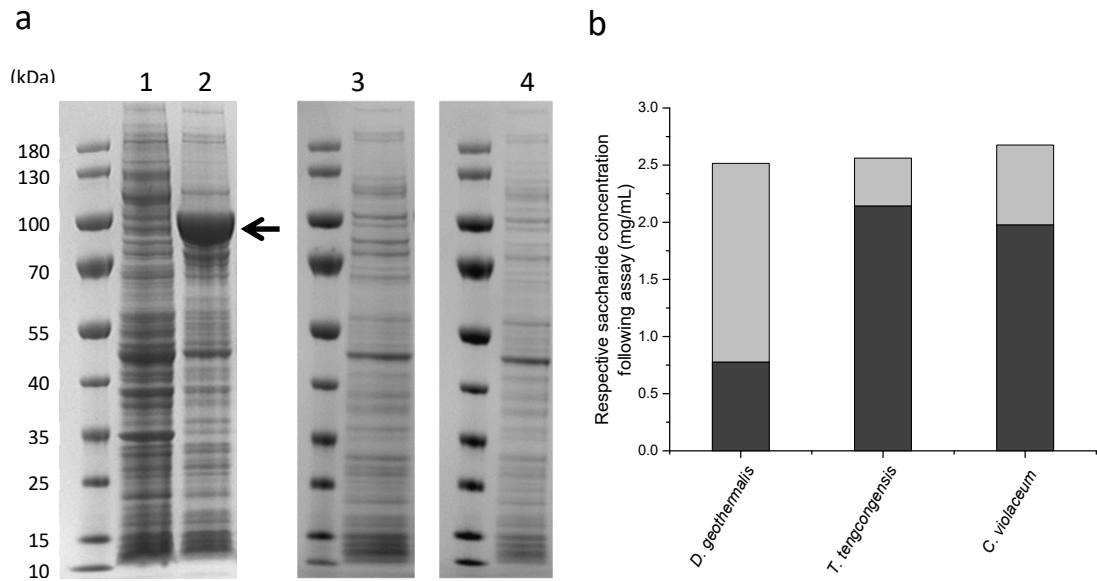


Figure 4.8 Glucoamylase expression and lysate activity

a) SDS page analysis of crude lysates from overnight cultures of *E. coli* BL21(DE3) harbouring either pQR1703 (lane 2), pQR1704 (lane 3), or pQR1705 (lane 4), with BL21(DE3) as untransformed control (lane 1), inoculated with 0.4 mM IPTG at an OD of 0.6-0.8 and cultured in LB for 24 hours at 30°C, 250 rpm. Arrow indicates presence of *D. geothermalis* glucoamylase (87.5 kDa) (lane 2) b) Clarified lysate activity measured at a single time point during amylase assay (16hr) and displayed as amount (mg/mL) of remaining starch (dark grey) determined by absorbance of starch/iodine complex at 600nm, and amount (mg/mL) of glucose accumulated (light grey) determined by Glucose GO assay kit (Sigma-Aldrich).

4.4.2 Further analysis of *D. geothermalis*, *T. tengcongensis* and *C. violaceum* glucoamylases

With initial investigations confirming all three enzymes displayed glucoamylase activity, a more detailed approach was applied to identify any differences between the already characterised *T. tengcongensis* glucoamylase, and the two novel enzymes from *D. geothermalis* and *C. violaceum*. Furthermore, in an attempt to increase the expression of each enzyme, and increase the likelihood they would be present in the soluble fraction, the incubation temperature was lowered to 25°C and LB was replaced by terrific broth (TB).

4.4.2.1 Expression of *D. geothermalis*, *T. tengcongensis* and *C. violaceum* glucoamylases and their conversion of starch to glucose

Both crude and clarified lysates of *E. coli* BL21(DE3) harbouring pQR1706, pQR1707, and pQR1708 (the pET28a based vectors) were run on SDS page (Fig 4.9a) following growth in terrific broth (TB) for 24 hours at a reduced culture temperature of 25°C (induction with 0.4 mM IPTG at an OD₆₀₀ of 0.8). As seen from initial expression studies the *D. geothermalis* glucoamylase crude lysate displayed a prominent band at 87.5 kDa, however there were no prominent bands in the clarified lysate sample, suggesting the majority of protein expressed was not soluble. Unlike initial expression studies the *C. violaceum* glucoamylase crude lysate under these conditions did contain a prominent band at 92.7 kDa, however again there were no noticeable bands in the clarified lysate. For the *T. tengcongensis* glucoamylase samples there were no obvious bands at the expected size (79.1 kDa) in either crude or clarified lysate. The clarified lysates for each enzyme were used in an amylase assay carried out at 37°C, from which samples were removed at specific time points and analysed for starch degradation and glucose accumulation (the latter determined using high performance anion exchange chromatography, section 2.5.10). Glucose accumulation measurements supported previous results determined enzymatically, showing that at an arbitrary time point within the amylase assay (1 hour in this case) the mass of starch remaining and the mass of glucose accumulated was more or less equal to the initial mass of starch at the beginning of the assay (2.5 mg/mL) (Fig 4.9b). It is worth noting at this point that cell densities were not normalised and expression levels were not the focus of the investigation, therefore the amount of starch degradation/glucose accumulation is not indicative of enzyme rate, as the amount of enzyme present was not known. One observation that can be made is that the combined mass of remaining starch and accumulated glucose for the *T. tengcongensis* enzyme was lower than for either of the two novel enzymes, coming in below the initial 2.5 mg/mL. The

logical conclusion is that the *T. tengcongensis* glucoamylase was converting a proportion of that starch into a different product, accounting for the negative value in the mass balance.

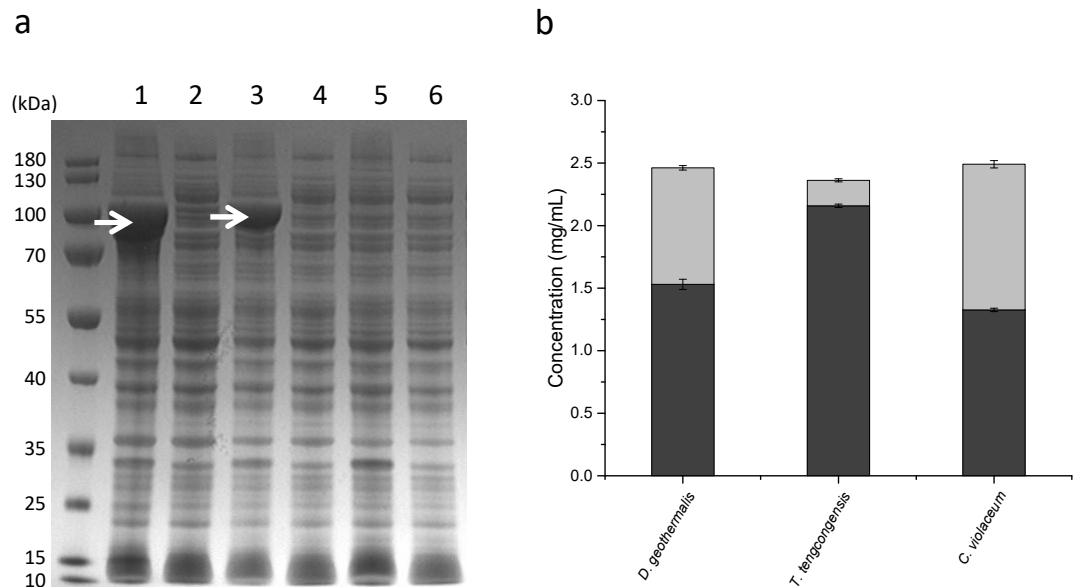


Figure 4.9 Further expression studies and clarified lysate effects on starch degradation and glucose accumulation for *D. geothermalis*, *T. tengcongensis* and *C. violaceum* glucoamylases

BL21(DE3) harbouring either pQR1706, pQR1707, or pQR1708, induced (0.4mM IPTG) at OD₆₀₀ of 0.8 and grown in TB for 24 hours at 25°C. a) Crude (whole cell) and clarified lysates analysed on SDS page for each construct; *D. geothermalis* glucoamylase whole cell lysate (lane 1) and clarified lysate (lane 2), *C. violaceum* glucoamylase whole cell lysate (lane 3) and clarified lysate (lane 4), *T. tengcongensis* glucoamylase whole cell lysate (lane 5) and clarified lysate (lane 6). Arrows indicate the presence of *D. geothermalis* glucoamylase (87.5 kDa) and *C. violaceum* glucoamylase (92.7 kDa) within the crude lysates (lanes 1 and 3 respectively). b) Clarified lysate activity measured at single time point during amylase assay (1hr) and displayed as amount (mg/mL) of remaining starch (dark grey) (starch degradation assay) and amount (mg/mL) of glucose accumulated (light grey) (High performance anion exchange chromatography). Error bars represent standard deviation, n=3.

4.4.2.2 Hydrolysis products of *D. geothermalis*, *T. tengcongensis* and *C. violaceum* glucoamylases

The chromatograms from the high performance anion exchange chromatography analysis of amylase assay samples at 1 hour for each clarified lysate show a clear difference in action between the *T. tengcongensis* enzyme and the two previously uncharacterised enzymes (Fig 4.10). The relatively small amount of glucose produced compared with other oligosaccharides suggests the *T. tengcongensis* glucoamylase had some endo-activity, whereas the *D. geothermalis* and *C. violaceum* glucoamylases produced more glucose relative to other oligosaccharides suggesting they had more pronounced exo-acting capabilities.

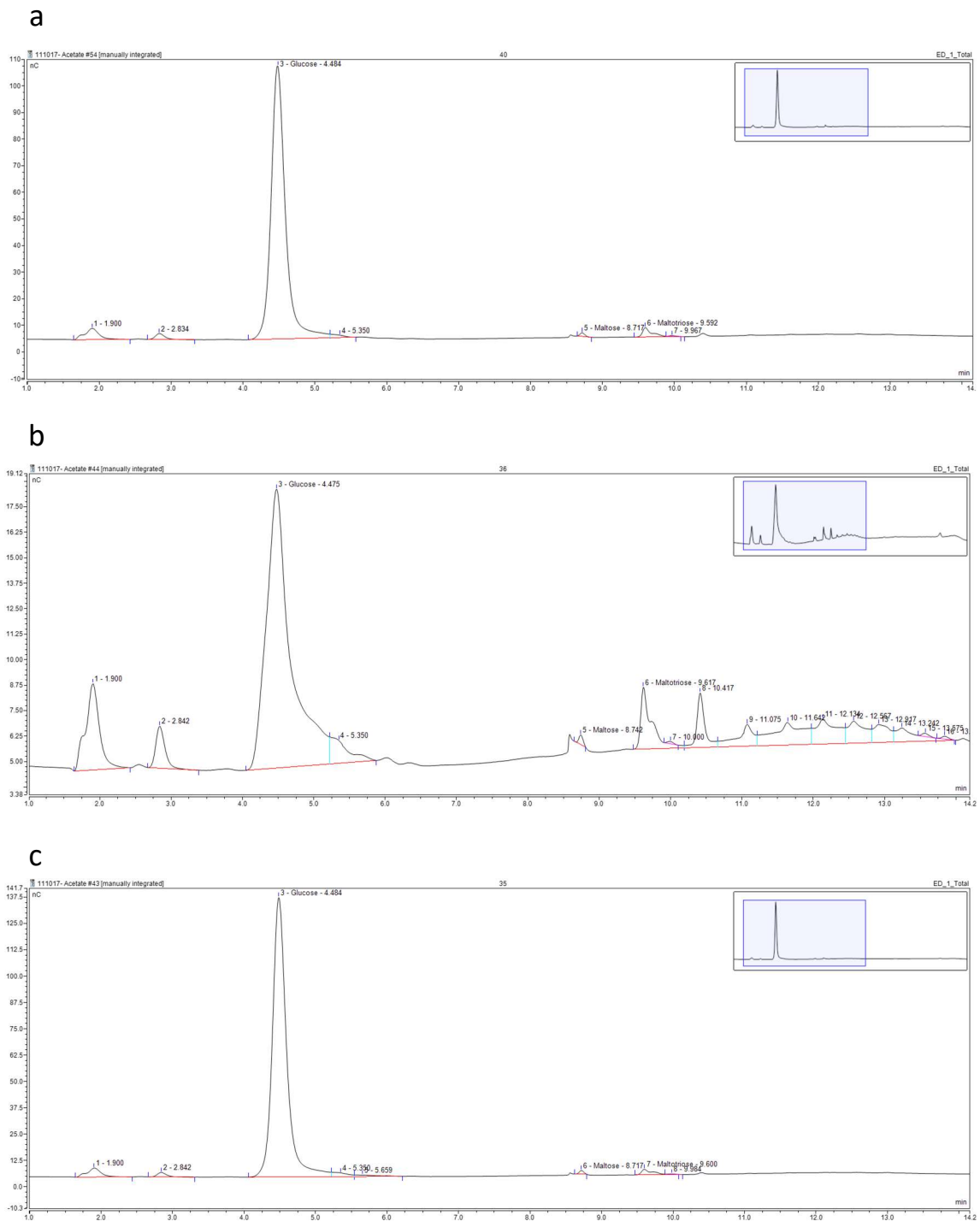


Figure 4.10 Chromatograms of *D. geothermalis*, *T. tengcongensis* and *C. violaceum* glucoamylase hydrolysis products

Example ICS chromatograms for amylase assay samples removed after 1 hour, for clarified lysates of *E. coli* BL21(DE3) expressing a) pQR1706, b) pQR1707, and c) pQR1708, cultured in TB for 24 hours at 25°C, 180 rpm (induced with 0.4 mM IPTG at an OD₆₀₀ of 0.8).

4.4.2.3 Clarified lysate activities for *D. geothermalis*, *T. tengcongensis* and *C. violaceum* glucoamylases

Amylolytic activity from clarified lysate has also been expressed in terms of units of amylase activity per mL of culture (Fig 4.11a), with units, in this case, defined as the disappearance of 1 mg/mL of starch/iodine complex per minute at an assay temperature of 37°C. Owing to the disparity in cell density between cultures amylase activity units have been normalised to dry cell weight (Fig 4.11b). (BL21(DE3) expressing the *T. tengcongensis* glucoamylase consistently achieved lower cell densities than the other two enzymes, in both LB and TB. Example OD₆₀₀ values from a single experimental run after 24 hours growth in TB at 25°C were as follows; OD₆₀₀ of 10 for *T. tengcongensis* glucoamylase; OD₆₀₀ of 33 for *D. geothermalis* glucoamylase; and OD₆₀₀ of 28 for *C. violaceum* glucoamylase) The normalised values indicate that despite an early observation that the *D. geothermalis* glucoamylase had higher expression levels compared with the other two enzymes, it is actually the *C. violaceum* glucoamylase which had the highest activity per gram of dry cell weight. When combined with glucose accumulation data (U defined as 1 mg/mL of glucose produced per minute at 37°C) normalised to dry cell weight (Fig 4.11c), the discrepancy between starch hydrolysis and glucose production for the *T. tengcongensis* glucoamylase is emphasised; further supporting the notion that the *T. tengcongensis* glucoamylase was not as exclusively exo-acting as the *D. geothermalis* and the *C. violaceum* glucoamylases.

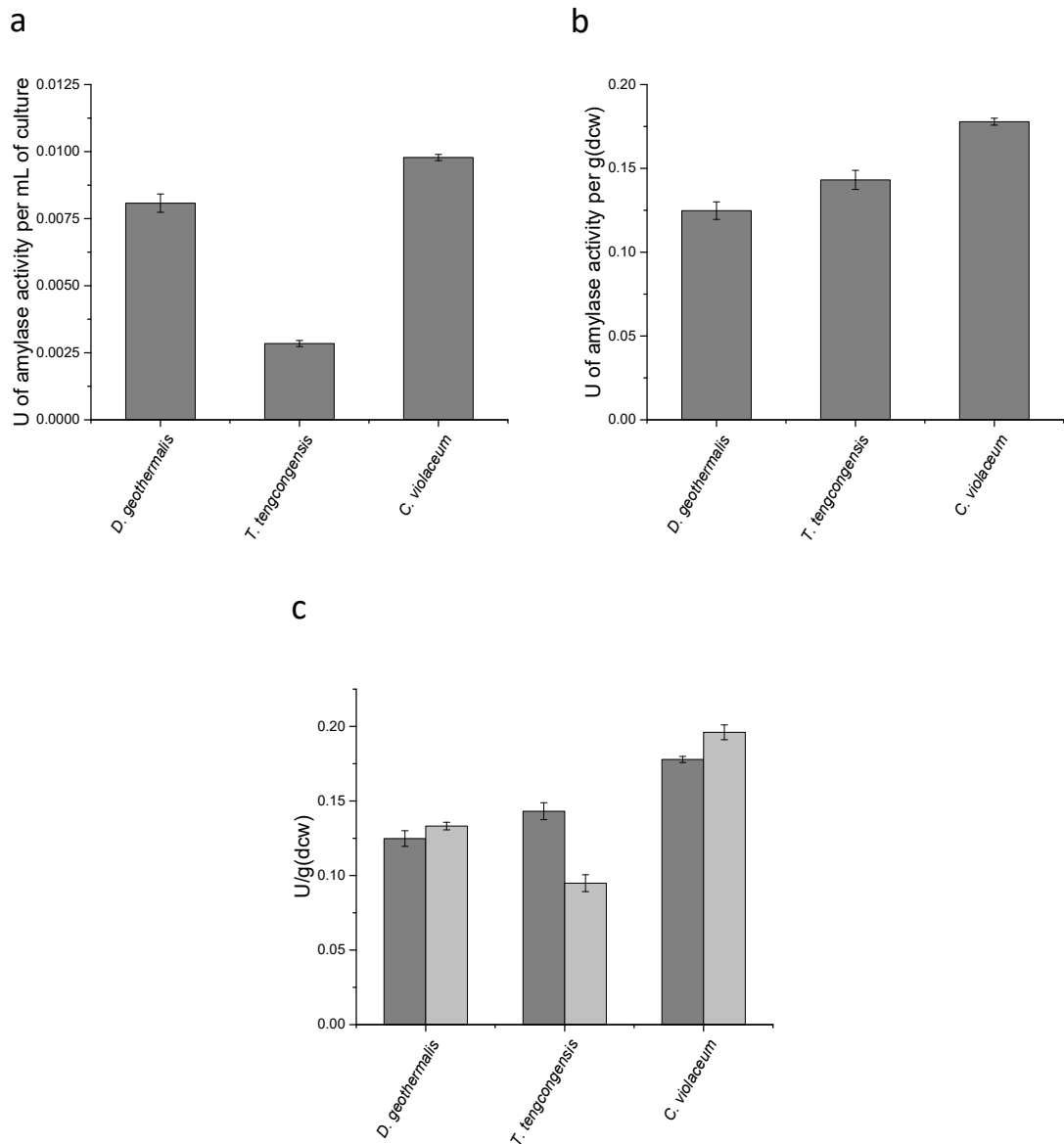


Figure 4.11 Clarified lysate activities for *D. geothermalis*, *T. tengcongensis* and *C. violaceum* glucoamylases expressed in terms of starch degradation and glucose production

a) Activity in units (disappearance of 1 mg/mL of starch/iodine complex per minute) per mL of culture. b) Activity in units (disappearance of 1 mg/mL of starch/iodine complex per minute) per gram of dry cell weight. c) Comparison in units of starch degradation (dark grey) (disappearance of 1 mg/mL of starch/iodine complex per minute) and glucose production (light grey) (accumulation of 1 mg/mL of glucose per minute) per gram of dry cell weight. Error bars represent standard deviation, n=3.

4.5 Investigating glucoamylase secretion

Owing to the fact that the already characterised *T. tengcongensis* glucoamylase appears less desirable in terms of application than the two novel glucoamylases, no further work has involved the use of this enzyme. The next section investigates secretion of *D. geothermalis* and *C. violaceum* glucoamylases, using both native signal sequences and the fusion of exogenous signal sequences.

4.5.1 Secretion of glucoamylases from native signal sequences

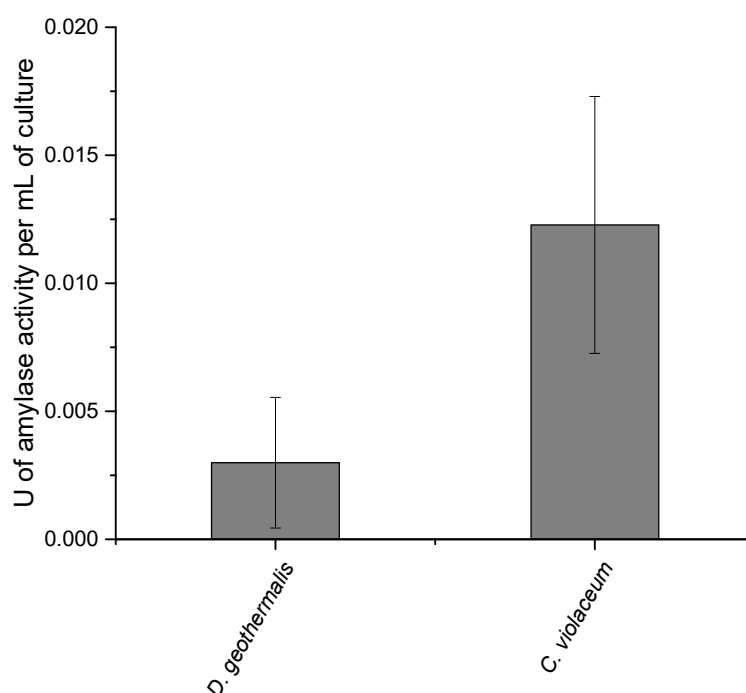


Figure 4.12 Extracellular media activity of *D. geothermalis* and *C. violaceum* glucoamylases

Cultures of *E. coli* BL21(DE3) harbouring either pQR1703 or pQR1705 grown in LB media for 24 hours at 37°C, 250 rpm and induced with 0.4 mM IPTG at an OD₆₀₀ of 0.6-0.8. Glucoamylase activity within the extracellular media expressed as units (defined as the disappearance of 1 mg/mL of starch-iodine complex per minute) per mL of culture media. Error bars represent standard deviation, n=6.

The two novel glucoamylases were analysed using the SignalP 4.1 server [95] to determine whether the enzymes contained native signal sequences. Only the *C. violaceum* glucoamylase was positive for a signal sequence, a result confirmed experimentally when the extracellular media of *E. coli* BL21(DE3) harbouring each of the two glucoamylase constructs (pQR1703 and pQR1705) was measured for amylolytic activity. The *C. violaceum* glucoamylase culture (pQR1705) displayed significantly higher amylolytic activity in the extracellular media than the *D. geothermalis* culture (pQR1703) (Fig 4.12). Despite the latter not containing a native signal sequence, there was still detectable amylolytic activity within the extracellular media. This could conceivably be explained by small amounts of *D. geothermalis* glucoamylase being released as a result of cell lysis during culture.

4.5.2 Improvement of secretion through addition of signal sequences

In an attempt to improve secretion for *D. geothermalis* and *C. violaceum* glucoamylases, a strategy was developed to insert new signal sequences at the N-terminus of each gene (Fig 4.13). For the *D. geothermalis* glucoamylase the signal sequences selected were the DsbA signal sequence and the PelB signal sequence (section 1.6). Both of which were synthesised as complementary oligo nucleotides, with the 5' end of the sense strand and the 3' end of the antisense strand staggered to form a join compatible with an *Xba*I restriction site. The 3' end of the sense strand and the 5' end of the antisense strand were designed to be staggered forming a join compatible with an *Nde*I restriction site. A ribosome binding site and a spacer region were included between the *Xba*I restriction site and the start codon. Following *Xba*I/*Nde*I digestion of pQR1703 the annealed oligo nucleotides were ligated forming pQR1703-DsbA and pQR1703-PelB, designated pQR1709 and pQR1710 respectively. The addition of an alternative signal sequence to the *C. violaceum* glucoamylase was more complicated as the native sequence needed to be removed. To do this the enzyme was re-cloned using a forward primer which excluded the native signal

sequence but contained an *Nde*I site (including a start codon) in the overhanging region. The truncated gene was then cloned into pET29a forming pQR1711, whereby the same strategy as above could be applied. Only the DsbA signal sequence was used in this case, forming the vector pQR1712.

Given that *D. geothermalis* glucoamylase did not contain a native signal sequence the initial lack of secretion was not unexpected. Surprisingly however, the addition of the DsbA signal sequence or the PelB signal sequence to the N-terminus of the gene did not improve secretion (Fig 4.14a). Furthermore, the clarified lysate activities of *D. geothermalis* glucoamylase containing additional signal sequences were reduced when compared to the native enzyme. The attempts to secrete the *D. geothermalis* glucoamylase with each type of signal peptide were unsuccessful, and actually appeared to have a negative impact on overall expression. Conversely, the addition of the DsbA signal sequence to the *C. violaceum* glucoamylase enhanced secretion (Fig 4.14b). Prior to addition, the removal of the native signal sequence reduced both extracellular media and clarified lysate activities, but these were rescued following addition of the DsbA signal sequence which displayed increased activity in the extracellular media compared with the native signal sequence. This was further enhanced when the activity was normalised to dry cell weight (Fig 4.14c).

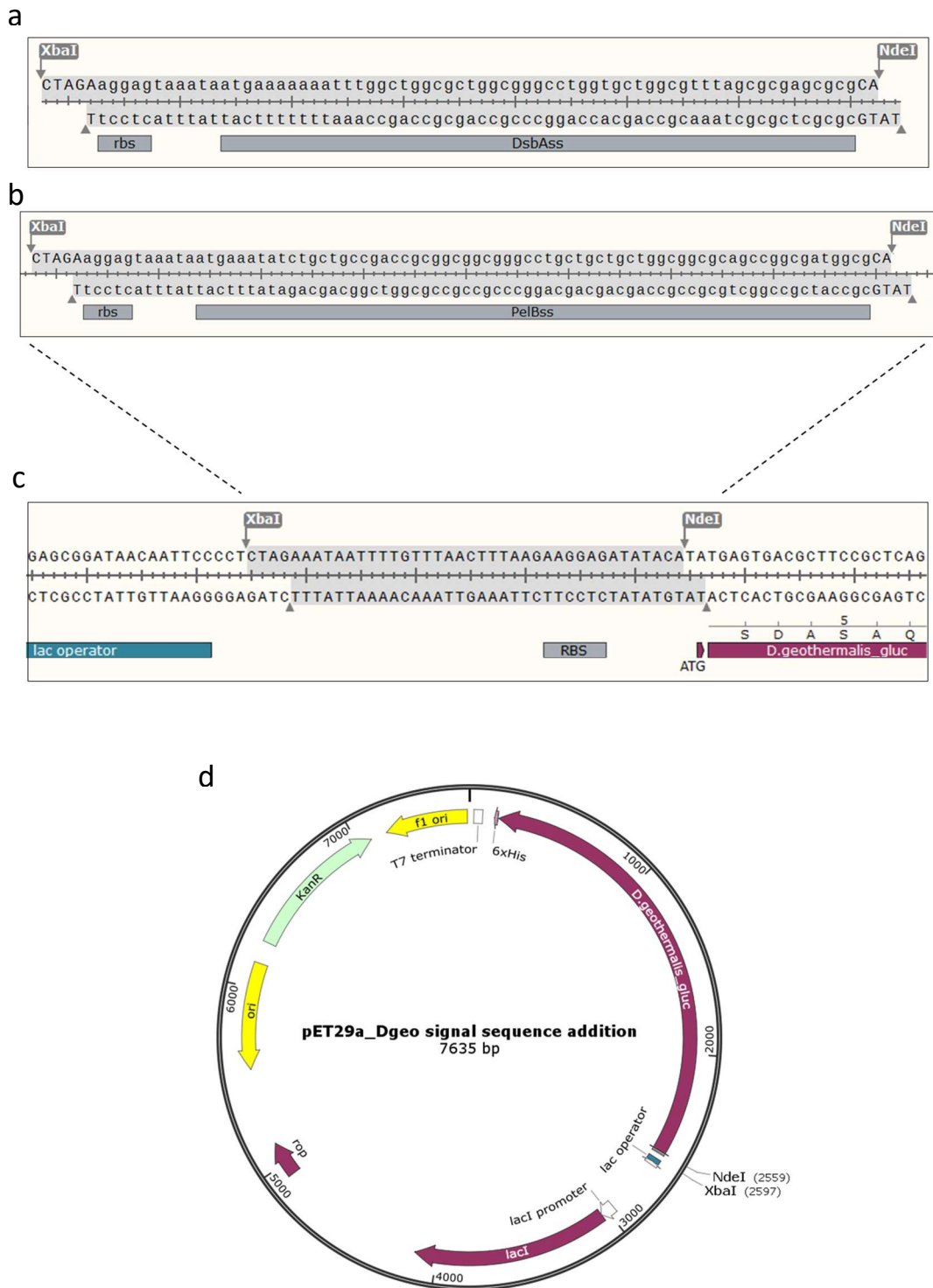


Figure 4.13 Diagram of signal sequence insertion using complementary oligonucleotides

Two oligonucleotides annealed to form the DsbA (a) and the PelB (b) signal sequence, plus an additional RBS and jagged ends complementary to an *XbaI* restriction site upstream and an *NdeI* restriction site downstream of the sequence. c) The location in to which the signal sequences are ligated, between the *XbaI* and *NdeI* sites within the original vector (d) (pQR1703 has been used as an example).

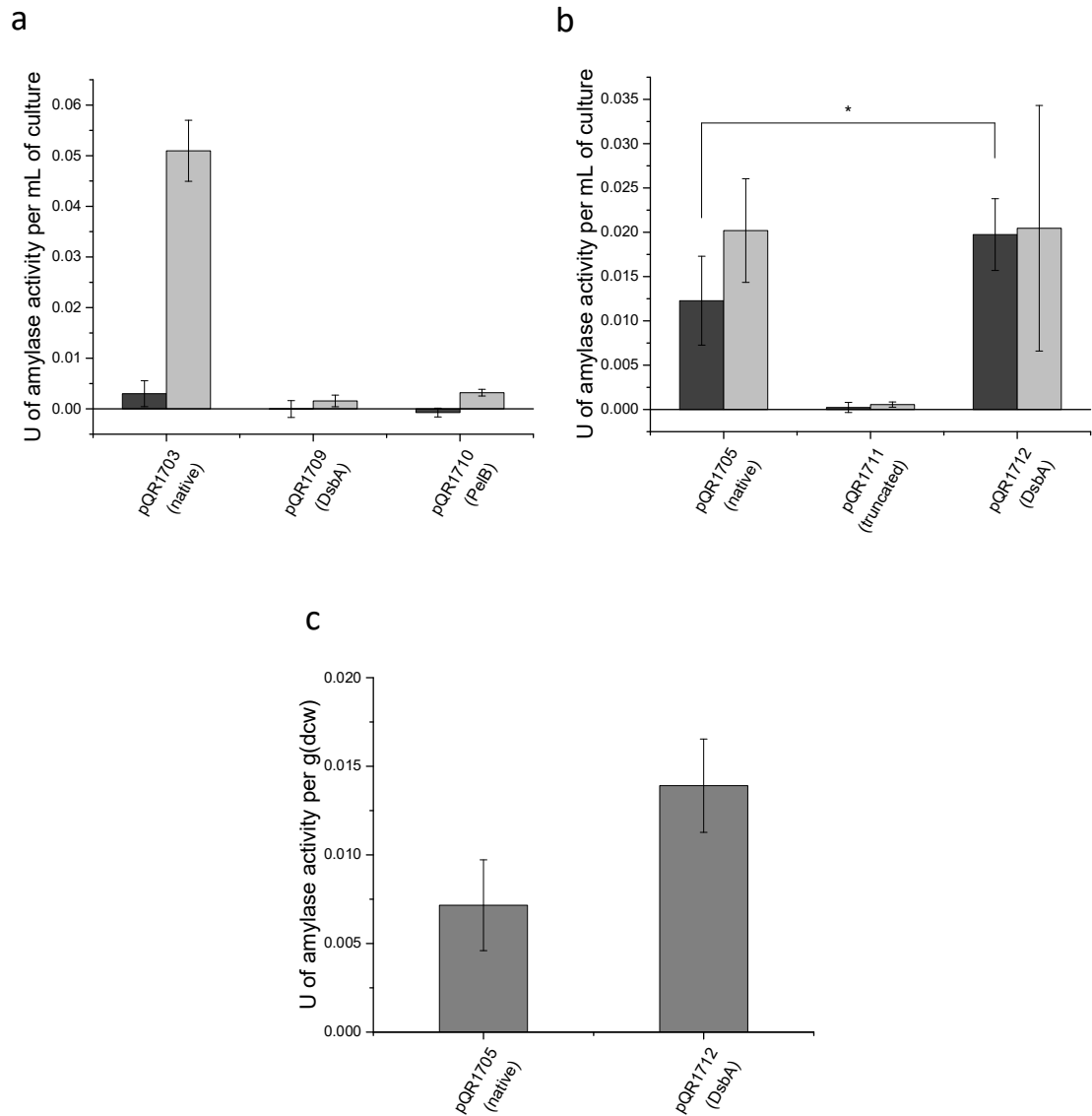


Figure 4.14 Activity of *D. geothermalis* and *C. violaceum* glucoamylases following addition of exogenous signal sequences

E. coli BL21(DE3) harbouring either a) pQR1703, pQR1709 (*D. geothermalis* glucoamylase with DsbA signal sequence) or pQR1710 (*D. geothermalis* glucoamylase with PelB signal sequence), or b) pQR1705, pQR1711 (truncated *C. violaceum* glucoamylase) or pQR1712 (*C. violaceum* glucoamylase with DsbA signal sequence), cultured for 24 hours in LB (induced with 0.4 mM IPTG at an OD₆₀₀ of 0.6-0.8). Either extracellular media activity (dark grey) or clarified lysate activity (light grey) determined by amylase assay and expressed in units per mL of culture volume. c) Extracellular media activity of *C. violaceum* glucoamylase with native (pQR1705) or exogenous (pQR1712) signal sequence normalised to dry cell weight. Error bars represent standard deviation, n=6.

4.6 Growth characteristic of *E. coli* expressing and secreting *C. violaceum* glucoamylase

Following the unsuccessful secretion attempts of *D. geothermalis* glucoamylase, the *C. violaceum* glucoamylase was identified as the most suitable candidate enzyme for use in a starch degrading, self-feeding *E. coli* strain. The following section describes the degradation of starch in culture conditions and the ability of *E. coli* expressing this enzyme to utilise starch as a sole carbon source.

4.6.1 Effects of temperature on the relative activity of *C. violaceum* glucoamylase

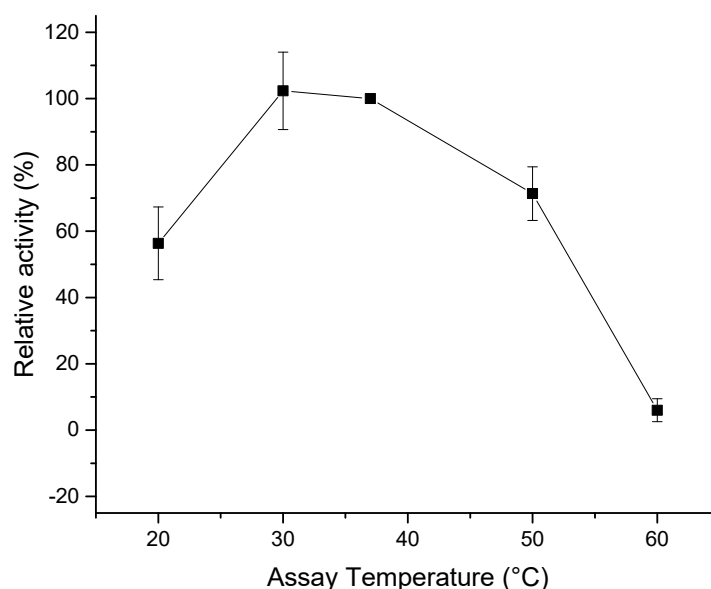


Figure 4.15 Relative enzyme activity of *C. violaceum* glucoamylase over a range of temperatures

Extracellular media activity from 24 hour cultures of *E. coli* BL21(DE3) harbouring pQR1705 grown in LB (induced with 0.4 mM IPTG at an OD₆₀₀ of 0.6-0.8), determined using amylase assays carried out at a range of temperatures (20°C to 60°C). Activity expressed as a percentage of the standard assay carried out at 37°C. Error bars represent standard deviation, n=3.

It is already known that *C. violaceum* glucoamylase can degrade starch at 37°C. Activity assays using extracellular media samples following an overnight culture were used to conduct an amylase assay at a range of temperatures in order to determine the relative activity, particularly at more typical *E. coli* culture temperatures of 25°C to 37°C. It was found that the optimum temperature for this enzyme was about 30°C (Fig 4.15), further emphasising its candidacy for the particular role to which it is being applied.

4.6.2 *E. coli* secreting *C. violaceum* glucoamylase and its utilisation of starch as a sole carbon source

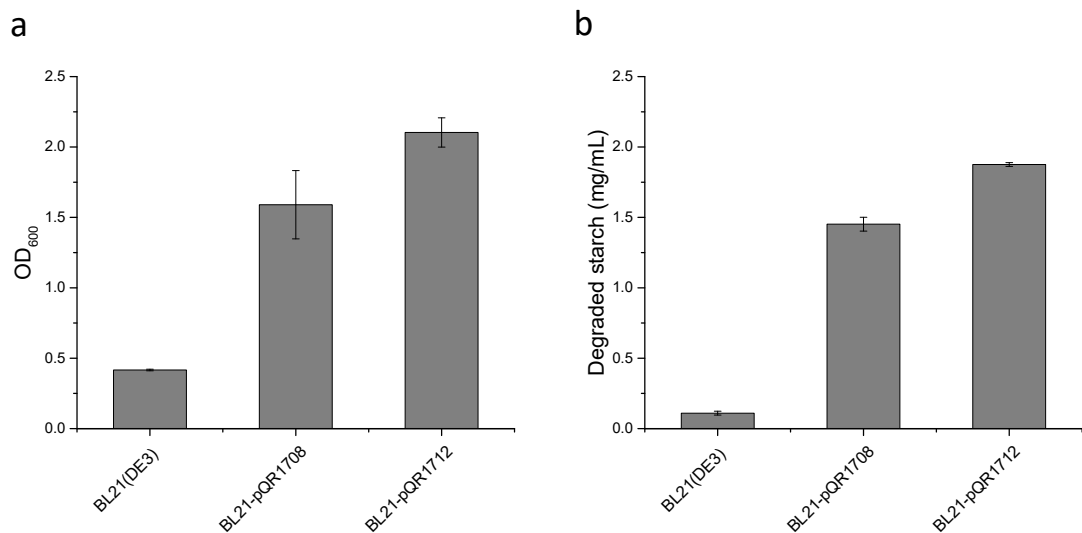


Figure 4.16 *E. coli*'s utilisation of starch as a sole carbon source through the expression and secretion of *C. violaceum* glucoamylase

E. coli BL21(DE3) harbouring either pQR1708 (native signal sequence) or pQR1712 (DsbA signal sequence) cultured over a 24 hour period at 30°C 250 rpm, in glucose free MSM, supplemented with 2.5 mg/mL starch. a) Cell density (OD₆₀₀) after 24 hours of culture. b) Amount of starch degraded (mg/mL) in culture media after 24 hours of culture, determined by starch degradation assay. Error bars represent standard deviation, n=3.

It has already been demonstrated that *E. coli* expressing *S. thermoviolaceus* α -amylase can grow using starch as a sole carbon source (Fig 3.14). BL21(DE3) harbouring either pQR1708

or pQR1712 were cultured in glucose free MSM supplemented with 2.5 mg/mL starch, and resulted in similar cell densities as those previously seen with *S. thermoviolaceus* α -amylase (Fig 4.16a, refer to Fig 3.14 for α -amylase data). Cell density appeared to be correlated with the amount of starch degraded (Fig 4.16b), with the enhanced secretion of glucoamylase from pQR1712 showing greater starch degradation in the media and leading to a higher cell density. Unfortunately no data involving these constructs is available for W3110, owing to the fact they include a T7 promoter and are not inducible. The following Chapter explores in greater detail vectors designed specifically for the expression of *C. violaceum* glucoamylase within W3110.

4.7 Discussion and conclusion

The *A. niger* glucoamylase was the initial target for recombinant expression within *E. coli*, given its prior use within an enzyme-based fed-batch fermentation system [34]. However, difficulties were encountered expressing this enzyme within *E. coli*, likely the reason why recombinant expression has not been reported previously. As a result other glucoamylases which have previously been successfully expressed in *E. coli* were investigated. The glucoamylase gene from *S. diastaticus*, which had been heterologously expressed in *E. coli* [65], was cloned from genomic DNA, however no functional expression was detected. An alternative approach was to investigate bacterial glucoamylases, based on the notion that *E. coli* is better equipped to express bacterial proteins than fungal proteins, particularly in the case of glucoamylases which generally require complex post-translational modification [64]. A literature search revealed that there were surprisingly few bacterial glucoamylases which had been characterised, however, one was found from *T. tengcongensis* which had been successfully expressed in *E. coli* [66]. Using this previously characterised enzyme as a basis, a bioinformatics approach was used to identify enzymes with a similar homology

which were present in a library of organisms available in-house. Out of the 17 enzymes which matched the criteria, two putative glucoamylases from *D. geothermalis* and *C. violaceum* were the most closely related to the *T. tengcongensis* glucoamylase, and were therefore selected for cloning and characterisation.

Characterisation studies revealed that the two novel enzymes were more exo-acting than the previously characterised *T. tengcongensis* glucoamylase, with high performance anion exchange chromatography data displaying an increased accumulation of glucose relative to longer chain oligosaccharides when the two novel glucoamylases hydrolysed starch. Furthermore, the mass balance of starch hydrolysis and glucose accumulation was less negative for both the *D. geothermalis* and the *C. violaceum* glucoamylases, than for the *T. tengcongensis* glucoamylase, suggesting an accumulation of product other than glucose for the latter enzyme.

The ability of the *D. geothermalis* and the *C. violaceum* glucoamylases to be secreted into the extracellular media was also investigated. The *C. violaceum* glucoamylase contains a native signal sequence in contrast to the *D. geothermalis* glucoamylase, which was reflected in measured amylolytic activities in the respective extracellular media. The addition of exogenous signal sequences to the N-terminus of the *D. geothermalis* glucoamylase did not appear to improve secretion; however, the replacement of the native signal sequence from the *C. violaceum* glucoamylase with the DsbA signal sequence did improve secretion. The fact that the *D. geothermalis* glucoamylase does not contain a recognisable native signal sequence suggests it is not usually exported and therefore may not be the best candidate enzyme for an extracellular application. Indeed, despite the addition of the DsbA signal sequence or the PelB signal sequence, no activity in the extracellular media was detected, suggesting that *D. geothermalis* glucoamylase is not easily secreted through either the SRP or Sec pathways. Conversely, the *C. violaceum*

glucoamylase is naturally secreted, and apparently capable of secretion by *E. coli* via both the native signal sequence and the exogenous DsbA signal sequence.

Secreted *C. violaceum* glucoamylase via either signal peptide showed considerable glucose releasing amyolytic activity in the extracellular media, enough to allow expression strains to degrade starch contained within the medium during growth. Furthermore, *E. coli* BL21(DE3) expressing and secreting *C. violaceum* was able to utilise starch as a sole carbon source, which is to our knowledge the first example of *E. coli* converting starch directly to glucose for growth. The next Chapter describes the application of this as a novel feeding strategy to mimic fed-batch fermentation in batch cultures, and attempts to use the new chassis as a platform to increase yield of recombinant protein expression in shake flasks.

5 Towards a self-secreting enzyme-based fed-batch fermentation system

5.1 Introduction

Enzyme-based glucose limited fed-batch fermentation is an established technology which has been shown to enhance biomass and recombinant protein expression in lab scale cultures. However, to date there have been no successful attempts at designing a self-contained enzyme-based fed-batch system using a cell engineering approach. Having already demonstrated the ability of amyolytic enzyme secreting *E. coli* strains to utilise starch as a carbon source, this Chapter explores the application of these strains as a means to increase cell mass over traditionally used complex media, and ultimately provide a basis for recombinant protein expression using starch as a substrate, which can outperform glucose in batch culture.

As discussed, glucoamylases offer some advantages over α -amylases for this purpose, owing to their respective hydrolysis product profiles, with the slow release of glucose from the former mirroring both traditional fed-batch and current enzyme-based fed-batch fermentation strategies. As such, much of the work focusses on strains secreting the *C. violaceum* glucoamylase with the enhanced DsbA signal peptide. The regulation of amyolytic enzyme expression, in terms of both induction and rate of secretion throughout the culture, is also investigated, and involves the characterisation of a glucose sensitive promoter for the purpose of self-regulation. Finally, the ability of amyolytic self-secreting strains to provide a platform for recombinant protein expression using starch as a substrate, and ultimately achieving higher recombinant protein yield than is possible with glucose in batch culture, is examined using a combination of co- and dual-expression constructs.

5.1.1 Overview of Chapter 5

This Chapter draws together components from the two previous Chapters in an attempt to examine in greater detail a cell engineering approach to enzyme-based fed-batch fermentation. Given the multiple threads running throughout Chapter 5, the following overview provides a brief explanation and guide to its structure.

The Chapter begins by examining the growth of an amylolytic *E. coli* strain within a commercially available enzyme-based fed-batch high cell density media, as a proof of concept for self-secretion leading to increased biomass. This follows on from conclusions made in Chapter 3 which suggested the concentrations of starch and glucose tested within LB was not high enough for overflow metabolism to be an important factor. For the purposes of these initial experiments the original α -amylase secreting strain, W3110 harbouring pQR187, has been used (Figs 5.1 and 5.2).

The commercially available media then provides a basis for the development of a defined media (MSM) containing starch-agar layers in an attempt to allow for the sufficient provision of carbon necessary for high cell density growth (Fig 5.3). Shake flasks containing starch-agar layers and glucose-free MSM are used for growth characterisation studies throughout the rest of the Chapter. Initially W3110 expressing and secreting α -amylase is cultured using starch-agar layers as a proof of principle (Fig 5.4). Further investigations are then carried out to determine if there are any potential differences in growth between W3110 and BL21(DE3) expressing and secreting α -amylase and whether starch can provide any advantage over more traditionally used glucose at these higher concentrations (Fig 5.5). Incorporating some elements of Chapter 4, the growth of BL21(DE3) expressing and secreting *C. violaceum* glucoamylase with the exogenous DsbA signal sequence is then characterised using glucose free MSM with starch-agar layers (Fig 5.6).

Owing to the ability of the BL21(DE3) strain to be less susceptible to overflow metabolism than K12 strains, the next section focusses on the design and construction of vectors which contain promoters to allow for the expression of the *C. violaceum* glucoamylase in W3110. Firstly, a glucose sensitive promoter is identified and subsequently characterised using eGFP as a reporter protein (pQR1714, Figs 5.7 and 5.8). A vector is then constructed from which the glucose sensitive promoter drives the expression of the *C. violaceum* glucoamylase containing the DsbA signal sequence (pQR1715, Fig 5.9), and is further characterised via extracellular glucoamylase activity following growth in LB containing various concentrations of glucose (Fig 5.10). Lastly this construct is used in growth experiments and starch degradation studies, in both LB (Fig 5.11) and glucose free MSM with starch-agar layers (Fig 5.12).

The final part of the Chapter aims to establish whether the increased biomass achieved with the self-secreting amylolytic *E. coli* strains can be reflected by an increase in yield for a recombinant protein of interest. Firstly co-expression studies are carried out using α -amylase and an *E. coli* derived transketolase as the protein of interest, cultured in both LB and the commercially available media used previously (Fig 5.13). Co-expression is then attempted in glucose free MSM containing starch-agar layers, using the glucose sensitive *C. violaceum* glucoamylase construct alongside the transketolase (Fig 5.14). An alternative approach is also investigated, involving the design and construction of dual-expression vectors i.e. where the amylolytic enzyme and the recombinant protein of interest are expressed from the same plasmid. Initially a pUC19 backbone is used to express α -amylase alongside eGFP as the protein of interest (Fig 5.15 and 5.16), with expression of each enzyme characterised in LB media (Fig 5.17) and later using starch as a sole carbon source in glucose free MSM (Fig 5.18). Finally a dual-expression vector is designed and constructed containing the *C. violaceum* glucoamylase with the attached DsbA signal sequence alongside eGFP as the protein of interest (pQR1720, Fig 5.19). This is characterised in

glucose free MSM containing starch-agar layers, providing the first demonstration of enhanced recombinant protein production as a direct result of self-secreting enzyme-based fed-batch fermentation (Fig 5.20).

5.2 Expression and secretion of α -amylase within commercially available high density media

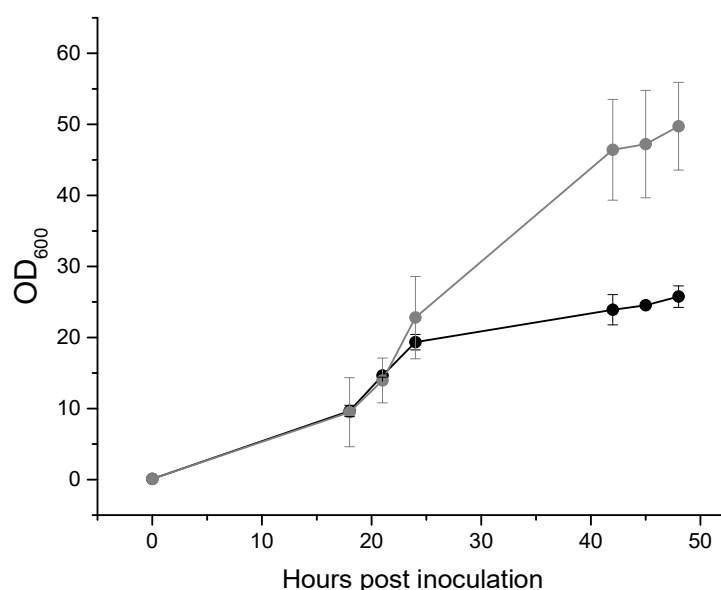


Figure 5.1 Growth curves of α -amylase secreting *E. coli* cultured in commercially available high cell density media

E. coli W3110 (black) and W3110 harbouring pQR187 (grey) cultured as per the EnPresso® growth system protocol (see materials and methods, section 2.4.4). The untransformed control (W3110) required the addition of reagent A (externally supplied amylolytic enzyme), whereas W3110 harbouring pQR187 was cultured in the absence of reagent A and instead induced with 0.4 mM IPTG at inoculation. Error bars represent standard deviation, n=3.

In media specifically designed for the slow release of glucose from starch, *E. coli* W3110 expressing α -amylase was able to grow to considerably higher densities than non-expressing W3110 (Fig 5.1). Both transformed and untransformed cells were grown according to the EnPresso® growth system protocol (see section 2.4.4), with the only

exception being that the α -amylase expressing strain did not require the addition of reagent A (a glucoamylase derived from *A. niger*), whereas the non-expressing control did require the addition of reagent A (i.e. starch degradation in cultures containing expressing cells was due to the self-secretion of α -amylase, but in cultures containing the non-expressing control, starch degradation was the result of externally supplied *A. niger* glucoamylase). The enhanced growth seen by W3110 expressing α -amylase over the externally supplied enzyme control not only establishes a proof of concept for self-secretion, but also highlights the potential in using a self-secreting strain to achieve cell densities in excess of those which can be achieved using current commercially available systems.

Consistent with previous results when W3110 harbouring pQR187 was grown in LB media (Fig 3.3), the expression levels of α -amylase increased throughout the EnPresso® culture period, as is seen from samples of clarified lysate analysed by SDS page (Fig 5.2a) i.e. qualitatively there was a more prominent α -amylase band (47 kDa) at 32 hours post booster addition than at 2 hours post booster addition. An increase in activity over time within the extracellular media was also observed (Fig 5.2b). As expected, there was an overall increase in activity within the extracellular media when normalised to cell density (dry cell weight) throughout the culture (Fig 5.2c). However, activity initially decreased, before increasing again, presumably because growth rate exceeded the rate of α -amylase expression when the booster was first added.

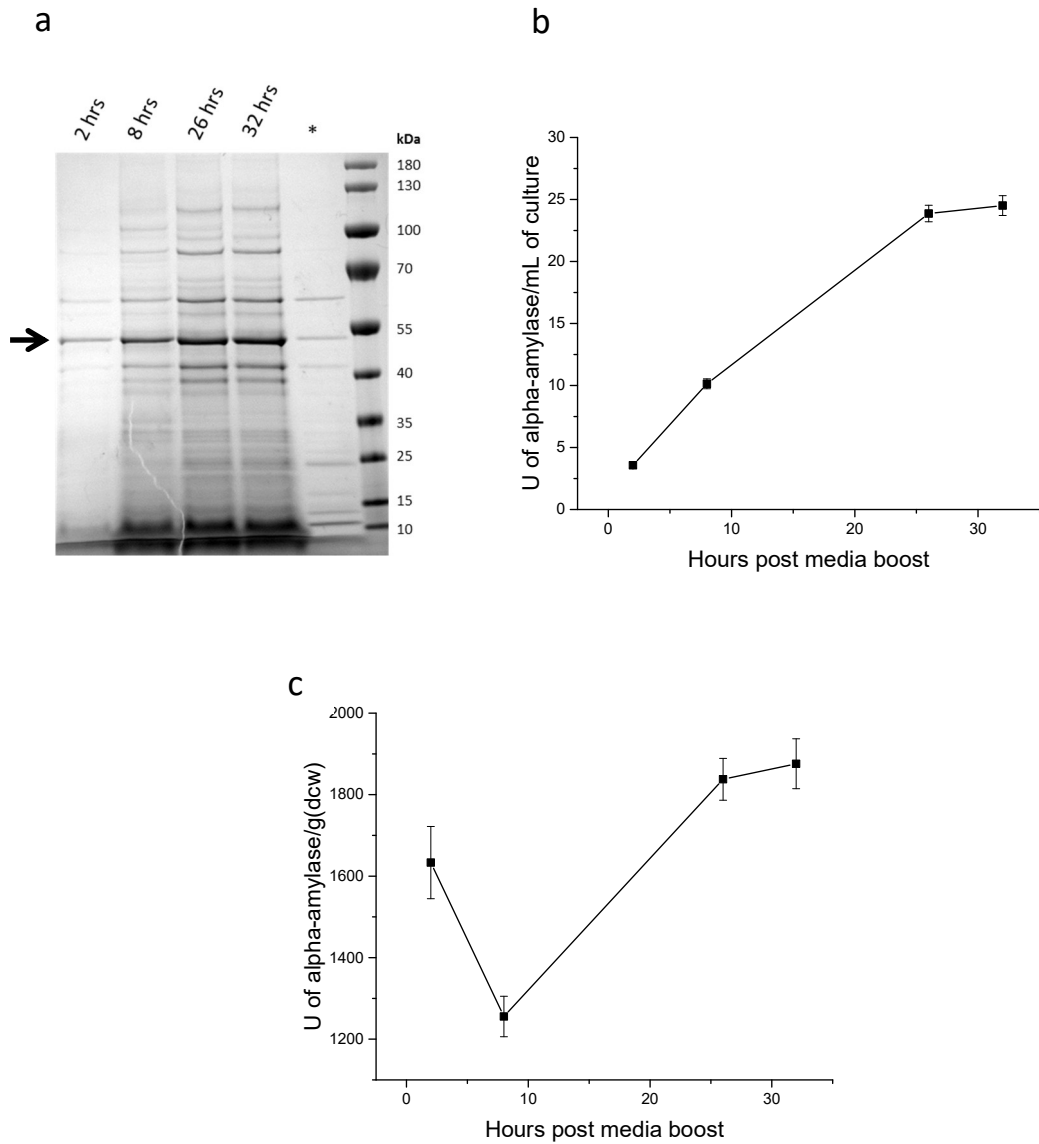


Figure 5.2 α-amylase expression over time in commercially available high density media

E. coli W3110 harbouring pQR187 grown as per the EnPresso® growth system protocol, induced at inoculation (0.4 mM IPTG) and excluding the additional reagent A. a) SDS page of clarified lysate at time points post induction. (*) indicates a repetition of the 2 hour time point. Arrow indicates *s. thermoviolaceus* α-amylase (47 kDa). Extracellular media activity determined by amylase assay and expressed in units of α-amylase activity per mL of culture volume (b) or units of α-amylase activity normalised to dry cell weight (c). Error bars represent standard deviation, n=3.

5.3 Starch-agar layer development for sufficient provision of carbon

Initial experiments described in Chapter 3 (Fig 3.7b and Fig 3.14b) indicated the amount of glucose added to the media (LB or MSM) thus far had not been large enough to have had any detrimental effects on growth i.e. the control groups containing an equivalent amount of glucose revealed that up to 20 mg/mL glucose did not have a negative influence on growth (albeit in microwell plate conditions), presumably meaning that overflow metabolism was not an important factor at this concentration in these conditions. Investigating growth in media with glucose concentrations beyond 20 mg/mL is fairly trivial, but dissolving starch at higher concentrations is particularly challenging. Given the difficulty of dissolving starch at concentrations in excess of 20 mg/mL, a commercially available media (EnPresso® growth system), in which starch is added in tablet form and dissolved into the media over time, was used as a proof of concept for achieving high densities with self-secreting cells (Fig 5.1). However, the exact composition of this media has been difficult to determine, a situation which necessitated the development of a high density media that is both defined and has the capacity to contain starch in a large enough quantity to support high density growth. As a result a previously established starch layer system [34] was modified to allow for sufficient release of starch into a liquid phase comprised of glucose free mineral salt medium (MSM) in 500 mL shake flasks (Fig 5.3). The process involved dissolving starch (using an autoclave) at a concentration of 50 mg/mL into 50 mL of 20 mg/mL agar, which once solidified was then capped with a 50 mL 50 mg/mL agar layer, preventing mechanical disruption by the liquid media above. Starch was then able to dissolve into the liquid media by diffusion throughout the culture period. Preliminary experiments revealed the actual method of starch diffusion was less reliant on the composition or size of the agar cap (contradicting the study in which the system was

developed, which itself suggested the agar percentage and thickness of the cap were important factors), but influenced to a greater extent by contact between the liquid media and the starch-agar layer via the sides of the flask. Although the starch-agar layer loses contact with the sides and bottom of the flask, allowing for mixing between the two phases, the conical shape of the flask prevents the agar cap from rising and therefore keeps the starch-agar layer beneath the liquid layer. At these specified concentrations the starch layer can theoretically provide up to 2.5 g of starch per flask. Fig 5.3c gives an indication of the diffusion of starch from the storage gel into the liquid media throughout the culture period, without the presence of cells. Within 24 hours, diffusion led to starch concentrations of over 10 mg/mL in the liquid phase.

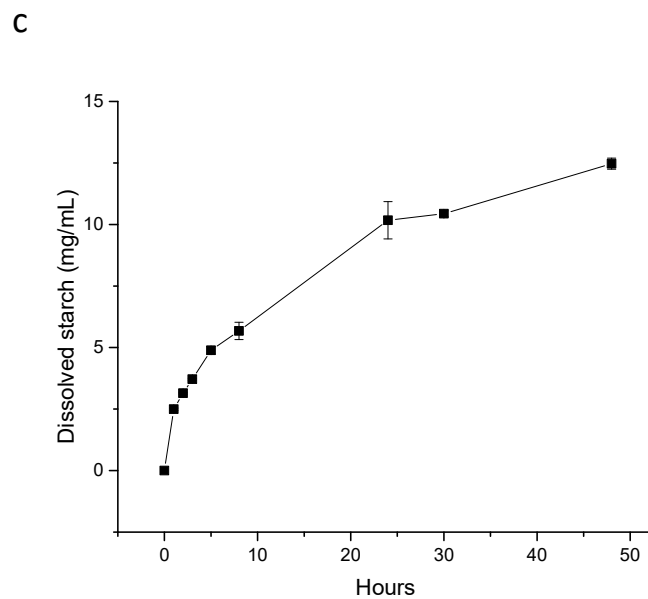
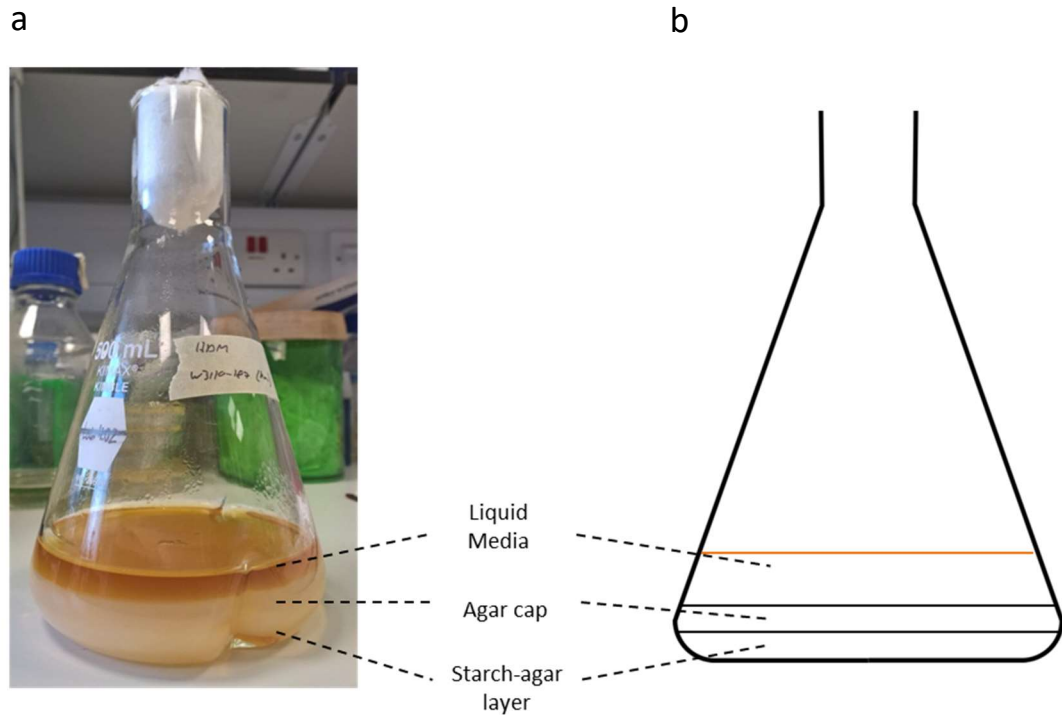


Figure 5.3 Design of starch-agar layer system for sufficient provision of carbon for high cell density applications

Photograph (a) and diagram (b) of the starch-agar layer design containing as a bottom layer 50 mL of 50 mg/mL starch and 20 mg/mL agar. Above this an agar cap consisting of 50 mL of 50 mg/mL agar and a top layer of liquid media (glucose free MSM). c) Diffusion of starch from the starch-agar layer into the liquid media from flasks containing no cells measured by starch degradation assay of liquid media samples over time with concentration calculated using a standard curve. Error bars represent standard deviation, $n=3$.

5.3.1 Growth studies using starch-agar layers and *E. coli* secreting *S. thermoviolaceus* α -amylase

E. coli W3110 expressing *S. thermoviolaceus* α -amylase was able to grow in flasks containing glucose free MSM with starch-agar layers, whereas non-expressing cells were unable to grow beyond initial inoculum densities (Fig 5.4). This mirrors previous results showing W3110 expressing α -amylase was able to utilise starch as a sole carbon source (Fig 3.14a). Moreover, these results go further by indicating W3110 expressing α -amylase can achieve higher cell densities than are generally seen with LB when a sufficient amount of starch is supplied within glucose free MSM.

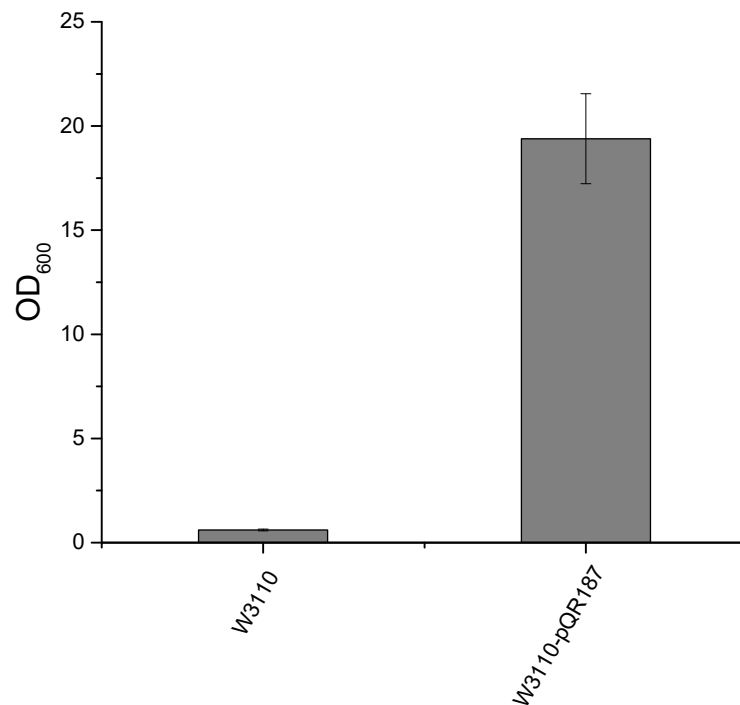


Figure 5.4 Increased cell densities for *E. coli* W3110 expressing *S. thermoviolaceus* α -amylase using the starch-agar layer system

Final cell densities for either untransformed *E. coli* W3110 or W3110 harbouring pQR187 grown in flasks containing the starch-agar layer system and glucose free MSM, incubated at 30°C, 180 rpm for 24 hours (induced with 0.4 mM IPTG at inoculation (inoculum equivalent to an initial OD₆₀₀ of 0.1)). Error bars represent standard deviation, n=3.

To determine whether or not growth on starch offers any advantage in terms of final cell density compared with growth on glucose, an equivalent amount of glucose (50 mg/mL) was dissolved in MSM. Cultures of *E. coli* W3110 or BL21(DE3) expressing α -amylase were grown in flasks containing either MSM supplemented with glucose (50 mg/mL) or glucose free MSM with starch-agar layers. It is apparent that the increased concentration of glucose did have a detrimental effect on final cell density for the K12 strain, with cultures achieving densities approximately half that of cultures grown on starch (Fig 5.5). However, for BL21(DE3) there appeared to be no advantage when replacing glucose with starch. To some extent this supports the literature which suggests BL21 strains are more tolerant to excessive concentrations of glucose and are less affected by overflow metabolism [51].

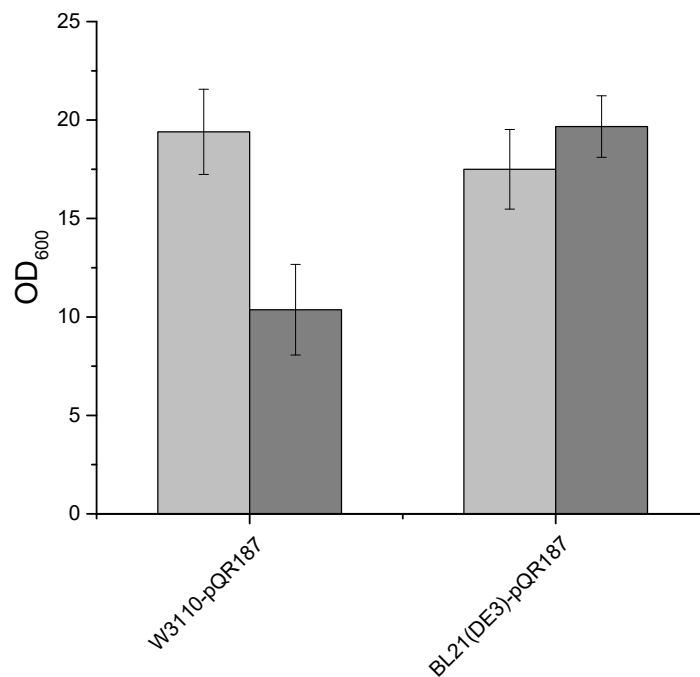


Figure 5.5 Comparison of amylolytic strain growth on high concentrations of starch or glucose in MSM

An end point analysis of *E. coli* W3110 or BL21 harbouring pQR187 cultured in flasks containing glucose free MSM with starch-agar layers (light grey) or MSM supplemented with 50 mg/mL glucose (dark grey) for 24 hours at 30°C, 180 rpm (induced with 0.4 mM IPTG at inoculation (inoculum equivalent to an initial OD₆₀₀ of 0.1)). Error bars represent standard deviation, n=3.

5.3.2 Growth studies using starch-agar layers with *E. coli* secreting *C. violaceum* glucoamylase

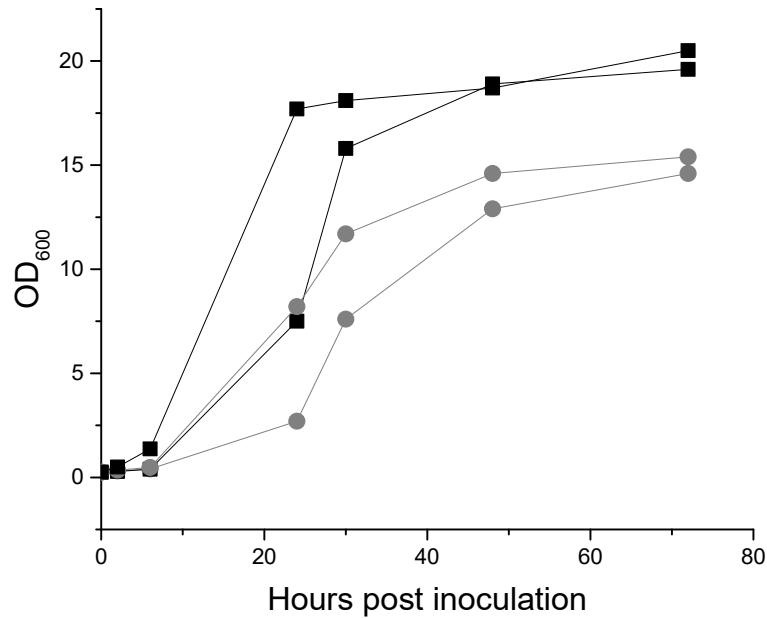


Figure 5.6 Growth curves for *E. coli* expressing *C. violaceum* glucoamylase

Growth curves in duplicate for *E. coli* BL21(DE3) harbouring pQR1712 cultured in MSM containing starch-agar layers (circle) or MSM supplemented with 50 mg/mL glucose (square) (induced with 0.4 mM IPTG at inoculation (inoculum equivalent to an initial OD₆₀₀ of 0.1)).

As seen previously, secreted *S. thermoviolaceus* α -amylase has high activity in the extracellular media, meaning rapid degradation of available starch and a complex product profile (Figs 3.5 and 3.6). Furthermore, glucose, the most advantageous carbon source in terms of growth for *E. coli*, is not produced in any sufficient quantity. To mimic traditional fed-batch fermentation systems, and indeed commercially available enzyme-based fed-batch fermentation systems, a glucoamylase from *C. violaceum* has been cloned into *E. coli* for subsequent expression and secretion within the glucose free MSM starch-agar layer setup. It has already been established in Chapter 4 that BL21(DE3) expressing and secreting *C. violaceum* glucoamylase can grow on starch as a sole carbon source (Fig 4.16). When

cultured using glucose free MSM in shake flasks containing starch-agar layers, BL21(DE3) secreting *C. violaceum* glucoamylase achieved densities beyond those typically seen in LB (Fig 5.6). However, once again growth on starch for BL21(DE3) secreting glucoamylase appeared to offer no advantage over glucose in terms of final cell density. In fact, glucose may have even led to higher cell densities than starch. More experimental repeats would be required to differentiate between the two but given that the results are consistent with previous observations in both this study and in previous literature, it was not investigated any further.

5.4 Regulation of *C. violaceum* glucoamylase expression

As seen previously, amyolytic expression strains of *E. coli* BL21(DE3) exhibited no growth advantage when supplemented with starch instead of glucose (Fig 5.6). This is true even at high concentrations of glucose. Conversely, *E. coli* W3110 secreting α -amylase has already demonstrated a 2 fold increase in cell density when grown on 50 mg/mL starch over an equivalent amount of glucose. The construction method for all *C. violaceum* glucoamylase vectors to date have used pET derived backbones, which contain the T7 promoter, inducible in BL21(DE3) but not in W3110. A K12 compatible promoter was therefore required for expression studies using W3110. Ideally this promoter would also provide the added benefit of being self-regulating rather than requiring induction, an important aspect from the perspective of enzyme-based fed-batch fermentation (see section 1.7 for details).

5.4.1 Cyclic AMP dependant promoter

The promoter, *PcstA*, characterised by the Edinburgh 2008 iGEM team, was selected as a candidate promoter for self-regulation based on its sensitivity to glucose concentration. To

characterise the promoter, eGFP was used as a reporter gene, with fluorescence measured at varying glucose concentrations within LB media.

5.4.2 Vector design and characterisation of *PcstA*

Using Biobrick Standard Assembly, eGFP was incorporated into BBa-K118011 (supplied by the 2016 iGEM distribution kit), to allow for *PcstA* to be characterised based on fluorescence. eGFP was cloned from pQR1344 using a forward primer with an overhanging region containing an *Xba*I restriction site upstream of an RBS site, and a reverse primer with an overhanging region containing a *Pst*I site downstream of an *Spe*I site. Following PCR purification and subsequent digestion of the fragment with *Xba*I and *Pst*I, the insert was ligated to a purified *Spe*I/*Pst*I digested BBa_K118011 backbone, resulting in BBa_K118011-eGFP, designated pQR1714 (Fig 5.7).

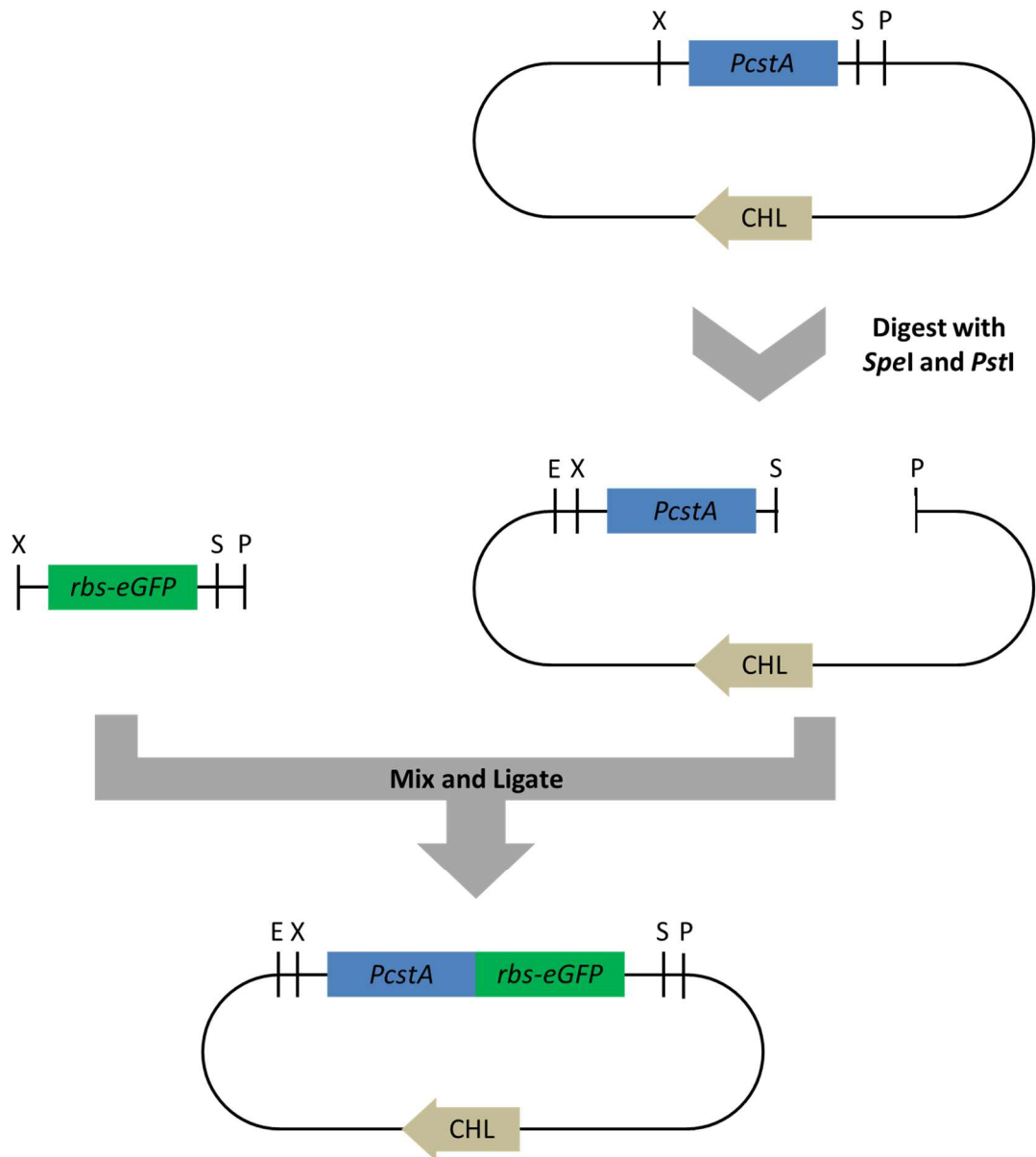


Figure 5.7 A schematic diagram of the Biobrick standard assembly method for suffix insertion

The insert fragment containing an RBS upstream of the eGFP gene was amplified using PCR primers with overhangs specific to the Biobrick prefix and suffix (containing an *Xba*I restriction site, and both *Spe*I and *Pst*I sites respectively). The PCR product was purified and digested with *Xba*I and *Pst*I. The vector, BBa_K118011 containing the *PcstA* promoter, was digested with *Spe*I and *Pst*I and both were ligated together to form pQR1714.

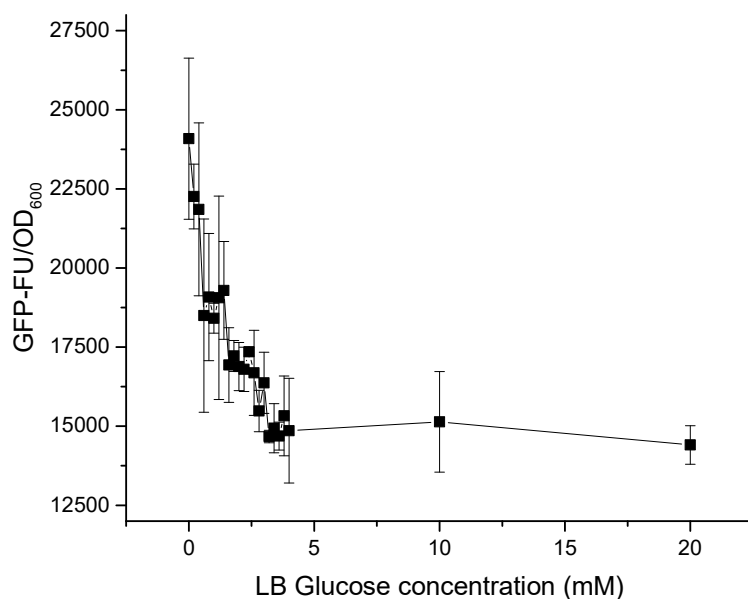


Figure 5.8 Characterisation of *PcstA* over a range of glucose concentrations using eGFP fluorescence

E. coli W3110 harbouring pQR1714 grown in LB overnight and used to inoculate (with a 1 in 20 dilution) LB supplemented with a range of glucose concentrations within a 96-well plate. Cultured for 8 hours at 37°C, 800 rpm. eGFP fluorescence intensity of neat whole cell samples was measured (with an excitation wavelength of 483 nm, and an emission wavelength of 535 nm (Tecan infinite 200 pro). Fluorescence units were normalised to OD₆₀₀. Error bars represent standard deviation, n=3.

E. coli W3110 harbouring pQR1714 was grown in LB overnight and was used to inoculate (with a 1 in 20 dilution) a 96-well plate containing LB with varying concentrations of glucose (0-20 mM). Following 8 hours incubation at 37°C the whole cell eGFP fluorescence was measured. eGFP fluorescence (fluorescence units normalised to OD₆₀₀) decreased with glucose concentration from 0-5 mM (Fig 5.8), indicating that as glucose concentration increased, eGFP expression decreased. It is worth noting that because the inoculum was grown in LB containing no additional glucose, each well initially contained cells expressing eGFP, accounting for the background fluorescence seen in Fig 5.8. The result supports previous characterisation of *PcstA*, in which the promoter was found to be sensitive to glucose at concentrations between 0 and 10 mM in LB.

5.4.3 *PcstA* regulation of *C. violaceum* glucoamylase

The characterisation of *PcstA* using eGFP has confirmed sensitivity to glucose within a concentration range applicable to glucose limited fed-batch fermentation i.e. glucose at a concentration of 5 mM is equivalent to 0.9 g/L, with typical values in the literature for direct feedback control mechanisms maintaining glucose concentrations to between 0.5 and 2 g/L [22, 96, 97]. To establish whether the expression level is high enough for effective secretion of an amylolytic enzyme, the *C. violaceum* glucoamylase containing the enhanced signal sequence (DsbA) was incorporated into the BBa_K118011 backbone producing pQR1715 (Fig 5.9).

5.4.3.1 Vector design

The Biobrick Standard Assembly method as previously described was not used to create pQR1715, owing to the presence of an internal *PstI* site within the *C. violaceum* glucoamylase gene. Instead, primers were designed to replace the *PstI* site with a *BamHI* site in the BBa_K118011 backbone. The forward primer (K118011*BamHI*.fw) was complementary to the sequence immediately downstream of the *PstI* site and included in the overhanging region the *BamHI* site. The reverse primer (K118011*BamHI*.rv) was complementary to the sequence immediately upstream of the *PstI* site. The PCR product was gel extracted, purified, and digested with *SpeI* and *BamHI*. Primers were designed to amplify the *C. violaceum* glucoamylase gene from pQR1712. The forward primer (K118011_CV2DsbA.fw) was complementary to the 5' end of the gene and the region upstream of the start codon, including the RBS, spacer and *XbaI* site present in pQR1712. The reverse primer (K118011_CV1.rv) was complementary to the C-terminus of the gene (including the stop codon) and contained within the overhanging region a *BamHI* site. The PCR product was gel extracted, purified, and digested with *XbaI* and *BamHI*. The fragment was ligated to the K118011-*BamHI* backbone, with *SpeI* and *XbaI* sites combining to form a

scar (which cannot be digested by either original enzyme) between the *PcstA* promoter and the gene, and the two *Bam*HI sites combining downstream of the gene.

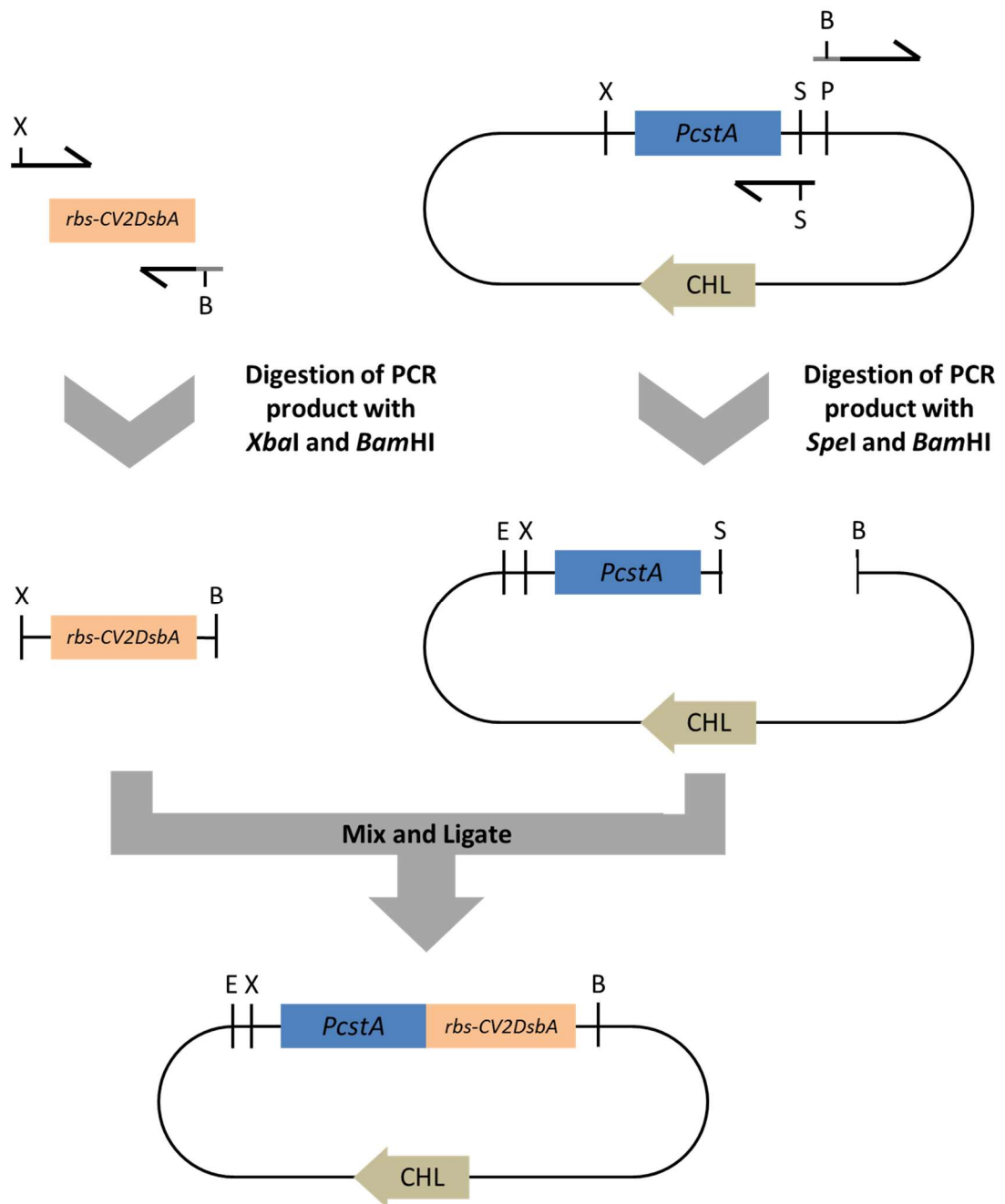


Figure 5.9 Schematic diagram for the insertion of *C. violaceum* glucoamylase gene into the BBa_K118011 backbone

Primers were designed to replace the *Pst*I (P) restriction site in the original BBa_K118011 vector with a *Bam*HI (B) site. Following PCR, the purified product was digested with *Spe*I (S) and *Bam*HI (B) and ligated to the amplified *rbs-CV2DsbA* fragment containing an *Xba*I (X) upstream and a *Bam*HI (B) site downstream, forming the construct pQR1715.

5.4.3.2 Characterisation of *PcstA* regulated *C. violaceum* glucoamylase secretion

To ensure *PcstA* allows for expression and secretion of *C. violaceum* glucoamylase, amyolytic activity within the extracellular media was measured following 24 hours of culture in LB supplemented with glucose in concentrations ranging from 0-20 mM (Fig 5.10). Firstly, there was clear amyolytic activity detected in the extracellular media indicating glucoamylase was secreted via regulation from *PcstA*. Secondly, the amyolytic activity detected decreased as glucose concentration increased, mirroring observations from the previous characterisation of *PcstA* using eGFP (Fig 5.8).

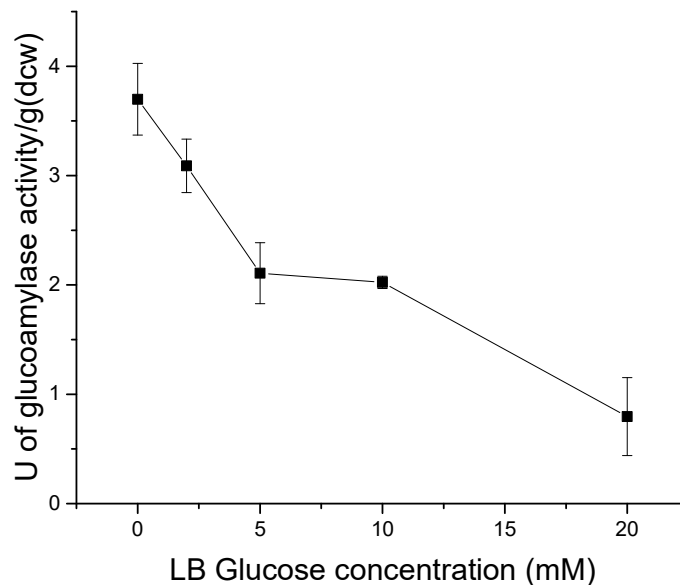


Figure 5.10 Characterisation of *PcstA* regulated *C. violaceum* glucoamylase secretion in LB media supplemented with 0-20 mM glucose

Glucoamylase activity in the extracellular media of *E. coli* W3110 harbouring pQR1715 cultured for 24 hours at 37°C, 250 rpm, determined by amyase assay (degradation of starch measured by the absorbance of starch-iodine complex at 600 nm) and expressed in units (defined as the disappearance of 1 mg/mL starch-iodine complex per minute) per gram of dry cell weight. Error bars represent standard deviation, n=3.

5.4.4 The influence of *PcstA* regulated *C. violaceum* glucoamylase expression on starch degradation within LB media

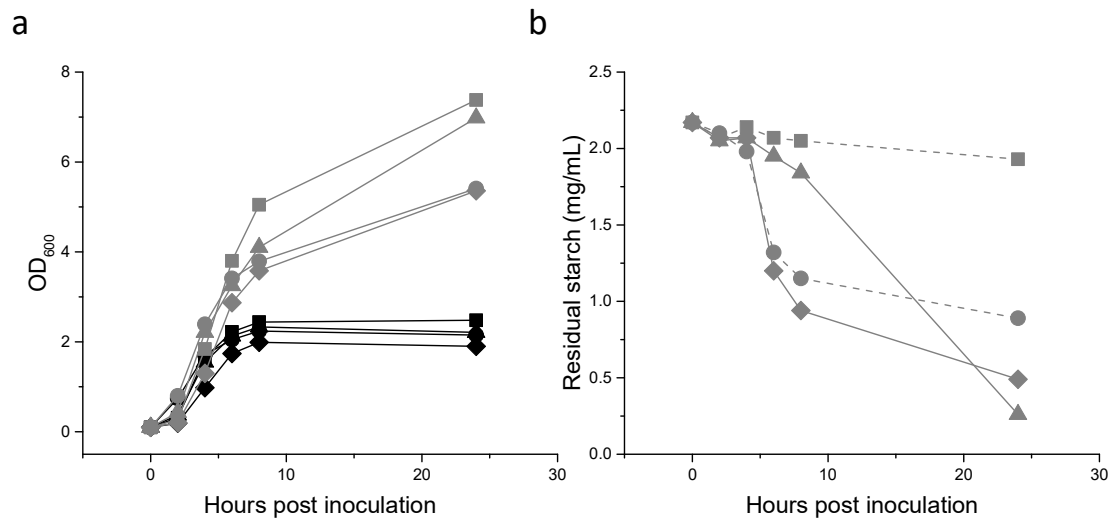


Figure 5.11 *PcstA* regulated expression of *C. violaceum* glucoamylase by *E. coli* and its influence on growth and the degradation of starch within LB media

E. coli strains cultured at 37°C, 250 rpm over 24 hours in either LB (black) or LB supplemented with 2.5 mg/mL starch (grey). a) Growth curves from single experimental run for untransformed W3110 (square), W3110 harbouring pQR1715 (triangle), untransformed BL21(DE3) (circle), or BL21(DE3) harbouring pQR1715 (diamond) in both media compositions. b) Residual starch concentrations for untransformed W3110 (square, dashed), W3110 harbouring pQR1715 (triangle), untransformed BL21(DE3) (circle, dashed), or BL21(DE3) harbouring pQR1715 (diamond).

When cultured in LB media supplemented with 2.5 mg/mL starch the expression of the *C. violaceum* glucoamylase under the *PcstA* promoter offered no advantage in terms of cell density over the untransformed controls (Fig 5.11a). This is consistent with previous results seen in Chapter 3 in which the expression of the *S. thermoviolaceus* α -amylase also offered no advantage (Figs 3.7a and 3.10a), and supports the conclusion that the starch provided as a supplement in LB enhances growth regardless of amylolytic enzyme expression. However, in terms of starch degradation within the media, the *PcstA* regulated expression and secretion of glucoamylase had a significant influence on the W3110 strains ability to degrade starch (Fig 5.11b). Given that untransformed BL21(DE3) is capable of rapid starch degradation anyway (Fig 3.10b), the *PcstA* regulated expression of glucoamylase offered

little increase and further investigation would be needed to determine whether there was a real difference between the two. However, seeing as it has already been established that high glucose concentration in shake flasks has little effect on the growth of BL21(DE3), this is an avenue which has not been pursued any further.

5.4.5 Growth characteristics of *E. coli* W3110 expressing *PcstA* regulated *C. violaceum* glucoamylase cultured in glucose free MSM with starch-agar layers

E. coli W3110 expressing *C. violaceum* glucoamylase under the regulation of *PcstA* was able to grow with starch as a sole carbon source, and was capable of achieving densities approximately twice that of cultures grown in an equivalent amount of glucose (Fig 5.12a). This is the first demonstration of increased cell densities having been achieved as a direct result of self-regulated enzyme-based fed-batch fermentation. Based on the previous characterisation studies of *PcstA*, it was expected that secretion of *C. violaceum* glucoamylase would be lower in cultures containing glucose, and higher in cultures containing starch. Surprisingly, when amyolytic activity in the extracellular media was measured there was no obvious difference between media containing starch and media containing glucose (Fig 5.12b). When normalised to dry cell weight, amyolytic activity in the extracellular media for both starch and glucose reduced and then plateaued, but again there was no discernible difference between the two media types. Further investigation would be required to explain why expression in culture conditions did not completely reflect the previous characterisation studies, however, for the purposes of this study the increase in cell density seen in starch compared to glucose is of greater importance, and provides a proof of principle that biomass can be enhanced via the self-secretion of an amyolytic enzyme when cells are grown in media containing starch compared with an equivalent amount of glucose.

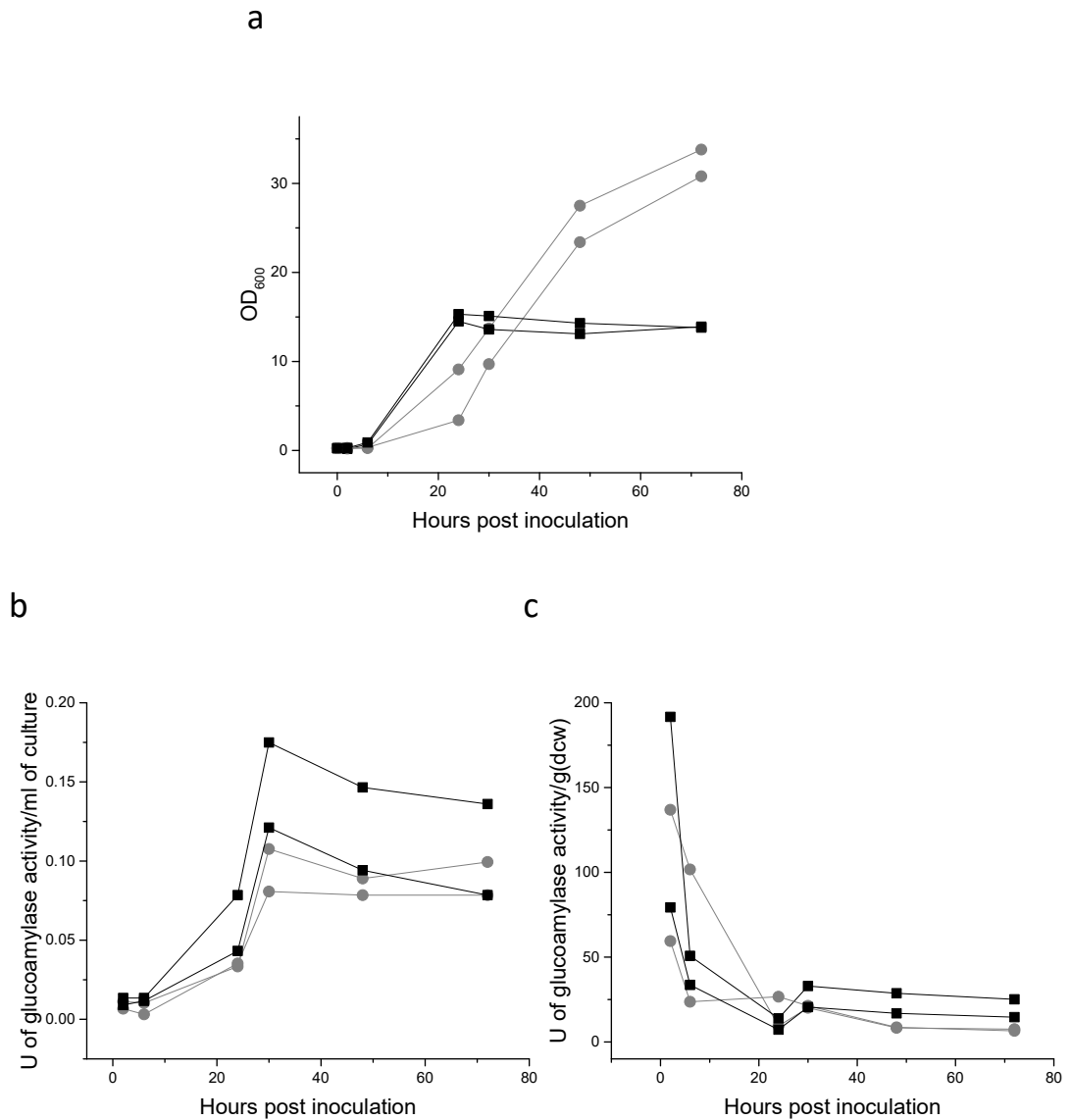


Figure 5.12 *PcstA* regulated *C. violaceum* glucoamylase expression and its influence on growth in MSM containing starch-agar layers

E. coli W3110 harbouring pQR1715 (BBa_K118011-CV2DsbA) cultured for 72 hours at 30°C, 180 rpm, in either glucose free MSM with starch-agar layers (grey) or MSM supplemented with 50 mg/mL glucose (black). a) Growth curves for each condition in duplicate. b) Glucoamylase activity in the extracellular media determined by amylase assay at 37°C and expressed as units per mL of culture. c) Glucoamylase activity in the extracellular media determined by amylase assay at 37°C and expressed as units per gram of dry cell weight.

5.5 Co-expression studies as a method for developing a heterologous protein expression system utilising starch as a carbon source

5.5.1 Co-expression of *S. thermoviolaceus* α -amylase and an *E. coli* derived transketolase

To investigate if a recombinant protein of interest could be co-expressed alongside *S. thermoviolaceus* α -amylase, a transketolase (TK) originally derived from *E. coli* was used. *E. coli* BL21(DE3) was co-transformed with pQR187 and the compatible plasmid pQR411 [80] (a pMMB67HE backbone vector containing an RSF1010 origin of replication and the *E. coli* derived TK), and grown up in LB for 24 hours at 37°C, 250 rpm (induced with 0.4 mM IPTG at inoculation (1 in 20 dilution of an overnight culture)). Although co-expression of the two enzymes was achieved, SDS page analysis revealed a qualitative reduction in TK expression (band at 75 kDa) from the co-expression strain compared with the strain expressing TK only (Fig 5.13a). In this particular example the expression of α -amylase was also clear in the co-expressing strain (band at 47 kDa). Given that the expression of α -amylase was highly visible on SDS page, and extracellular activity is generally known to be very high (Chapter 3 discussion), it may be possible that the marked reduction in expression of TK was due to the over expression of α -amylase.

To investigate the potential of using the increased cell mass gained from high density cultures to increase expression of heterologous protein, experiments were conducted using the commercially available EnPresso® growth system. Co-transformed BL21(DE3) were cultured using the EnPresso® protocol described in the materials and methods (section 2.4.4), alongside controls of BL21(DE3) expressing TK only and BL21(DE3) expressing TK only, but without the addition of reagent A. Despite matching the final cell density with an OD₆₀₀ of approximately 33 (OD₆₀₀ data shown in Figure legend), the co-expressing strain did

not express TK as highly as the single expressing TK strain under the EnPresso® conditions (Fig 5.13b). In fact, qualitatively, the co-expressing strain produced a similar amount of TK as the strain expressing TK only, without the addition of reagent A. This suggests expression levels of TK were decreased in the co-expression strain to such an extent that even the associated increase in cell density did not offset the reduction in expression.

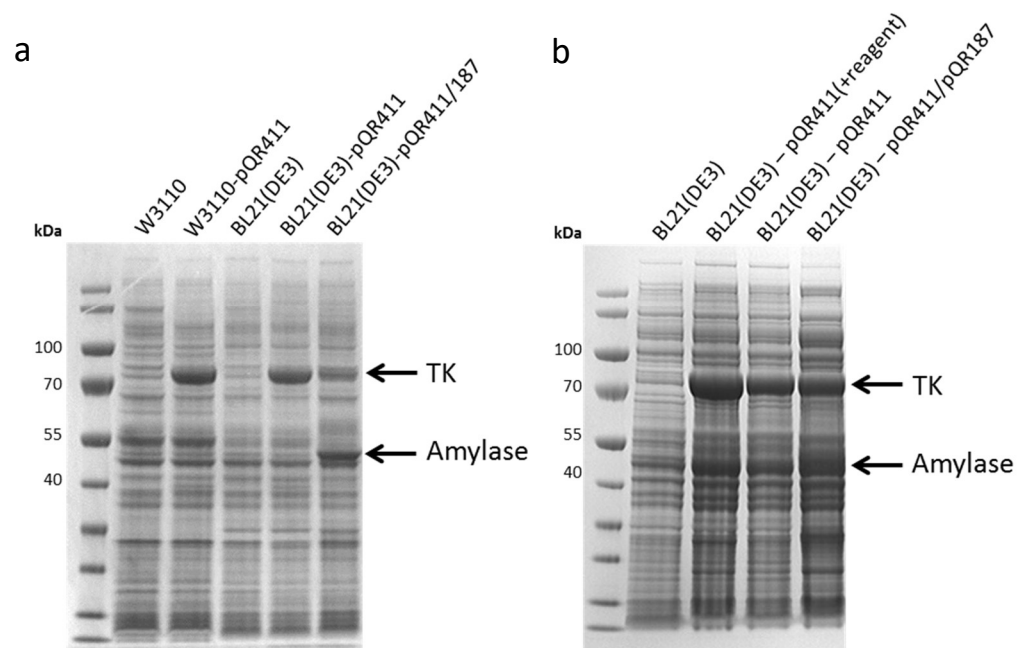


Figure 5.13 SDS-page analysis for the co-expression of *S. thermoviolaceus* α -amylase and an *E. coli* derived transketolase

a) SDS-page of clarified lysate for untransformed *E. coli* W3110, W3110 harbouring pQR411, untransformed BL21(DE3), BL21(DE3) harbouring pQR411, and BL21(DE3) harbouring both pQR411 and pQR187, grown in LB for 24 hours at 37°C, 250 rpm. Sample volume processed was normalised to cell density b) SDS-page of clarified lysate for BL21(DE3) (OD₆₀₀ of 18), BL21(DE3) harbouring pQR411 (with reagent A) (OD₆₀₀ of 29), BL21(DE3) harbouring pQR411 (without reagent A) (OD₆₀₀ of 21), and BL21(DE3) harbouring both pQR411 and pQR187 (without reagent A) (OD₆₀₀ of 33) grown in EnPresso® growth media as per the standard protocol (see section 2.4.4). Cultures contained the appropriate antibiotics when necessary to maintain plasmid stability (see materials and methods), and were induced with 0.4 mM IPTG at inoculation (1 in 20 dilution from an overnight culture) when necessary. Labeled arrows indicate position of TK (75 kDa) and α -amylase (47 kDa).

5.5.2 Co-expression of *C. violaceum* glucoamylase and an *E. coli* derived transketolase

Previous studies have indicated that co-expression does not necessarily lead to a reduction in expression [6], however, it is possible that the overexpression of *S. thermoviolaceus* α -amylase results in a metabolic burden rendering co-expression non-viable. To determine whether co-expression could be a viable option, TK from pQR411 was co-transformed into *E. coli* W3110 with the lesser expressed *PcstA* regulated *C. violaceum* glucoamylase. Co-expression of TK from pQR411 and the *PcstA* regulated *C. violaceum* glucoamylase containing the DsbA signal sequence (pQR1715) was carried out in flasks containing glucose free MSM with starch-agar layers. The growth curves for the co-expressing strain mirrored those seen in cells expressing *C. violaceum* glucoamylase only, albeit with a slightly delayed onset of log phase (Fig 5.14a). This was likely due to the decrease in glucoamylase activity within the media (Fig 5.14b) compared to cells expressing *C. violaceum* glucoamylase only, indicating that glucoamylase expression was reduced when expressed alongside pQR411. When this co-expressing strain was grown in MSM containing an equivalent amount of glucose, the final densities achieved were similar to those seen previously by the strain expressing glucoamylase only. However, when final cell pellets were analysed by SDS page, TK expression was not obvious (Fig 5.14d).

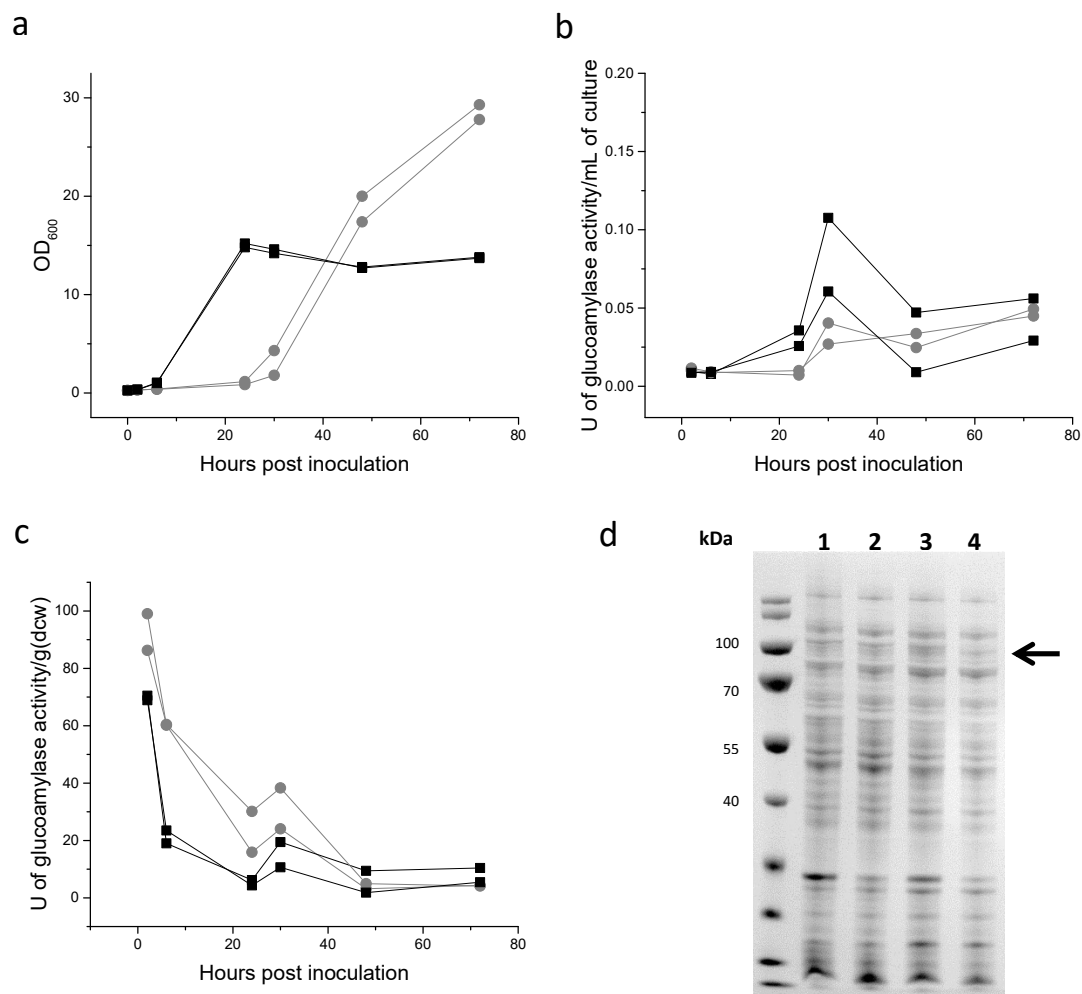


Figure 5.14 Co-expression of *PcstA* regulated *C. violaceum* glucoamylase and an *E. coli* derived transketolase

E. coli W3110 harbouring pQR1715 (BBa_K118011-CV2DsbA) and pQR411 cultured for 72 hours at 30°C, 180 rpm, in either glucose free MSM with starch-agar layers (grey) or MSM supplemented with 50 mg/mL glucose (black). a) Growth curves for each condition in duplicate. b) Glucoamylase activity in the extracellular media determined by amylase assay at 37°C and expressed as units per mL of culture. c) Glucoamylase activity in the extracellular media determined by amylase assay at 37°C and expressed as units per gram of dry cell weight. d) SDS page of samples removed at 72 hours (1) whole cell lysate of W3110 harbouring pQR1715 cultured in glucose free MSM with starch-agar layer, (2) clarified cell lysate of W3110 harbouring pQR1715 cultured in glucose free MSM with starch-agar layer, (3) whole cell lysate of W3110 harbouring pQR1715 cultured in MSM supplemented with 50 mg/mL glucose, (4) Clarified cell lysate of W3110 harbouring pQR1715 cultured in MSM supplemented with 50 mg/mL glucose. Arrow indicates expected position of TK (at 75 kDa).

5.6 Dual-expression studies as a method for developing a heterologous protein expression system utilising starch as a carbon source

Some of the complications surrounding co-expression could be potentially mitigated by constructing an operon on a single plasmid, termed here dual-expression. Compatibility issues and the metabolic burden associated with multiple antibiotic resistance genes would be eliminated, along with simplifying the transformation method. It would also provide a basis for a versatile system whereby a plasmid already containing a self-regulated amylolytic enzyme could be designed to contain a multiple cloning site for insertion of an additional gene of interest, similar in concept to current commercially available vectors such as pETDuet™ (Novagen) or pACYCDuet™ (Novagen), but specifically for high density growth using starch as the substrate.

5.6.1 Construction of pQR1716 (pUC19-Amy) and pQR1717 (pUC19-GFP)

Initially, control vectors containing either *S. thermoviolaceus* α -amylase or eGFP were constructed using circular polymerase extension cloning (CPEC) (Fig 5.15). The vector backbones were derived from pUC19 [81], which carries ampicillin resistance, and contains the *lac* promoter allowing for expression in both *E. coli* BL21(DE3) and W3110. CPEC construction involved the designing of overlapping primers at each intersection between insert and vector. In the case of pQR1716 and pQR1717, there is one insert in each vector, resulting in two primer pairs used for initial amplification reactions. pQR1716 construction used AmyCPEC1.fw and AmyCPEC1.rv primers for insert amplification, and pUC19CPEC1.fw and pUC19CPEC1.rv primers for vector amplification, with pQR187 and pUC19 acting as respective templates in standard PCR conditions (described in section 2.2.3). pQR1717 construction used CPEC2_GFP.fw and CPEC2_GFP.rv primers for insert amplification, and

CPEC2_pUC19.fw and CPEC2_pUC19.rv primers for vector amplification, with pET29a-GFP and pUC19 acting as respective templates. PCR products were gel extracted, purified, and combined for respective CPEC reactions (see section 2.2.4 for details). Both resulting constructs were confirmed using restriction digestion analysis and sequencing.

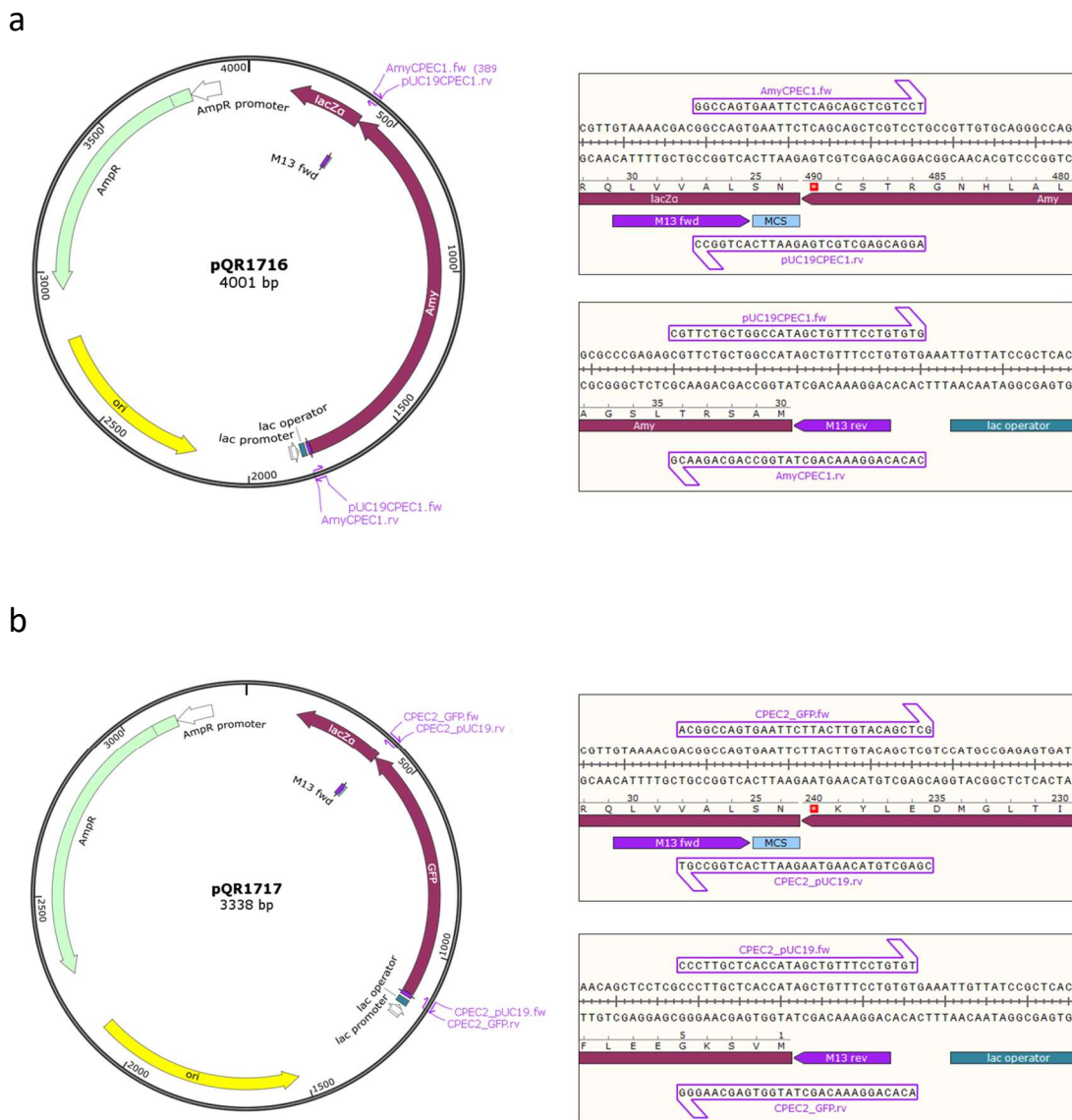


Figure 5.15 Construction of pQR1716 (pUC19-Amy) and pQR1717 (pUC19-GFP) using Circular Polymerase Extension Cloning
 Vector maps and primer design for construction of a) pQR1716 and b) pQR1717, using Circular Polymerase Extension Cloning (CPEC).

5.6.2 Construction of dual-expression vectors pQR1718 (pUC19-AmyGFP) and pQR1719 (pUC19-GFPAmy)

The first construction of a dual-expression vector combined *S. thermoviolaceus* α -amylase and eGFP, using CPEC in the same way as above. Two inserts required three primer pairs (one at each intersection between the vector and insert 1, insert 1 and insert 2, and insert 2 and the vector), as highlighted in Fig 5.16. Prior to the CPEC reaction three separate PCRs were required to amplify the two inserts and one vector. Insert 1 (*S. thermoviolaceus* α -amylase) was amplified using AmyCPEC1.rv and CPEC7_Amy.fw primers, with pQR187 as the template. Insert 2 (eGFP) was amplified using CPEC7_GFP.rv and CPEC2_GFP.rv primers, with pET29a-eGFP as the template. The vector (pUC19 backbone) was amplified using CPEC2_pUC19.rv and pUC19CPEC1.fw primers, with pUC19 as the template. PCR reactions followed standard conditions described in section 2.2.3. Following gel extraction and purification the subsequent PCR products were used in a CPEC reaction with conditions optimised for multiple inserts (see section 2.2.4 for details). The resulting construct, pQR1718 was confirmed using restriction digestion analysis and sequencing. A vector was also constructed using the same method but with primers containing the inserts in the reverse order i.e. eGFP upstream of the *S. thermoviolaceus* α -amylase. This was in an attempt to optimise GFP expression, adhering to the notion that genes are more highly expressed on an operon the closer they are to the promoter [98]. The resulting construct was designated pQR1719.

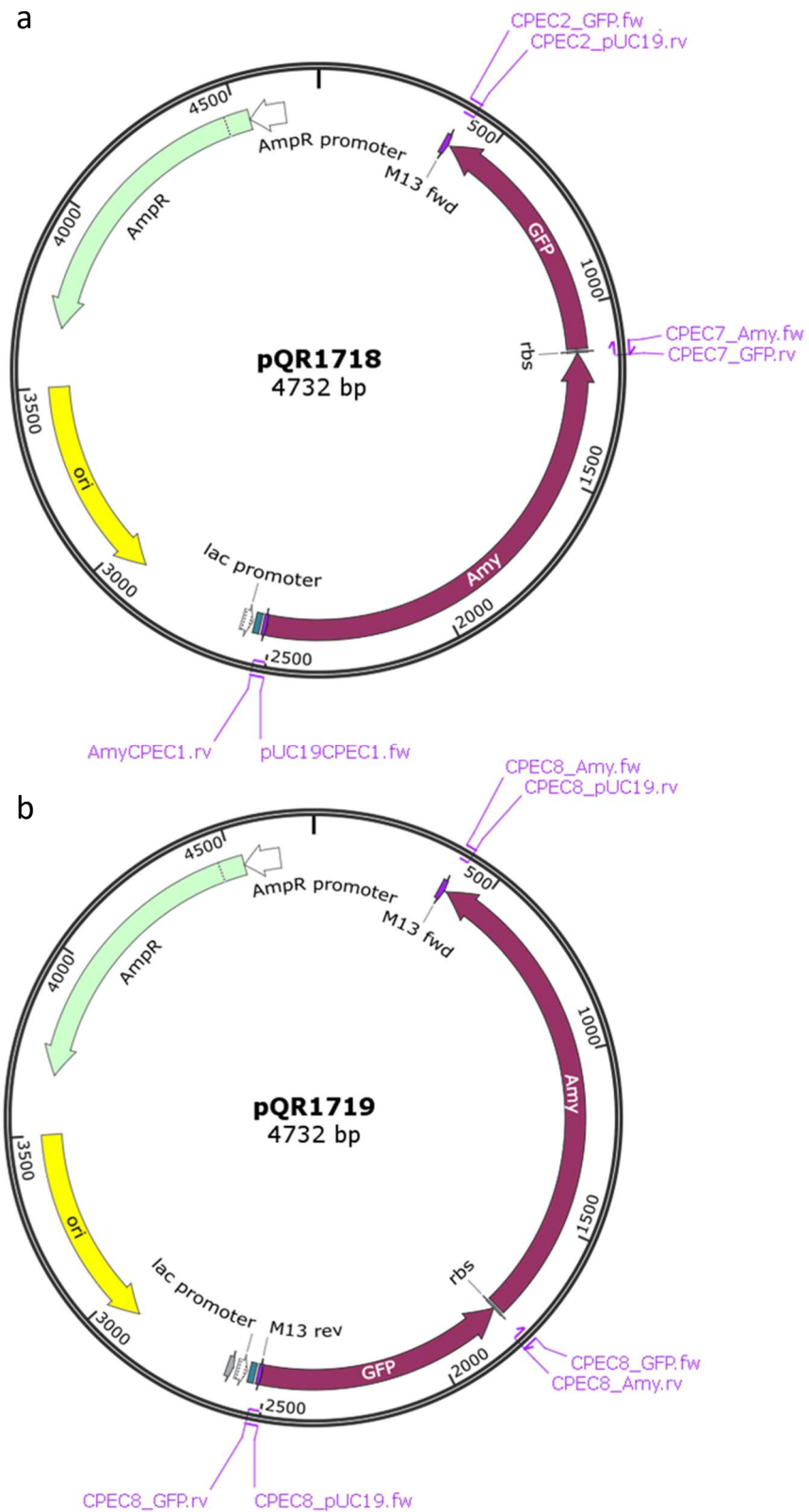


Figure 5.16 Vectors designed for dual-expression of eGFP and α -amylase
 Vector maps of a) pQR1718 (pUC19AmyGFP) and b) pQR1719 (pUC19GFPAmy) along with primers used for initial PCR reactions. The final construction step used multi insert CPEC.

5.6.3 Expression and activity from dual-expression plasmids

As expected cells harbouring pQR1719 showed increased GFP fluorescence over those harbouring pQR1718 (Fig 5.17a), though surprisingly the reverse was not true for amylase activity. In fact, amylase activity in the extracellular media was marginally increased in cells harbouring pQR1719 compared with those harbouring pQR1718 (Fig 5.17b). Overall, expression from the dual-expression plasmid mirrored previous co-expression results in that expression of a recombinant protein of interest was significantly reduced when expressed concurrently with an amyolytic enzyme.

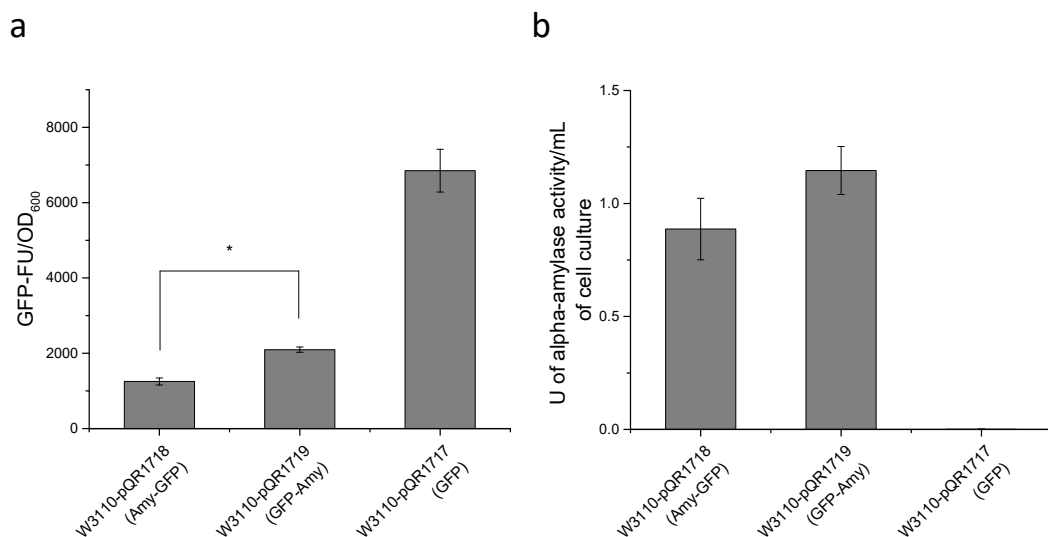


Figure 5.17 eGFP fluorescence and α -amylase activity from dual-expression vectors *E. coli* W3110 harbouring pQR1718 (pUC19AmyGFP), pQR1719 (pUC19GFPAmy) or pQR1717 (pUC19GFP), cultured in LB media at 37°C, 250 rpm for 24 hours (induced with 0.4 mM IPTG at an OD₆₀₀ of 0.6-0.8). a) eGFP fluorescence intensity measured from neat whole cell samples using an excitation wavelength of 483 nm and an emission wavelength of 535 nm (Tecan infinite 200 pro). Fluorescence units were normalised to OD₆₀₀. b) Extracellular media α -amylase activity determined by amylase assay and expressed as units per mL of cell culture volume. Error bars represent standard deviation, n=3.

5.6.4 Dual-expression using starch as a sole carbon source

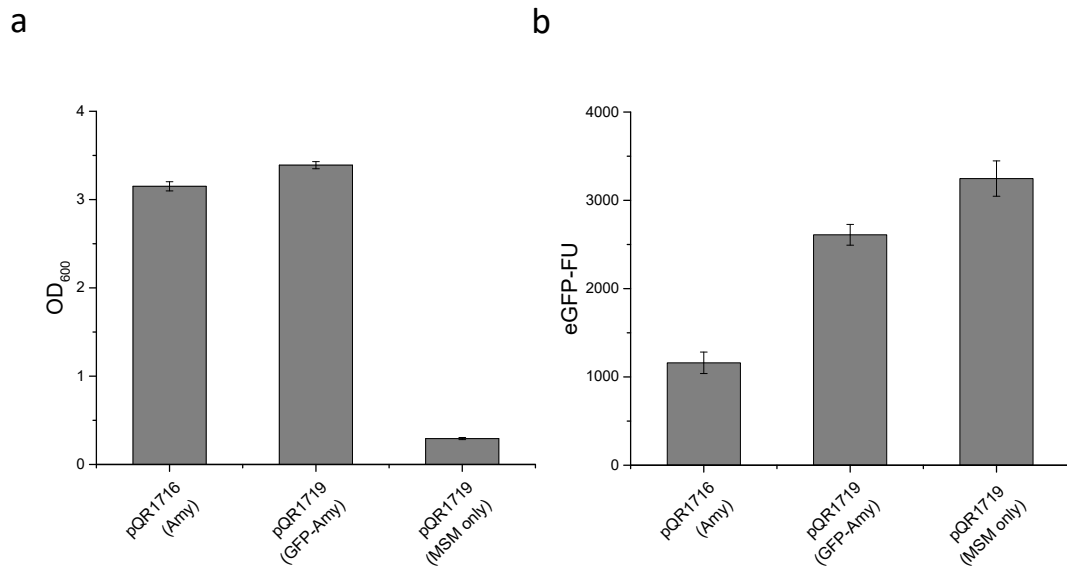


Figure 5.18 Growth and eGFP expression of *E. coli* W3110 harbouring the pQR1719 dual-expression vector cultured in glucose free MSM supplemented with 2.5 mg/mL starch

E. coli W3110 harbouring either pQR1716 (pUC19-Amy) or pQR1719 (pUC19-GFPAmy), cultured in glucose free MSM supplemented with 2.5 mg/mL starch, or MSM only (control), at 37°C, 250 rpm for 24 hours (induced with 0.4 mM IPTG at inoculation (initial OD₆₀₀ of 0.25)). a) Cell density determined by OD₆₀₀ following a culture period of 24 hours. b) Total eGFP fluorescence intensity measured from neat whole cell samples using an excitation wavelength of 483 nm and emission wavelength of 535 nm (Tecan infinite 200 pro). Error bars represent standard deviation, n=3.

E. coli W3110 harbouring pQR1719 was able to grow in glucose free MSM supplemented with 2.5 mg/mL starch i.e. the dual-expression strain was able to utilise starch as a sole carbon source (Fig 5.18a), and was capable of achieving cell densities similar to those seen with W3110 harbouring the amylase only vector, pQR1716. However, total eGFP expression, despite being greater than the pQR1716 control, did not increase throughout the 24 hour culture, as indicated by the inoculum control (Fig 5.18b). The inoculum control comprised glucose free MSM only, and was inoculated with the same volume of LB starter culture. The lack of carbon prevented cells from growing in density beyond the initial inoculum and gave an indication of eGFP expression already present within the inoculum.

Despite observing eGFP expression in LB media, these results indicate dual-expression from pQR1719 did not lead to significant production of eGFP in defined media with starch as a sole carbon source.

5.6.5 Dual-expression of *C. violaceum* glucoamylase and eGFP

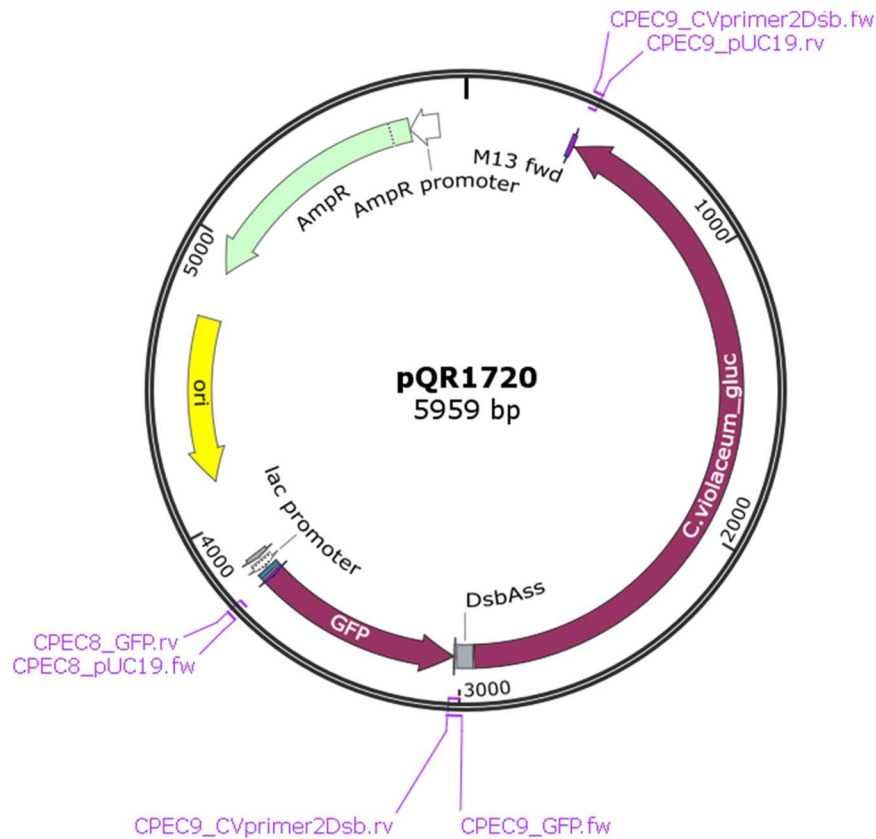


Figure 5.19 Vector designed for dual-expression of eGFP and *C. violaceum* glucoamylase
 Vector map of pQR1720, constructed using multiple insert CPEC following insert and vector PCR reactions using primer pairs indicated.

Given the apparent problems associated with the dual-expression of eGFP and α -amylase, a vector was constructed replacing α -amylase with *C. violaceum* glucoamylase containing the DsbA signal sequence, in an attempt to increase eGFP expression while utilising starch as a sole carbon source. The rationale followed previous observations whereby *C. violaceum* glucoamylase is generally less well expressed than *S. thermoviolaceus* α -amylase regardless

of the promoter and RBS combination used, yet still leads to an enhancement of cell mass when starch is used as the sole carbon source. With the assumption that a less well expressed enzyme will assert a lower metabolic burden on the cell, it may be possible that the expression of a second protein would be increased, even in defined media containing starch as the only carbon source. The pQR1720 vector (Fig 5.19) was constructed using CPEC in the same way as pQR1719; with insert 1 (eGFP) amplified using CPEC8_GFP.rv and CPEC9_GFP.fw primers, with pQR1344 as the template, insert 2 (*C. violaceum* glucoamylase with attached DsbA signal sequence) amplified using CPEC9_CVprimer2Dsb.rv and CPEC9_CVprimer2Dsb.fw primers, with pQR1712 as the template, and the vector backbone amplified using CPEC9_pUC19.rv and CPEC8_pUC19.fw primers, with pUC19 as the template. Construction was confirmed by sequencing.

When cultured in flasks containing glucose free MSM and starch-agar layers, *E. coli* W3110 harbouring pQR1720 achieved densities similar to those which have been seen previously with the pQR1715 construct, driving expression of the *C. violaceum* glucoamylase alone. Furthermore, total eGFP expression was greatly increased throughout the culture period, particularly when compared to cultures containing an equivalent amount of glucose. This is the first demonstrated example of enhanced recombinant protein expression resulting directly from a self-secreting enzyme-based fed-batch fermentation system.

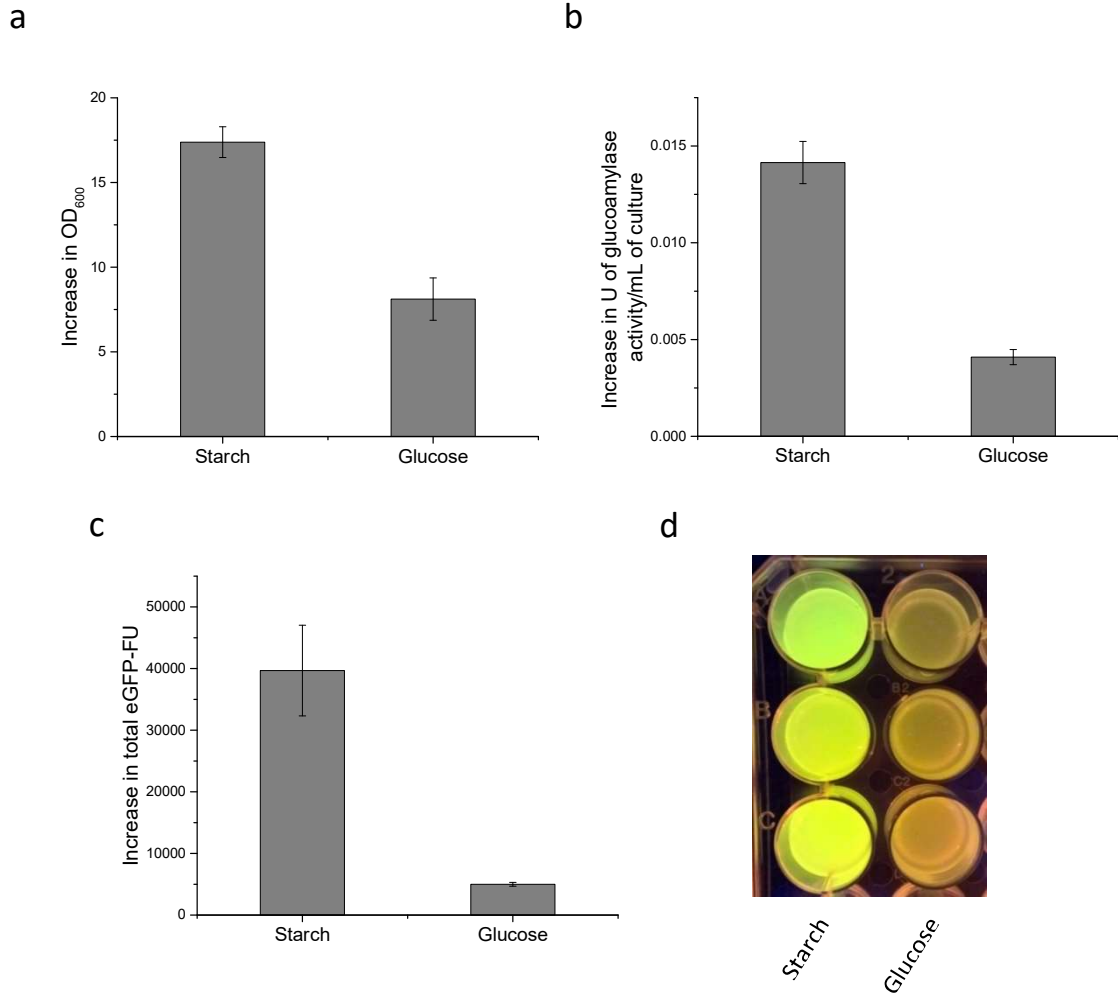


Figure 5.20 Dual-expression of *C. violaceum* glucoamylase and eGFP in *E. coli* W3110 harbouring pQR1720

E. coli W3110 harbouring pQR1720, cultured in flasks containing glucose free MSM with starch-agar layers or MSM supplemented with 50 mg/mL glucose, at 37°C, 250 rpm for 48 hours (induced with 0.4 mM IPTG at inoculation (initial OD₆₀₀ of 0.25)). a) Increase in cell density (OD₆₀₀) over 48 hours of culture for each media type. b) Increase in extracellular media glucoamylase activity over 48 hours for each media type, expressed in units of glucoamylase activity per mL of culture, determined by amylase assay (absorbance of starch-iodine complex at 600 nm). c) Increase in total eGFP fluorescence units over 48 hours for each media type, measured from neat whole cell samples using an excitation wavelength of 483 nm and emission wavelength of 535 nm (Tecan infinite 200 pro). d) Image of eGFP expression under blue light for each media composition, displayed in triplicate. Error bars represent standard deviation, n=3.

5.7 Discussion and Conclusion

A major objective of this Chapter was to examine the application of a cell engineering approach to enzyme-based fed-batch fermentation. As a proof of concept, *E. coli* secreting *S. thermoviolaceus* α -amylase cultured in EnPresso® growth media, lacking the additional amylolytic reagent, was shown to achieve cell densities in excess of the control that lacked α -amylase but included the exogenously added amylolytic reagent A. The enhanced cell growth observed confirms cell engineering is a viable option for enzyme-based fed-batch fermentation, however, given the rate at which extracellular starch is degraded by *S. thermoviolaceus* α -amylase, it also raises some questions as to whether the true mechanism is based on the slow release of utilisable carbon or simply that utilisable carbon is liberated from starch. Given that the predominant hydrolysis products of *S. thermoviolaceus* α -amylase are short oligosaccharides rather than glucose (see section 3.3.5), the latter seems more likely. Furthermore, owing to the degree of impenetrability surrounding the identity of components within EnPresso® growth media, there were difficulties in determining the exact nature of carbon present in the cultures to begin with.

To investigate the slow release of utilisable carbon and truly mimic fed-batch fermentation, a combination of defined media (glucose free MSM) and starch-agar layers were developed alongside *E. coli* W3110 strains able to express and secrete *C. violaceum* glucoamylase using a glucose sensitive promoter. The increase in cell density within flasks containing starch compared with those containing glucose is the first demonstration of a cell engineering approach to self-regulated enzyme-based fed-batch fermentation. The main caveat to this system is that, for shake flasks at least, it may be specific to K12 strains, as BL21(DE3) appear not to benefit from the slow release of glucose from starch, presumably because they do not demonstrate any detrimental effects in terms of growth from high concentrations of glucose in the first place. As discussed previously this is likely a result of

the B strains ability to employ a glyoxylate shunt, reducing the accumulation of acetate and minimising the detrimental effects of overflow metabolism [47-51].

In an attempt to use this enhanced cell mass as a platform for recombinant protein expression, simultaneous expression of both an amylolytic enzyme and a recombinant protein of interest was investigated. Initial experiments using a two vector system indicated that co-expression had the effect of reducing the level of expression for each individual protein, compared with expression from the same constructs when present on their own. Despite the increased cell density, expression of the recombinant protein of interest (TK) remained at a lower level than the single expressing control. Single vectors containing operons were constructed as an alternative to multi-vector co-expression. While these dual-expression vectors provide certain technical advantages such as eliminating the need for co-transformation and reducing the requirement for multiple types of antibiotic, it was thought that they may also lead to higher levels of protein due to a reduced metabolic burden on the host cell. The construction of pQR1720 which includes an operon containing eGFP immediately followed by the *C. violaceum* glucoamylase, regulated by the *lac* promoter, demonstrated for the first time recombinant protein expression using starch as a sole carbon source. Furthermore, the yield of recombinant protein (eGFP) was greater in cultures containing starch than in cultures containing an equivalent amount of glucose. This is the first example of enhanced recombinant protein expression resulting directly from a cell engineered approach to enzyme-based fed-batch fermentation.

6 Conclusions and Future work

This study has provided evidence to suggest that the construction of amylolytic *E. coli* strains could allow starch to be used as a viable alternative to other carbon sources during fermentation. More specifically, through the identification and characterisation of novel bacterial glucoamylases, and the combination of these with regulatory elements and secretory signal peptides, a cell engineering approach to enzyme-based fed-batch fermentation has been demonstrated for the first time via enhanced cell growth and an associated increase in recombinant protein yield.

With a proof of concept firmly established, further development of this project can be divided into a number of areas. One avenue would be to integrate the *C. violaceum* glucoamylase into the host genome, ideally using a glucose sensitive promoter for regulation. This should theoretically eliminate some of the issues associated with maintaining multiple plasmids within one cell, and increase the systems versatility. Preliminary investigations into genome integration were carried out using a temperature sensitive vector pGRG36 designed for site-specific insertions of transgenes using the transposon Tn7 [99]. Growth at permissive temperatures of 32°C allows for the recombination machinery present on the plasmid to insert the transgene (present within the plasmids multiple cloning site) into the Tn7 attachment site (*attTn7*) in the genome. Increasing the temperature to 37°C cures the cells of the vector. The *C. violaceum* glucoamylase along with the *PcstA* promoter and the DsbA signal peptide were sub-cloned into the pGRG36 and transformed into chemically competent *E. coli* W3110 cells, however no amylolytic activity was detected from colonies tested. Further work is needed to determine the reasons for this, and to explore whether the substantial reduction in gene copy number compared with vector based expression would be adequate within this particular system.

Alternatively, the dual-expression vector-based system could be further optimised, and modified to include a multiple cloning site to facilitate the insertion of genes for recombinant expression. The dual-expression vectors used in this study contain an operon regulated by the *lac* promoter; further modifications could include separate promoters independently regulating the expression of the amylolytic enzyme and the recombinant protein of interest, essentially mimicking current commercially available dual-expression vectors such as pETDuet™ (Novagen) or pACYCDuet™ (Novagen), whereby two genes are regulated by independent promoters. However, unlike these commercially available vectors the amylolytic enzyme would ideally be self-regulated i.e. controlled by a *PcstA*-like promoter, while the recombinant protein cloned into the multiple cloning site could be regulated by a strong inducible promoter. Given that self-secreting enzyme-based fed-batch fermentation has been realised only in *E. coli* W3110 and not in BL21(DE3), it is important to select a promoter compatible with K12 strains, such as *Ptac*.

This method of self-secreting enzyme-based fed-batch fermentation is not limited to the degradation of starch. The same principle could be applied to alternative carbon sources such as cellulose. By engineering an *E. coli* strain with the ability to secrete cellulase into the extracellular media, it may be possible to release glucose in a similar manner. Initial investigations using the CAZY database [54] identified a number of cellulases of potential interest from *D. geothermalis*. It is possible that a combination of cellulases would be required, including endo-acting cellulases (EC 3.2.1.4) for the initial hydrolysis of cellulose, exo-acting cellulases (EC 3.2.1.91) to form cellobiose, and cellobiases (EC 3.2.1.21) for final hydrolysis of cellobiose into glucose. An obvious advantage, much like starch, is the ubiquity of cellulose as a carbon source. However, the insolubility of cellulose in water could provide a major obstacle in applying it to a liquid based culture.

Another potential improvement over the current system lies with altering the mechanism behind secretion. It may be possible to avoid relying on outer membrane permeability for secretion by anchoring amylolytic enzymes to the cells outer surface. This may allow for a smaller amount of enzyme to be produced whilst still maintaining the desired feed rate, based on the rationale that when the enzyme is targeted to the periplasm for periplasmic release, a proportion of that enzyme never comes into contact with its substrate in the extracellular media. Whereas, if the amylolytic enzyme is targeted directly to the outer surface, all enzyme produced will have access to the substrate. If less amylolytic enzyme is required this has the potential to reduce the overall metabolic burden on the cell and may allow for increased cell growth and increased recombinant protein yield. Furthermore, the mechanism behind periplasmic leakage itself is not completely understood, with reports suggesting a possible correlation between periplasmic protein concentration and release [100], and others suggesting additional factors such as outer membrane composition playing a more significant role [101]. Either way, avoiding this step would provide a more direct link between transcription and functional expression, allowing for more precise regulatory control. In addition, having the amylolytic enzyme attached to the cell membrane could simplify any issues in downstream processing, which may arise from the amylolytic enzyme and the recombinant protein of interest being present in the same subcellular fraction. The idea of cell surface display for polysaccharide degradation has been explored previously, with one example being a cello-oligosaccharide assimilating *E. coli* strain displaying an active β -glucosidase anchored to the cell surface via the Blc protein [102]. The Blc protein itself is an outer membrane lipoprotein endogenous to *E. coli*, and was in this case fused via its C-terminus to the N-terminus of the β -glucosidase. Another example has been the use of auto-transporters, a family of proteins which use the type V secretion pathway to deliver proteins to the cell surface in Gram-negative bacteria [103]. The advantage of this system is that it is modular, consisting of an N-terminal signalling

sequence, a passenger domain containing the protein to be displayed, and a membrane anchored C-terminal translocation unit [104]. More recently an auto-transporter was used to display a thermophilic β -glucosidase from *Thermobifida fusca* onto the cell surface of the *E. coli* strain MS04, for the purposes of carrying out simultaneous saccharification and fermentation in the production of lignocellulosic biofuels [105].

Investigations within this study have also shed light on previously unreported observations that *E. coli*, particularly BL21(DE3), is able to degrade starch without the heterologous expression of an amylolytic enzyme, however the reasons behind this remain unclear. Further work is needed to gain a more complete picture about the endogenous enzyme responsible, and why there is such a disparity between BL21(DE3) and W3110. It is already known that expression levels of certain proteins including those of the maltose transporter are increased in BL21 compared to K12 strains [106]. It is certainly possible that amylolytic enzymes involved in this pathway are also upregulated in BL21(DE3), explaining the increased ability to degrade starch within the media. An interesting observation is that the amylolytic enzyme in question is not secreted, but is instead associated with the cell itself, indicating that starch molecules are capable of being degraded by enzymes residing in either the periplasmic space or at the outer membrane. A key piece of work still remaining is to identify the hydrolysis products from this endogenous enzyme, and establish why *E. coli* BL21(DE3) appears not to be able to utilise those products for growth.

In summary this study has investigated the utilisation of starch as a carbon source in both untransformed and engineered amylolytic *E. coli* strains. The characterisation of *S. thermoviolaceus* α -amylase secreting *E. coli* reveals it to be a particularly potent amylolytic strain, with potential applications as a microbial platform to convert starch into valuable products. The development of additional novel amylolytic strains has allowed for the direct conversion of starch to glucose within the culture media. The outcome is an innovative

solution to one of the fundamental issues associated with microbial fermentation, and provides the first reported example of self-secreting enzyme-based fed-batch fermentation, resulting in both increased cell density and increased recombinant protein yield.

7 References

1. Davy, A.M., H.F. Kildegaard, and M.R. Andersen, *Cell Factory Engineering*. Cell Systems, 2017. **4**(3): p. 262-275.
2. Lim, Y., et al., *Engineering mammalian cells in bioprocessing – current achievements and future perspectives*. Biotechnology and Applied Biochemistry, 2010. **55**(4): p. 175-189.
3. Humphreys, D.P., et al., *Engineering of Escherichia coli to improve the purification of periplasmic Fab' fragments: changing the pI of the chromosomally encoded PhoS/PstS protein*. Protein Expression and Purification, 2004. **37**(1): p. 109-118.
4. Velur Selvamani, R., et al., *Antibiotic-free segregational plasmid stabilization in Escherichia coli owing to the knockout of triosephosphate isomerase (tpiA)*. Microbial Cell Factories, 2014. **13**(1): p. 58.
5. Cooke, G.D., et al., *A modified Escherichia coli protein production strain expressing staphylococcal nuclease, capable of auto-hydrolysing host nucleic acid*. Journal of Biotechnology, 2003. **101**(3): p. 229-239.
6. Nesbeth, D.N., et al., *Growth and productivity impacts of periplasmic nuclease expression in an Escherichia coli Fab' fragment production strain*. Biotechnology and Bioengineering, 2012. **109**(2): p. 517-527.
7. Makrides, S.C., *Strategies for achieving high-level expression of genes in Escherichia coli*. Microbiological Reviews, 1996. **60**(3): p. 512-38.
8. Archer, C.T., et al., *The genome sequence of E. coli W (ATCC 9637): comparative genome analysis and an improved genome-scale reconstruction of E. coli*. BMC Genomics, 2011. **12**: p. 9-9.
9. Scalfaferrri, F., et al., *Role and mechanisms of action of Escherichia coli Nissle 1917 in the maintenance of remission in ulcerative colitis patients: An update*. World Journal of Gastroenterology, 2016. **22**(24): p. 5505-5511.
10. Monod, J., *Recherches Sur la Croissance Des Cultures Bactériennes*. 1942: Hermann & Cie.
11. Jahreis, K., et al., *Ins and outs of glucose transport systems in eubacteria*. FEMS Microbiology Reviews, 2008. **32**(6): p. 891-907.
12. Ferenci, T., *Adaptation to life at micromolar nutrient levels: the regulation of Escherichia coli glucose transport by endoinduction and cAMP*. FEMS Microbiology Reviews, 1996. **18**(4): p. 301-317.
13. Dippel, R. and W. Boos, *The Maltodextrin System of Escherichia coli: Metabolism and Transport*. Journal of Bacteriology, 2005. **187**(24): p. 8322-8331.

14. Szmelcman, S. and M. Hofnung, *Maltose transport in Escherichia coli K-12: involvement of the bacteriophage lambda receptor*. Journal of Bacteriology, 1975. **124**(1): p. 112-118.
15. Schneider, E., et al., *Molecular characterization of the MalT-dependent periplasmic alpha-amylase of Escherichia coli encoded by malS*. Journal of Biological Chemistry, 1992. **267**(8): p. 5148-54.
16. Ferenci, T. and U. Klotz, *Affinity chromatographic isolation of the periplasmic maltose binding protein of Escherichia coli*. FEBS Letters, 1978. **94**(2): p. 213-217.
17. Ranquin, A. and P. Van Gelder, *Maltoporin: sugar for physics and biology*. Research in Microbiology, 2004. **155**(8): p. 611-616.
18. Ferenci, T., *The Recognition of Maltodextrins by Escherichia coli*. European Journal of Biochemistry, 1980. **108**(2): p. 631-636.
19. Boos, W. and H. Shuman, *Maltose/Maltodextrin System of Escherichia coli: Transport, Metabolism, and Regulation*. Microbiology and Molecular Biology Reviews, 1998. **62**(1): p. 204-229.
20. Bren, A., et al., *Glucose becomes one of the worst carbon sources for E.coli on poor nitrogen sources due to suboptimal levels of cAMP*. Scientific Reports, 2016. **6**: p. 24834.
21. Bauer, K.A., et al., *Improved expression of human interleukin-2 in high-cell-density fermentor cultures of Escherichia coli K-12 by a phosphotransacetylase mutant*. Applied and Environmental Microbiology, 1990. **56**(5): p. 1296-1302.
22. Luli, G.W. and W.R. Strohl, *Comparison of growth, acetate production, and acetate inhibition of Escherichia coli strains in batch and fed-batch fermentations*. Applied and Environmental Microbiology, 1990. **56**(4): p. 1004-1011.
23. Åkesson, M., et al., *On-line detection of acetate formation in Escherichia coli cultures using dissolved oxygen responses to feed transients*. Biotechnology and Bioengineering, 1999. **64**(5): p. 590-598.
24. Majewski, R.A. and M.M. Domach, *Simple constrained-optimization view of acetate overflow in E. coli*. Biotechnology and Bioengineering, 1990. **35**(7): p. 732-738.
25. Wolfe, A.J., *The Acetate Switch*. Microbiology and Molecular Biology Reviews, 2005. **69**(1): p. 12-50.
26. Abdel-Hamid, A.M., M.M. Attwood, and J.R. Guest, *Pyruvate oxidase contributes to the aerobic growth efficiency of Escherichia coli*. Microbiology, 2001. **147**(6): p. 1483-1498.
27. Chang, Y.Y., A.Y. Wang, and J.E. Cronan, *Expression of Escherichia coli pyruvate oxidase (PoxB) depends on the sigma factor encoded by the rpoS(katF) gene*. Molecular Microbiology, 1994. **11**(6): p. 1019-1028.

28. Eiteman, M.A. and E. Altman, *Overcoming acetate in Escherichia coli recombinant protein fermentations*. Trends in Biotechnology, 2006. **24**(11): p. 530-536.
29. Yee, L. and H.W. Blanch, *Recombinant Protein Expression in High Cell Density Fed-Batch Cultures of Escherichia Coli*. Bio/Technology, 1992. **10**: p. 1550.
30. Betts, J.I. and F. Baganz, *Miniature bioreactors: current practices and future opportunities*. Microbial cell factories, 2006. **5**: p. 21-21.
31. Tyrrell, E.A., R.E. Mac Donald, and P. Gerhardt, *BIPHASIC SYSTEM FOR GROWING BACTERIA IN CONCENTRATED CULTURE*. Journal of Bacteriology, 1958. **75**(1): p. 1-4.
32. Lübbe, C., A.L. Demain, and K. Bergman, *Use of controlled-release polymer to feed ammonium to Streptomyces clavuligerus cephalosporin fermentations in shake flasks*. Applied Microbiology and Biotechnology, 1986. **23**(5): p. 411-411.
33. Jeude, M., et al., *Fed-batch mode in shake flasks by slow-release technique*. Biotechnol Bioeng, 2006. **95**.
34. Panula-Perala, J., et al., *Enzyme controlled glucose auto-delivery for high cell density cultivations in microplates and shake flasks*. Microbial Cell Factories, 2008. **7**(1): p. 31.
35. Hernández-Montalvo, V., et al., *Expression of galP and glk in a Escherichia coli PTS mutant restores glucose transport and increases glycolytic flux to fermentation products*. Biotechnology and Bioengineering, 2003. **83**(6): p. 687-694.
36. De Anda, R., et al., *Replacement of the glucose phosphotransferase transport system by galactose permease reduces acetate accumulation and improves process performance of Escherichia coli for recombinant protein production without impairment of growth rate*. Metabolic Engineering, 2006. **8**(3): p. 281-290.
37. Cho, S., et al., *High-level recombinant protein production by overexpression of Mlc in Escherichia coli*. Journal of Biotechnology, 2005. **119**(2): p. 197-203.
38. Aristidou, A.A., K.Y. San, and G.N. Bennett, *Metabolic Engineering of Escherichia coli To Enhance Recombinant Protein Production through Acetate Reduction*. Biotechnology Progress, 1995. **11**(4): p. 475-478.
39. Farmer, W.R. and J.C. Liao, *Reduction of aerobic acetate production by Escherichia coli*. Applied and Environmental Microbiology, 1997. **63**(8): p. 3205-3210.
40. Gokarn, R.R., M.A. Eiteman, and E. Altman, *Metabolic Analysis of Escherichia coli in the Presence and Absence of the Carboxylating Enzymes Phosphoenolpyruvate Carboxylase and Pyruvate Carboxylase*. Applied and Environmental Microbiology, 2000. **66**(5): p. 1844-1850.
41. Vemuri, G.N., M.A. Eiteman, and E. Altman, *Increased recombinant protein production in Escherichia coli strains with overexpressed water-forming NADH oxidase and a deleted ArcA regulatory protein*. Biotechnology and Bioengineering, 2006. **94**(3): p. 538-542.

42. Andersen, K.B. and K. von Meyenburg, *Are growth rates of Escherichia coli in batch cultures limited by respiration?* Journal of Bacteriology, 1980. **144**(1): p. 114-123.
43. Aristidou, A.A., K.Y. San, and G.N. Bennett, *Improvement of Biomass Yield and Recombinant Gene Expression in Escherichia coli by Using Fructose as the Primary Carbon Source.* Biotechnology Progress, 1999. **15**(1): p. 140-145.
44. Luo, Q., et al., *Optimization of culture on the overproduction of TRAIL in high-cell-density culture by recombinant Escherichia coli.* Applied Microbiology and Biotechnology, 2006. **71**(2): p. 184-191.
45. Han, K., J. Hong, and H.C. Lim, *Relieving effects of glycine and methionine from acetic acid inhibition in Escherichia coli fermentation.* Biotechnology and Bioengineering, 1993. **41**(3): p. 316-324.
46. Wang, H., et al., *Improving the Expression of Recombinant Proteins in E. coli BL21 (DE3) under Acetate Stress: An Alkaline pH Shift Approach.* PLOS ONE, 2014. **9**(11): p. e112777.
47. van de Walle, M. and J. Shiloach, *Proposed mechanism of acetate accumulation in two recombinant Escherichia coli strains during high density fermentation.* Biotechnology and Bioengineering, 1998. **57**(1): p. 71-78.
48. Noronha, S.B., et al., *Investigation of the TCA cycle and the glyoxylate shunt in Escherichia coli BL21 and JM109 using 13C-NMR/MS.* Biotechnology and Bioengineering, 2000. **68**(3): p. 316-327.
49. Phue, J.-N., et al., *Glucose metabolism at high density growth of E. coli B and E. coli K: Differences in metabolic pathways are responsible for efficient glucose utilization in E. coli B as determined by microarrays and Northern blot analyses.* Biotechnology and Bioengineering, 2005. **90**(7): p. 805-820.
50. Phue, J.-N., et al., *Evaluating microarrays using a semiparametric approach: Application to the central carbon metabolism of Escherichia coli BL21 and JM109.* Genomics, 2007. **89**(2): p. 300-305.
51. Shiloach, J., et al., *Effect of glucose supply strategy on acetate accumulation, growth, and recombinant protein production by Escherichia coli BL21 (λ DE3) and Escherichia coli JM109.* Biotechnology and Bioengineering, 1996. **49**(4): p. 421-428.
52. de Souza, P.M. and P. de Oliveira Magalhães, *Application of microbial α -amylase in industry – A review.* Brazilian Journal of Microbiology, 2010. **41**(4): p. 850-861.
53. Henrissat, B. and G. Davies, *Structural and sequence-based classification of glycoside hydrolases.* Current Opinion in Structural Biology, 1997. **7**(5): p. 637-644.
54. Cantarel, B.L., et al., *The Carbohydrate-Active EnZymes database (CAZy): an expert resource for Glycogenomics.* Nucleic Acids Research, 2009. **37**(Database issue): p. D233-D238.

55. Kumar, P. and T. Satyanarayana, *Microbial glucoamylases: characteristics and applications*. Critical Reviews in Biotechnology, 2009. **29**(3): p. 225-255.
56. Rosales-Colunga, L.M. and A. Martínez-Antonio, *Engineering Escherichia coli K12 MG1655 to use starch*. Microbial Cell Factories, 2014. **13**: p. 74-74.
57. Bahri, S.M. and J.M. Ward, *Cloning and expression of an α -amylase gene from Streptomyces thermoviolaceus CUB74 in Escherichia coli JM107 and S. lividans TK24*. Journal of General Microbiology, 1990. **136**(5): p. 811-818.
58. Bahri, S.M. and J.M. Ward, *Sequence of the Streptomyces thermoviolaceus CUB74 α -amylase-encoding gene and its transcription analysis in Streptomyces lividans*. Gene, 1993. **127**(1): p. 133-137.
59. French, C., E. Keshavarz-Moore, and J.M. Ward, *Development of a simple method for the recovery of recombinant proteins from the Escherichia coli periplasm*. Enzyme and Microbial Technology, 1996. **19**(5): p. 332-338.
60. Spratt, B.G., et al., *Kanamycin-resistant vectors that are analogues of plasmids pUC8, pUC9, pEMBL8 and pEMBL9*. Gene, 1986. **41**(2-3): p. 337-342.
61. Summers, D.K. and D.J. Sherratt, *Resolution of ColE1 dimers requires a DNA sequence implicated in the three-dimensional organization of the cer site*. The EMBO Journal, 1988. **7**(3): p. 851-858.
62. French, C. and J. Ward, *Improved production and stability of E. coli recombinants expressing transketolase for large scale biotransformation*. Biotechnology Letters, 1995. **17**(3): p. 247-252.
63. Norouziyan, D., et al., *Fungal glucoamylases*. Biotechnology Advances, 2006. **24**(1): p. 80-85.
64. Coutinho, P.M. and P.J. Reilly, *Glucoamylase structural, functional, and evolutionary relationships*. Proteins: Structure, Function, and Bioinformatics, 1997. **29**(3): p. 334-347.
65. Kobayashi, F. and Y. Nakamura, *Efficient production by Escherichia coli of recombinant protein using salting-out effect protecting against proteolytic degradation*. Biotechnology Letters, 2003. **25**(10): p. 779-782.
66. Zheng, Y., et al., *Cloning, expression, and characterization of a thermostable glucoamylase from Thermoanaerobacter tengcongensis MB4*. Applied Microbiology and Biotechnology, 2010. **87**(1): p. 225-233.
67. Fekkes, P. and A.J.M. Driessen, *Protein Targeting to the Bacterial Cytoplasmic Membrane*. Microbiology and Molecular Biology Reviews, 1999. **63**(1): p. 161-173.
68. Valent, Q.A., *Signal recognition particle mediated protein targeting in Escherichia coli*. Antonie van Leeuwenhoek, 2001. **79**(1): p. 17-31.

69. Robinson, C. and A. Bolhuis, *Tat-dependent protein targeting in prokaryotes and chloroplasts*. Biochimica et Biophysica Acta (BBA) - Molecular Cell Research, 2004. **1694**(1–3): p. 135-147.
70. Green, E.R. and J. Meccas, *Bacterial Secretion Systems – An overview*. Microbiology spectrum, 2016. **4**(1): p. 10.1128/microbiolspec.VMBF-0012-2015.
71. Luirink, J. and B. Dobberstein, *Mammalian and Escherichia coli signal recognition particles*. Molecular Microbiology, 1994. **11**(1): p. 9-13.
72. Schierle, C.F., et al., *The DsbA Signal Sequence Directs Efficient, Cotranslational Export of Passenger Proteins to the Escherichia coli Periplasm via the Signal Recognition Particle Pathway*. Journal of Bacteriology, 2003. **185**(19): p. 5706-5713.
73. Lei, S.P., et al., *Characterization of the Erwinia carotovora pelB gene and its product pectate lyase*. Journal of Bacteriology, 1987. **169**(9): p. 4379-4383.
74. Schultz, J.E. and A. Matin, *Molecular and functional characterization of a carbon starvation gene of Escherichia coli*. Journal of Molecular Biology, 1991. **218**(1): p. 129-140.
75. Busby, S. and R.H. Ebright, *Transcription activation by catabolite activator protein (CAP)*. Journal of Molecular Biology, 1999. **293**(2): p. 199-213.
76. Notley-McRobb, L., A. Death, and T. Ferenci, *The relationship between external glucose concentration and cAMP levels inside Escherichia coli: implications for models of phosphotransferase-mediated regulation of adenylate cyclase*. Microbiology, 1997. **143**(6): p. 1909-1918.
77. Wang, J., et al., *Optimization of carbon source and glucose feeding strategy for improvement of L-isoleucine production by Escherichia coli*. Biotechnology, Biotechnological Equipment, 2015. **29**(2): p. 374-380.
78. Hayashi, K., et al., *Highly accurate genome sequences of Escherichia coli K-12 strains MG1655 and W3110*. Molecular Systems Biology, 2006. **2**(1).
79. Studier, F.W. and B.A. Moffatt, *Use of bacteriophage T7 RNA polymerase to direct selective high-level expression of cloned genes*. Journal of Molecular Biology, 1986. **189**(1): p. 113-130.
80. Ingram, C.U., et al., *One-pot synthesis of amino-alcohols using a de-novo transketolase and β -alanine: Pyruvate transaminase pathway in Escherichia coli*. Biotechnology and Bioengineering, 2007. **96**(3): p. 559-569.
81. Yanisch-Perron, C., J. Vieira, and J. Messing, *Improved M13 phage cloning vectors and host strains: nucleotide sequences of the M13mpl8 and pUC19 vectors*. Gene, 1985. **33**(1): p. 103-119.
82. Krause, M., et al., *A novel fed-batch based cultivation method provides high cell-density and improves yield of soluble recombinant proteins in shaken cultures*. Microbial Cell Factories, 2010. **9**(1): p. 1-11.

83. Blanchin-Roland, S. and J.-M. Masson, *Protein secretion controlled by a synthetic gene in Escherichia coli*. Protein Engineering, 1989. **2**(6): p. 473-480.
84. Pierce, J.J., et al., *A comparison of the process issues in expressing the same recombinant enzyme periplasmically in Escherichia coli and extracellularly in Streptomyces lividans*. Journal of Biotechnology, 2002. **92**(3): p. 205-215.
85. Bahri, S.M. and M. Ward, *Regulation of a thermostable α -amylase of Streptomyces thermoviolaceus CUB74: maltotriose is the smallest inducer*. Biochimie, 1990. **72**(12): p. 893-895.
86. Müller-Hill, B., L. Crapo, and W. Gilbert, *Mutants that make more lac repressor*. Proceedings of the National Academy of Sciences of the United States of America, 1968. **59**(4): p. 1259-1264.
87. A., R., et al., *Characterization of the metabolic burden on Escherichia coli DH1 cells imposed by the presence of a plasmid containing a gene therapy sequence*. Biotechnology and Bioengineering, 2004. **88**(7): p. 909-915.
88. Glick, B.R., *Metabolic load and heterologous gene expression*. Biotechnology Advances, 1995. **13**(2): p. 247-261.
89. Schlegel, S., et al., *Optimizing heterologous protein production in the periplasm of E. coli by regulating gene expression levels*. Microbial Cell Factories, 2013. **12**: p. 24-24.
90. de Marco, A., *Recombinant polypeptide production in E. coli: towards a rational approach to improve the yields of functional proteins*. Microbial Cell Factories, 2013. **12**: p. 101-101.
91. Freundlieb, S. and W. Boos, *Alpha-amylase of Escherichia coli, mapping and cloning of the structural gene, malS, and identification of its product as a periplasmic protein*. Journal of Biological Chemistry, 1986. **261**(6): p. 2946-53.
92. Bailey, J.M. and W.J. Whelan, *Physical Properties of Starch: I. RELATIONSHIP BETWEEN IODINE STAIN AND CHAIN LENGTH*. Journal of Biological Chemistry, 1961. **236**(4): p. 969-973.
93. Cormack, B.P., R.H. Valdivia, and S. Falkow, *FACS-optimized mutants of the green fluorescent protein (GFP)*. Gene, 1996. **173**(1): p. 33-38.
94. Yoji, H., et al., *Nucleotide sequence and expression of the glucoamylase-encoding gene (glaA) from Aspergillus oryzae*. Gene, 1991. **108**(1): p. 145-150.
95. Petersen, T.N., et al., *SignalP 4.0: discriminating signal peptides from transmembrane regions*. Nature Methods, 2011. **8**: p. 785.
96. Kleman, G.L., et al., *A predictive and feedback control algorithm maintains a constant glucose concentration in fed-batch fermentations*. Applied and Environmental Microbiology, 1991. **57**(4): p. 910-917.

97. Luli, G.W., et al., *An automatic, on-line glucose analyzer for feed-back control of fed-batch growth of Escherichia coli*. Biotechnology Techniques, 1987. **1**(4): p. 225-230.
98. Lim, H.N., Y. Lee, and R. Hussein, *Fundamental relationship between operon organization and gene expression*. Proceedings of the National Academy of Sciences of the United States of America, 2011. **108**(26): p. 10626-10631.
99. McKenzie, G.J. and N.L. Craig, *Fast, easy and efficient: site-specific insertion of transgenes into Enterobacterial chromosomes using Tn7 without need for selection of the insertion event*. BMC Microbiology, 2006. **6**: p. 39-39.
100. Shokri, A., A. Sandén, and G. Larsson, *Growth rate-dependent changes in Escherichia coli membrane structure and protein leakage*. Applied Microbiology and Biotechnology, 2002. **58**(3): p. 386-392.
101. Ukkonen, K., et al., *Effect of culture medium, host strain and oxygen transfer on recombinant Fab antibody fragment yield and leakage to medium in shaken E. coli cultures*. Microbial Cell Factories, 2013. **12**: p. 73-73.
102. Tanaka, T., et al., *Creation of a Cellooligosaccharide-Assimilating Escherichia coli Strain by Displaying Active Beta-Glucosidase on the Cell Surface via a Novel Anchor Protein*. Applied and Environmental Microbiology, 2011. **77**(17): p. 6265-6270.
103. Leo, J.C., I. Grin, and D. Linke, *Type V secretion: mechanism(s) of autotransport through the bacterial outer membrane*. Philosophical transactions of the Royal Society of London. Series B, Biological sciences, 2012. **367**(1592): p. 1088-1101.
104. Nicolay, T., J. Vanderleyden, and S. Spaepen, *Autotransporter-based cell surface display in Gram-negative bacteria*. Critical Reviews in Microbiology, 2015. **41**(1): p. 109-123.
105. Munoz-Gutierrez, I., et al., *Ag43-mediated display of a thermostable beta-glucosidase in Escherichia coli and its use for simultaneous saccharification and fermentation at high temperatures*. Microbial Cell Factories, 2014. **13**(1): p. 106.
106. Marisch, K., et al., *A Comparative Analysis of Industrial Escherichia coli K-12 and B Strains in High-Glucose Batch Cultivations on Process-, Transcriptome- and Proteome Level*. PLoS ONE, 2013. **8**(8): p. e70516.